University of Alberta

Detection and Compensation For Stiction In Multi-loop Control Systems

by

Mahdi Alemohammad

A thesis submitted to the Faculty of Graduate Studies and Research in partial fulfillment of the requirements for the degree of

Master of Science

in

Process Control

Department of Chemical and Materials Engineering

Spring 2011
Edmonton, Alberta

Examining Committee

Prof. Biao Huang, Chemical and Materials Engineering

Dr. Vinary Prasad, Chemical and Materials Engineering

Prof. Bob Koch, Mechanical Engineering

To My ***Parents*** and ***Sisters***

Abstract

Unsatisfactory performance of a control system may have different root causes, of which diagnosis and control have been subjects of interest. Numerous approaches have been used to identify the source of the oscillatory behavior of control systems. This work will focus on the nonlinearities introduced by process equipment, more specifically, static friction (stiction) in control valves.

Using shape-based stiction detection methods and surrogate testing for time series, a new detection method is proposed for systems containing one or more sticky valves. Performance of this method is validated by both simulation and industrial data.

The existence of stiction in a control valve may lead to oscillations in all loops of the process. In this work, frequency analysis of multi-loop processes oscillating due to stiction will be presented. Derivation of a general mathematical representation of the condition, under which oscillations occur in a multi-loop system because of stiction, is the contribution of the proposed analysis.

The proposed condition for occurrence of oscillations provides a compensation framework for this problem. In this scheme, given dynamics of the system and severity of stiction, the appropriate tuning for the controller will be found which reduces or removes oscillations from the system.

An alternative compensation algorithm will also be proposed, which aims removal of oscillations from systems for which the previously proposed approach cannot permanently remove undesirable oscillations. Achieving a non-oscillatory output without making the valve stem to move more aggressively, is the main characteristic of this algorithm.

Acknowledgements

First, I acknowledge my supervisor, Prof. Biao Huang, for his endless directions, professional manner, constructive criticism and friendly support.

I had the honor of working with Dr. Amos Benzvi, Dr. Jongmin Lee and Dr. Dave Shook as their teaching assistant. The experiences I obtained during these tasks are treasures for my future career.

Financial support from Natural Sciences and Engineering Research Council of Canada (NSERC), Syncrude Canada Ltd. and Agrium Co. is greatly acknowledged.

Technical advices and cooperations from Professor Nina Thornhill (Imperial College London), Edward Bai (Agrium Co.), Dr Kwanho Lee and Xinguang Shao (Syncrude Canada Ltd.) is acknowledged.

I would also like to thank all of my colleagues in the computer process control group, especially Yuri Shardt.

Many thanks to my friends Sahar Salimi and Ata Kamyabi Gol for their helps with preparing and writing this work.

Last but not least, I appreciate my parents and sisters for the moral support they granted to me in my entire life.

Contents

List of Tables

List of Figures

List of Symbols

A_i	Magnitude of the i^{th} sinusoidal input to stiction describing function
C	Difference between cut-off frequencies of PI controller and the process
E	Number of columns of Y_{emb}
F_i	Fourier transform of time series in i^{th} frequency channel
F_{imag}	Imaginary value of FR at ω^*
$F_{surr,i}$	Surrogate of the fourier component in i^{th} frequency channel
$G_{(s)}$	Laplace transform of the process dynamics
$G_{c(s)}$	Laplace transform of the controller dynamics
H	Prediction horizon in Surrogate method
H_{real}	Real value of FR at ω^{**}
J	Slip-jump parameter in Choudhury's and Kano's two-parameter stiction models (% lift)
K	Gain of FOPDT transfer function
K_c	Controller gain
MV	Position of the valve stem (% lift)
MV_{ss}	Position of the sticky valve at steady state
$\widehat{MV}_{end}$	Final position of the valve in modified two-move approach
$\widehat{MV}_{mid}$	Intermediate position of the valve in modified two-move approach
$\widehat{MV}_t$	Proper position of the sticky valve at time step t

$N_{(A_i)}$	Describing function of stiction in i^{th} loop
N_T	Product of values of stiction DFs for all loops of the process
NI	Nonlinearity Index
OP	Output of the controller (% lift)
OP_{end}	Controller output equivalent to $\widehat{MV}_{end}$
OP_{mid}	Controller output equivalent to $\widehat{MV}_{mid}$
OP_{ss}	Controller output equivalent to MV_{ss}
$\widehat{OP}_t$	Controller output equivalent to $\widehat{MV}_t$
PV	Output of the process (% lift)
S	Stick-band parameter in Choudhury's and Kano's stiction models (% lift)
S_n	Number of samples per cycle of oscillation
SP	Setpoint (% lift)
X_i	Frequency responses of dynamic elements in a control system with sticky valve
Y_{emb}	Embedded matrix used in Surrogate Analysis
a_{cr}	Tuning parameter in Constant Reinforcement compensation method (% lift)
d	Stiction parameter in Stenman's one-parameter stiction model
f_t	Added signal (force) to OP at time step t
$\{f_s, f_d\}$	Stiction parameters in He's two-parameter stiction model
$g_{ij(s)}$	Transfer function from j^{th} input to i^{th} output
k_{opt}	Number of sticky valves in a system
l	Length of time series to be analyzed by Surrogate method
u_k	Input to the stiction model at time k
y_k	Output of the stiction model at time k

$\mathcal{H}$ — Condition matrix containing dynamics of process, controllers and sticky elements defined as

$$\begin{bmatrix} 1+g_{11}g_{c1}N_1 & g_{12}g_{c2}N_2 & \cdots & g_{1n}g_{cn}N_n \\ g_{21}g_{c1}N_1 & 1+g_{22}g_{c2}N_2 & \cdots & g_{2n}g_{cn}N_n \\ \vdots & & \ddots & \vdots \\ g_{n1}g_{c1}N_1 & g_{n2}g_{c2}N_2) & \cdots & 1+g_{nn}g_{cn}N_n \end{bmatrix}$$

$\mathcal{H}'$ — The matrix resulted from dividing i^{th} column of $\mathcal{H}$ by N_i, for a multi-loop system with one sticky valve in i^{th} loop

$\mathcal{H}''$ — The matrix resulted from dividing corresponding columns of $\mathcal{H}$ to loops with sticky valves, by their DF values

$\overline{\mathcal{H}}_{ij}$ — The matrix resulted from elimination of i^{th} row and j^{th} column of $\mathcal{H}$

$\overline{\mathcal{H}}'_{ij}$ — The matrix resulted from elimination of i^{th} row and j^{th} column of $\mathcal{H}'$

$\overline{\mathcal{H}}''_{ij}$ — The matrix resulted from elimination of i^{th} row and j^{th} column of $\mathcal{H}''$

$\mathcal{S}$ — Stiction nonlinear function, which for each time step t depends on OP_t, MV_{t-1} and stiction parameters

Γ_{test} — H step ahead prediction error in Surrogate method

$\bar{\Gamma}_{surr}$ — Average of H step ahead prediction errors of M Surrogate series

Λ — RGA matrix

α_k — Added signal to OP in Constant Reinforcement compensation method

δ — Half width of the envelope, within which OP_t oscillates after learning phase of the model-based compensation method

δ_{opt} — Half width of the envelope, within which OP changes cannot move the valve

ε_x — Threshold for changes in OP

ε_y — Threshold for changes in PV

θ — Time delay of FOPDT transfer function

λ_{ij} — Entry of Λ related to j^{th} input and i^{th} output

$\sigma_{\Gamma_{surr}}$	Standard deviation of M Surrogate series
τ	Time constant of FOPDT transfer function
τ_I	Integral time of the controller
ϕ_i	Random phase in Surrogate method, picked from uniform distribution
ω^*	The frequency at which trajectory of FR intersects imaginary axis for the first time (real part is zero)
ω^{**}	The frequency at which trajectory of FR intersects real axis for the first time (imaginary part is zero)

List of Abbreviations

ANSI	American National Standard Institute
ARMAX	AutoRegressive Moving Average with eXogenous Input
ARX	AutoRegressive with eXogenous Input
CCF	Cross Correlation Function
DCS	Distributed Control System
DF	Describing Function
FOPDT	First Order Plus Dead Time
FR	Frequency Response
MSE	Mean Square Error
PI	Proportional-Integral
RGA	Relative Gain Array

Chapter 1

Introduction

1.1 Stiction in Control Systems

A typical modern chemical plant includes hundreds or thousands of control loops. The main objectives of such control systems are maintaining the processes at proper operating conditions. Acceptable and reliable performance of these control loops ensures the high quality of the products. Different kinds of observed fluctuations in the signals of a control system are considered as a result of unsatisfactory performance. These deviations from desired values may have different root causes. Poor controller tuning, external disturbance and nonlinearity in the system are some known sources of poor performance [30]. This work focuses on the latter mentioned cause, nonlinearities in the control system, specifically nonlinearity as a result of failure in sensors and/or equipments.

As one of the vital parts of a control loop, which executes the control command on the manipulated variable, the control valve is a potential source of nonlinear behavior. Reports show that various nonlinearities in control valves, such as hysteresis, backlash, dead-band, dead-zone and stiction (static friction), are responsible for 20% to 30% of all oscillations occurred due to nonlinear sources [11, 9, 34, 2]. According to [36], stiction severity equivalent to or more than 1% of the valve travel length can cause the system to oscillate considerably. The upper limit for hysteresis nonlinearity is determined as 3%. Such facts make the stiction phenomenon an interesting area of study, in which researchers are faced with a wide range of challenges. Some of these challenges are stiction modeling, detection, quantification and compensation. Figure 1.1 elaborates different steps which have to be taken towards solving the stiction problem in a control valve. In next few sections of this chapter, all the mentioned aspects of solving this problem will be discussed in detail.

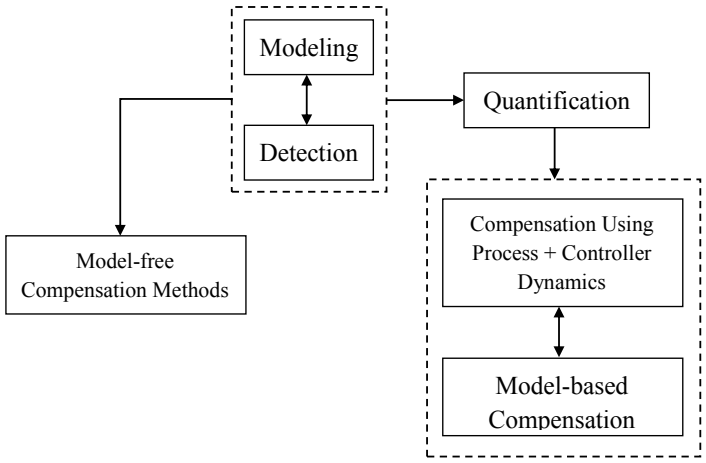

Figure 1.1: Stiction as an extended problem.

1.1.1 Definition of Stiction

Stiction phenomenon is defined by ANSI as "*The resistance to the start of motion, usually measured as the difference between the driving values required to overcome static friction upscale and downscale*" [37]. Moreover, other references [19, 12, 32, 36] have stated many phrases for the definition of stiction. Among all the definitions, the one by [7] may reflect the behavior of stiction nonlinearity more completely: "*Stiction is a property of an element such that its smooth movement in response to a varying input is preceded by a sudden abrupt jump called the slip-jump. Slip-jump is expressed as a percentage of the output span. Its origin in a mechanical system is static friction which exceeds the friction during smooth movement*". Figure 1.2 illustrates a typical pneumatic control valve used in a single-loop control system. In this figure, it is also shown that stiction occurs at interface of packing and the valve stem. It is noteworthy that in Figure 1.2, signals denoted by SP, OP, MV and PV represent setpoint, control signal, actual value of the manipulated variable (or position of the valve) and process output, respectively.

1.1.2 Effect of Stiction on Control System Performance

As a result of stiction presence in a control valve, its actual position (MV) will always be different from the desired (OP). In other words, the valve will not move in response to the control signal. When the cumulative value of the controller output overcomes the friction force in the valve, a sudden move (in positive or negative direction) is seen in the valve position. In some cases, even after the sudden dislocation, the valve will not move smoothly, i.e., consecutive step-wise changes will be applied to the manipulated variable. Several examples of oscillations induced by stiction for laboratory-scale or industrial plants can be seen in Figure 1.3.

Another effective tool to observe and even measure nonlinearities in the control valve is OP-MV plot, also called the valve signature. Plotting these two variables

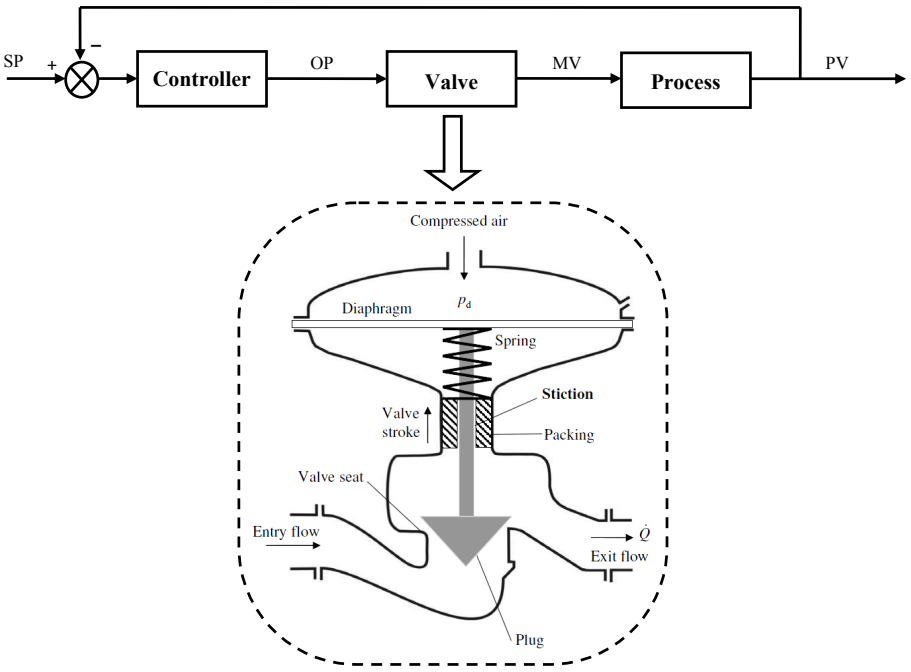

Figure 1.2: Stiction in a simple control system (diagram of the control valve by [23]).

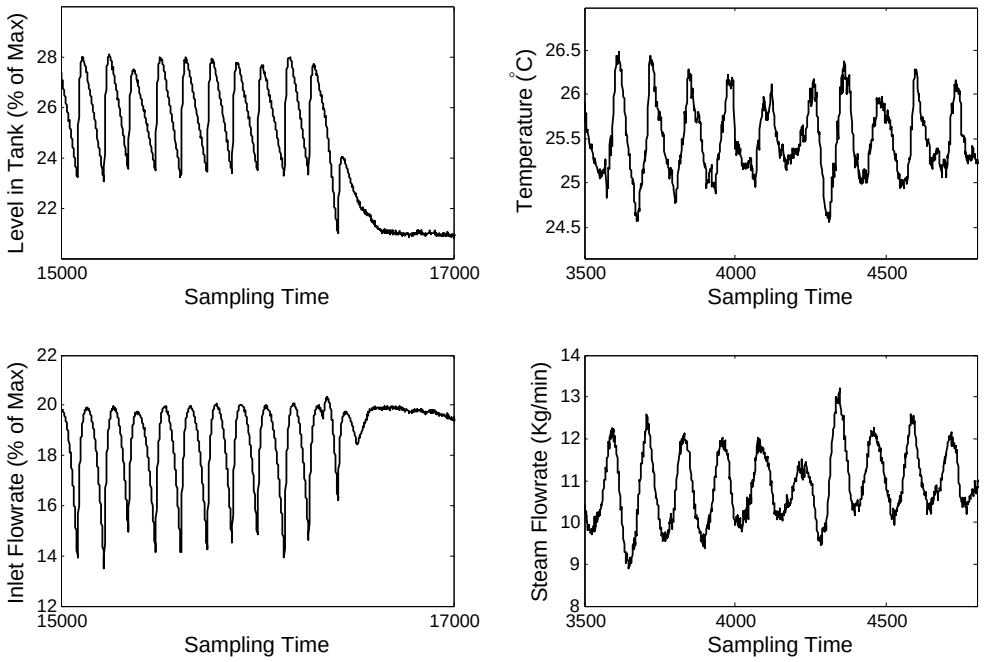

Figure 1.3: Examples of stiction-induced oscillations in pilot-scale temperature control system (Right) and industrial level control system (Left); Process outputs (Top) and control signals (Bottom).

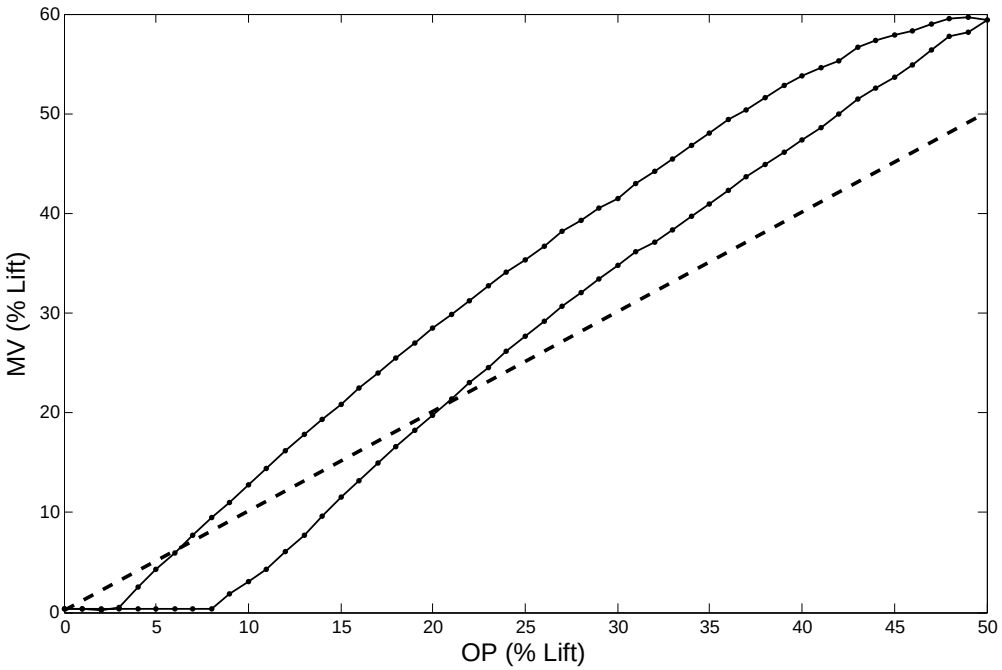

Figure 1.4: Example of the valve signature for a control valve with stiction and calibration problems (solid line) and ideal valve (dashed line).

(in the same unit) for an ideal valve leads to a line, shown by the dashed pattern in Figure 1.4. For used or faulty valves, some deviations from the diagonal line can be seen in their signatures (see Figure 1.4).

1.1.3 Other Nonlinearities of the Control Valves

Doubtlessly, stiction is not the only possible nonlinearity in control valves. Some other commonly seen problems have been addressed in the literature: hysteresis, dead-band and dead-zone. Definitions for these nonlinearities can be found in [37]. Also, Figure 1.5 illustrates simplified signatures of a hypothetical control valve with each problem, plotting output of the valve versus its input.

As mentioned before, the focus of this thesis will be on stiction (static friction) in control valves and challenges related to this nonlinearity. In the next section, existing works in the literature which have addressed stiction and the resulted issues will be reviewed.

1.2 Literature Review

1.2.1 Modeling of the Stiction Nonlinearity

Depending on the application of the model, modeling of stiction can be done using different approaches. All existing models for this phenomenon in mechanical systems

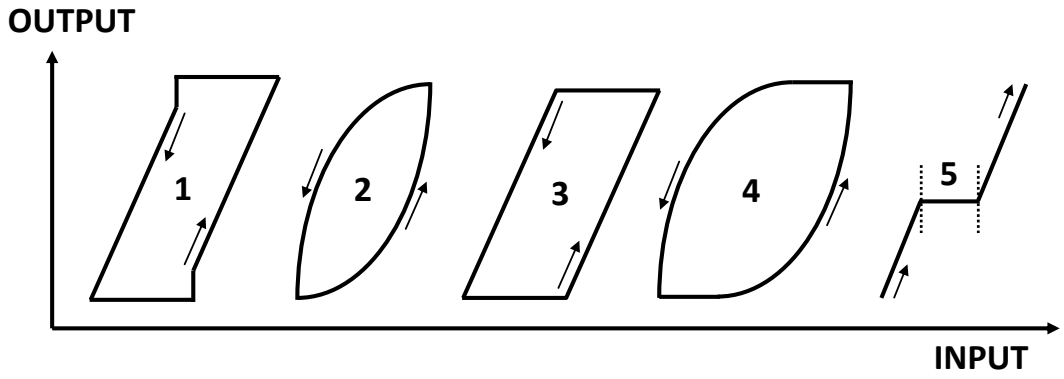

Figure 1.5: Common nonlinearities in control valves: (1) Stiction; (2) Hysteresis; (3) Dead-band; (4) Hysteresis + Dead-band and (5) Dead-zone.

can be classified into two major categories: (1) physics-based (first principle) and (2) data-driven models. Choosing between these two classes is a trade-off between accuracy of predictions and simplicity of the model.

Physics-based Models

Physics-based stiction models can be static or dynamic, based on the friction profile used for derivation of these models. In other words, dynamic models use a time-varying profile for friction force versus the velocity, while static models are assumed to follow a deterministic profile. Karnopp [25] and Classical [33] models are the most applicable static models describing friction in motive mechanical systems. Also, some dynamic models have been introduced by [1, 8], which have been used to model stiction in control valves. Although physics-based models have the ability to capture the behavior of a sticky control valve fairly well, their applications have been limited. Existence of numerous parameters and variables, of which values are difficult or even impossible to measure, can be one of the main reasons. Some of these parameters are stem position and velocity, mass of stem and plug, and different friction forces (e.g., Coulomb, static and viscous). Obviously, such information may not be available for a normal control valve which is already in use. An example to show the complexity of the application of such models, compared to data-driven approaches, is presented in [23].

Data-driven Models

Unlike physics-based models, data-driven models use least possible number of parameters in order to explain the behavior of a sticky control valve. A very simple model which uses only one parameter (d) was introduced by [46]. The proposed model is known as the only existing one-parameter model (Stenman's model), and is given as

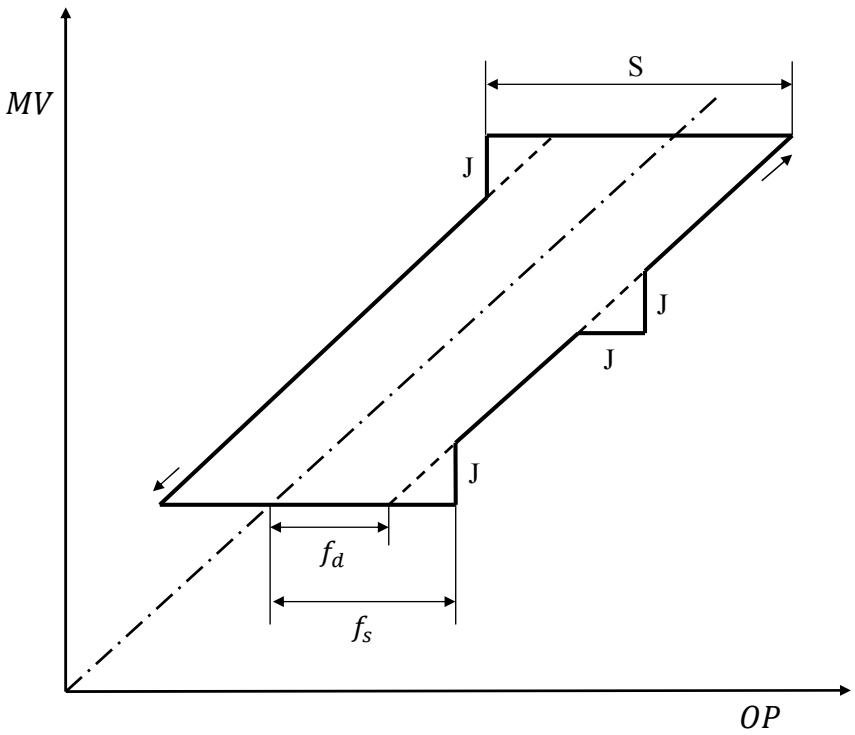

Figure 1.6: Signature of a hypothetical sticky valve, and values of the parameters used in two-parameter data-driven models.

$$y_k = \begin{cases} u_{k-1} & |u_k - y_{k-1}| < d \\ u_k & otherwise \end{cases} \tag{1.1}$$

where u_k is the control signal at time k, in terms of the percentage of stem travel length, and y_k is the predicted position of the valve. This model has been used for stiction quantification using Hammerstein identification algorithm because of its relative simplicity [45], although its accuracy has always been subject to discussion.

Among existing models with more parameters, two-parameter models seem to be the optimum since they show acceptable accuracy using fewer number of parameters. The most frequently used models in this category are proposed by Choudhury et al. [7], Kano et al. [24] and He et al. [17]. The first two models use parameters S (stick-band) and J (slip-jump), and He's model uses parameters f_s and f_d with the following formulation:

$$f_s = \frac{S+J}{2}, \qquad f_d = \frac{S-J}{2} \tag{1.2}$$

It is noteworthy that all the stiction parameters and inputs to these models should have the same units, e.g., percent of stem travel length (% lift). The stiction parameters used in two-parameter models have been shown on the signature of a sticky valve in Figure 1.6.

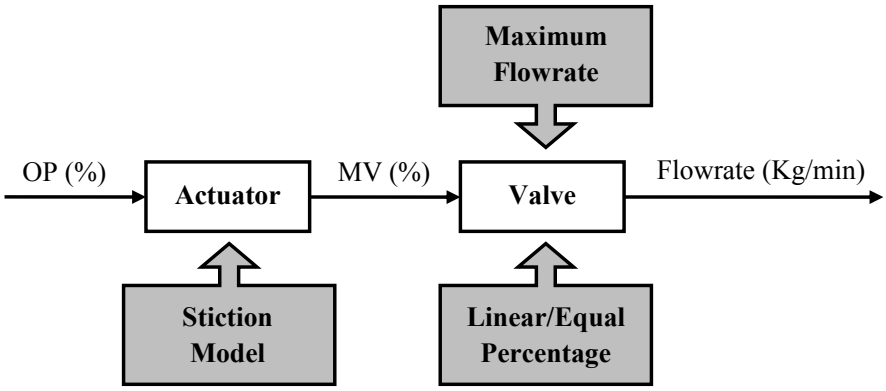

Figure 1.7: Required information to perform the comparison between stiction models and real laboratory data.

Comparison of Existing Stiction Models

Several comparisons have been carried out for existing models describing static friction in mechanical systems. A comparison between existing physics-based models is reported in [32]. Another similar comparative study between a first principle and the mentioned two-parameter models is presented in [23]. Probably, the work by [13] which engages both physics-based and data-driven models in some standard mechanical tests for control valves can be considered as the best amongst similar works. In the mentioned study, the authors have used both classes of the models to simulate response of a control valve to several routine valve tests.

In the current work, one and two-parameter data-driven models are compared to real laboratory data from a controlled pilot-scale process with sticky valves. According to Figure 1.7, to perform such an experiment, one needs to know: (1) the stiction severity (stiction parameters), (2) the manufacturing features of the valve and (3) the maximum flowrate of the fluid through the valve.

The experiment is done on a simple feed-back control system, which controls the level of water in a tank by manipulating the inlet water flowrate. The values of stiction parameters were estimated as $S = 5$ and $J = 1.4$ (the detailed procedure for stiction quantification will be explained in Section 3.4.2). Figure 1.8 illustrates the results of the experiment. Values of the Mean Square Error (MSE) for the predictions of different models are reported in Table 1.1.

According to the results, Choudhury's model appears to predict the behavior of the control valve more precisely than others. Only He's model is successful at capturing the stepwise movement of the stem in transition phases. As expected, the one-parameter model (Stenman's) ranks last based on the accuracy of the prediction.

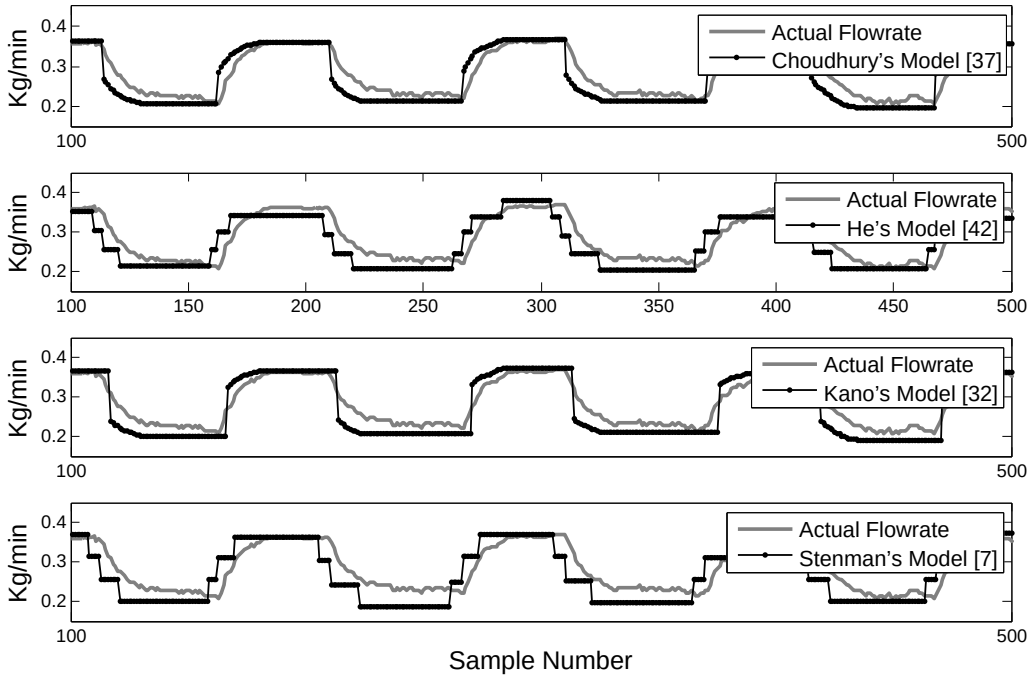

Figure 1.8: Predictions of data-driven models versus the actual laboratory data.

Table 1.1: Mean square error (MSE) for predictions of different models.

Model	Choudhry's	He's	Kano's	Stenman's
MSE	0.4705	0.5602	0.7591	0.8930

Modeling the stiction nonlinearity is the first step towards finding a solution for this common problem. The next step will be oscillation detection, regardless of any possible root cause. Some algorithms for detecting oscillations using routine plant data are presented in [23]. When the presence of oscillation in a system is confirmed, stiction detection procedures will be used to determine the source of such fluctuations. Stiction may not be identified as the only reason for poor performance of the control system. Therefore, other possibilities have to be considered in this step. In the next section, some common algorithms for detecting stiction will be reviewed.

1.2.2 Stiction Detection in Control Loops

Detection of stiction in control systems has been the subject of interest, as there exist numerous methods and algorithms proposed for this purpose in the literature. This fact also confirms that stiction is one of the most commonly observed problems in industrial control loops. Detection algorithms are so numerous that, in some cases, the users may get confused. These methods make either a qualitative or a quantitative statement about the presence of stiction in the control system. Accord-

ing to [20], the existing methods can be divided into three groups based on their approaches to solving the problem: (1) time domain shape analysis, (2) nonlinearity analysis and (3) fault detection and identification. The third group, also known as stiction quantification methods, will be discussed in Section 1.2.3.

Besides the difference in the approach, the inputs to algorithms may be completely different. A detection method is considered effective only when its final decision is relatively reliable, while using available routine information of the control system. Among all methods, there are some which use controller output signal (OP) and valve stem position (MV) in order to detect the problem. The main disadvantage of these methods is unavailability of MV in many industrial plants. Measuring the actual position of the control valve stem is not always possible. Usually, process output (PV) and OP are considered as routine operating data from an industrial plant. The methods which use this pair of data sets are more acceptable among users.

In the following, some of the common algorithms for stiction detection will be discussed briefly.

Cross Correlation Method

Introduced by [18], this method uses OP and PV to predict the presence of stiction in a system with none-integrating process and proportional-integral (PI) controller. This algorithm is based on cross correlation function (CCF) of the controller output and process output signals. The key idea is: "*If the CCF between controller output and process output is an odd function, the likely cause of the oscillation is stiction. If the cross-correlation function is even, then the likely cause is an external oscillation or too tight controller tuning*" [18]. The reason for this statement is that for a system which satisfies the assumptions for the process and the controller, for low-frequency oscillations, the phase difference between two signals will be a multiple of $\frac{-3\pi}{2}$, which makes the CCF an odd function (symmetric with respect to the origin of the coordinate system). The fact is that in contrast to stiction, tight controller tunings may lead to high-frequency oscillations in the system. If the calculated CCF is close enough to an odd function (considering a threshold), the algorithm will confirm the presence of a sticky valve.

Probability Distribution of the Control Error Signal

The key idea for this method is to detect sudden changes in the control error signal, using the probability distribution of the first derivative of error signal for self-regulating, and second derivative for integrating processes [21]. The criterion for an integrating process is stated as: "*Consider the second (filtered) derivative of the*

loop output. Check whether the probability density function is rather Gaussian (neglecting the pulse train) or the one of a sinusoid with additional Gaussian noise. A better fit to the first distribution indicates stiction, a better fit for the second one non-stiction" [21]. Similarly, the procedure can be carried out for a self-regulating process using the second derivative of the control error signal.

Nonlinearity and Non-Guassianity Analysis For the Control Error Signal

An automatic stiction detection algorithm is proposed in [4], which aims at the detection of general nonlinearity in a control system, not specifically stiction. The author has defined two different indices for nonlinearity and non-guassianity of the control signal. If results of both tests are positive, then presence of nonlinearity in the control system is confirmed. The author claims that the source of the problem is the final control element (control valve) if: (1) the process is locally linear, (2) nonlinear disturbance does not enter the loop, and (3) the installed characteristic of the control valve is reasonably linear in the current operating region. This method uses routine operating data (SP, OP and PV) and is model-free.

Measuring the Valve Stoppage, Varying OP

A basic and simple fact is used by [24] to conclude the presence of stiction in a system. This fact is that in the presence of stiction, no change in the position of the sticky valve will be observed in response to changes in the control command. The algorithm considers two different thresholds for changes in OP and PV, labeled ϵ_x and ϵ_y respectively. The changes in OP and PV are calculated relative to the previous time step. A time step where $\Delta OP > \epsilon_x$ and $\Delta PV < \epsilon_y$ indicates stiction in the valve. Finally, the ratio of the time steps when stiction is concluded over the entire time interval, indicates an index to judge the presence of stiction.

Fitting A Parallelogram to OP-PV Plot

Another method is proposed by [24] with a different approach. This method is based on the relationship between the input and output of a sticky valve. In the case of stiction, the OP-MV plot of the valve will take the shape of parallelogram, as seen in Figure 1.6 for the valve signature. PV can be substituted for MV when MV is not measurable. The main challenge for this method is automation of an algorithm to recognize a parallelogram from an ellipse, which is the general shape of the plot for linear oscillations. An algorithm is also proposed to carry out the shape fitting using routine operating data from industrial plants.

Qualitative Shape Analysis for the Valve Signature

This method is proposed by [53] and uses phase plot of PV versus OP for qualitative detection of stiction. First, some so called "primitives" are defined, which represent possible changes (and the directions) in the trajectory of OP-PV curve in the phase plane. Based on the sequence of the primitives which are fitted to the signature of the valve, an index can be defined to conclude the presence of stiction in the valve. This method is very similar to the previously described algorithm, since they both use the valve signature as input to the algorithms and their results are qualitative.

Area Calculation for Control Error Signal

The authors of [40] have proposed a detection method for self-regulating processes based on the calculation of the encircled area by oscillations of the control error signal. They claim: "*aggressive control usually results in a sinusoidal control error signal, while for a sticking valve, the signal typically follows exponential decay and rise. The reason for this behavior is that while the plant input is continuous for aggressive control (except when the controller output is saturated), valve stiction results in a discontinuous plant input that closely resembles a rectangular pulse signal*" [40]. The detection algorithm, first recognizes two consecutive zero-crossings, then finds the maximum (or minimum) of the signal between these two points. The vertical line passing through the maximum point divides the oscillation half-cycle into two sub-areas (A_1 and A_2). Equality of A_1 and A_2 concludes linearity of the oscillation, while the values for the ratio $\frac{A_1}{A_2}$ which are far from 1 indicate the existence of stiction.

Surrogate Analysis

This analysis can be described as a tool to judge linearity (or nonlinearity) of a time series [48]. The key idea is evaluating the predictability of a signal by changing it to a new form called "surrogate". Surrogate data can be produced from a time series, having the same power spectrum with the phase coupling removed by randomizing of phases. A time series with phase coupling is more structured and more predictable than its surrogate [47]. Therefore, the prediction error for the nonlinear time series is smaller than that of its surrogate. This method suggests that the time series is nonlinear, if the prediction error of original time series is less than that of the surrogate by more than three standard deviations. The details of this algorithm and the challenges this method faces will be discussed in Section 2.3.5. In the case of a nonlinear signal, stiction can be the possible source of oscillation.

Comparison of Signals versus Pre-defined Shapes

Oscillations induced by stiction in a control system usually have cycles with known shapes. This fact motivated authors of [38] and [44] to develop algorithms which are capable of recognizing oscillation patterns of a system and compare it with common pre-defined shapes. For this purpose, [44] suggests the comparison of PV with a sequence of square-shaped and triangular (sharp and smooth) pulses, which have been commonly seen in plants with stiction problem. The authors also suggest carrying out this procedure for each cycle separately. To make the algorithm more general, [38] chooses the step-response of a first order plus dead-time (FOPDT) process as the pre-defined pattern. In this case, by changing the values of the process gain (K), time constant (τ) and dead-time (θ) a wide variety of shape patterns can be created. The results of the mentioned methods are qualitative and they assume the only source of nonlinearity is stiction.

Comparisons carried out between all mentioned methods by [20] and [23] show that all of them do not predict the presence of stiction in control valves correctly. In some cases, there are grey areas where the methods are unable to decide whether or not stiction exists in the valve. This may be due to restrictive assumptions made in the derivation step of different methods, which may not be satisfied in practice. One of these assumptions, which is almost common in all of the methods, is that the oscillating loop is considered isolated from other loops; while the fact is that there is no isolated single-loop control system in practice. There are always interactions between neighboring loops in an industrial plant. In such cases, diagnosis and control of the source of oscillation requires more time and effort. The problem will be more complex when there are multiple faults in the system, e.g., several sticky control valves. Hence, a methodology is required to enable the detection of stiction in several interacting loops simultaneously by the user.

In the next section, the third group of detection methods based on classification of [20] (fault detection and identification methods) will be discussed.

1.2.3 Stiction Quantification

It is clear that in order to control the unsuitable influence of stiction on performance of the control system, this fault has to be quantified. Some of the explained methods explained in Section 1.2.2 provide indices which enable comparison and/or ranking of several different sticky valves in terms of severity of the problem. The fact is that the term "quantification" refers to methods which have aimed at assigning numerical values to the parameters used in stiction models, e.g., f_s and f_d for He's model. Some of the existing models for stiction were discussed in Section 1.2.1. These algorithms are considered as simultaneous detection and quantification meth-

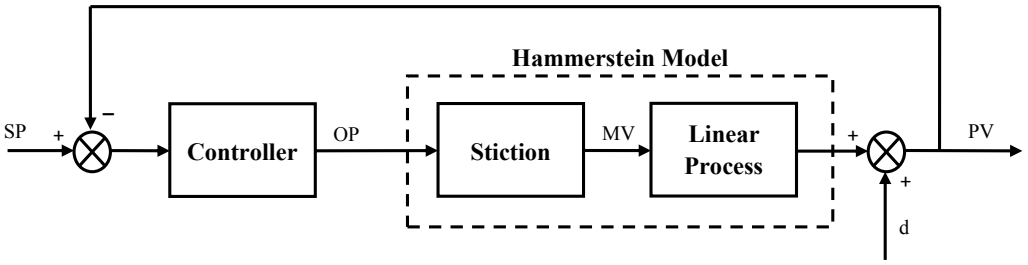

Figure 1.9: Block diagram of a closed-loop Hammerstein nonlinear process.

ods, because estimation of negligible values for stiction parameters is equivalent to absence of nonlinearity in the valve. They also allow data reproduction, comparison of sticky valves and taking future control actions. Some of the most commonly used approaches for this purpose will be explained in the following paragraphs.

Doubtlessly, the idea of separating nonlinear and linear dynamics of the process is the mostly used approach for the purpose of stiction quantification. Given a fairly accurate model for stiction, even only in the neighborhood of the operating region, Hammerstein and Wiener nonlinear process identification algorithms are useful. Hammerstein modeling has been used in many methods as the main framework for quantification [54, 51, 28, 45, 26]. Figure 1.9 shows the schematic of closed-loop Hammerstein process, where identification of the best linear model for the process is subject of interest. The authors of [45] used stenamn's one-parameter stiction model to produce the response of the stiction block. Lee et. al. [28] used He's two-parameter model and considered the first and second order ARX models for the linear dynamic. In [54], Choudhury's model has been used and the optimization problem is solved using Neural Network approach. Finally, [26] has solved the quantification problem by considering an extended ARMAX structure for the linear part, i.e., adding a non-stationary disturbance term to the model. The authors use this additive term to detect the other possible root cause, including external disturbance.

Nonlinear Wiener identification is another popular approach to quantify stiction. The block diagram of the closed-loop process is shown in Figure 1.10. Generally, evaluation of a Wiener model for a nonlinear process is more challenging, as the process transfer function is assumed to be followed by a nonlinear function, which is unknown. Usually, some assumptions for the structure and order of this function are required. This framework is used in [35] and [50] as the basic approach.

In addition to the nonlinear system identification, there are a few methods which consider different alternatives. The stiction is quantified in [5] by fitting an ellipsoid to the OP-PV plot of the valve. The geometry of the fitted shape will provide

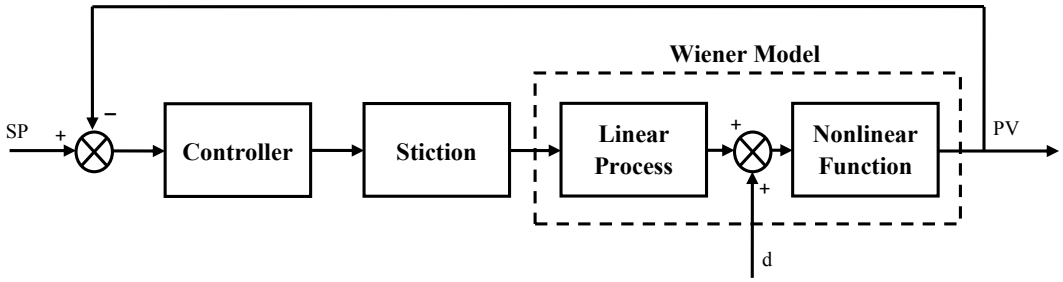

Figure 1.10: Block diagram of a closed-loop Wiener nonlinear process.

estimates for stiction parameters. Also, the authors of [3] have proposed a new methodology which estimates the valve position (MV) by considering it as an unknown input and employing a Kalman filter type unknown input estimator which uses a linear model of the process.

Once detection and quantification of the stiction in a valve is complete, a strategy is needed to compensate the effect of this nonlinearity on the performance of the system. As a matter of fact, all the mentioned steps are prerequisites for the final solution for the problem.

1.2.4 Compensation for Stiction

Certainly, scheduling the faulty valves to be repaired is the definite solution to stiction problem. But, since shutting down the process to isolate the faulty valve for maintenance purposes is not economical, this solution does not count as the primary option. A method to compensate the stiction phenomenon should be used, especially when maintenance is not available. In this section, some existing compensation algorithms will be reviewed. Unlike methods which are used for detection or quantification purposes, the methods to compensate stiction are few and limited.

Knocker or Dither

Presented by [15], this method can be considered as the first compensation method specifically targeting static friction in control valves. The idea is to add a predesigned signal to the controller output in order to prevent the fluctuations in the process output. A schematic of a control loop containing a compensator is shown in Figure 1.11.

The additive signal consists of a sequence of pulses with constant amplitude, width, and time between each two pulses in the direction of changes in the control output signal. Some suggestions for the geometry features of the knocker signal was proposed later in [42]. Figure 1.12 shows the control signal of a system which

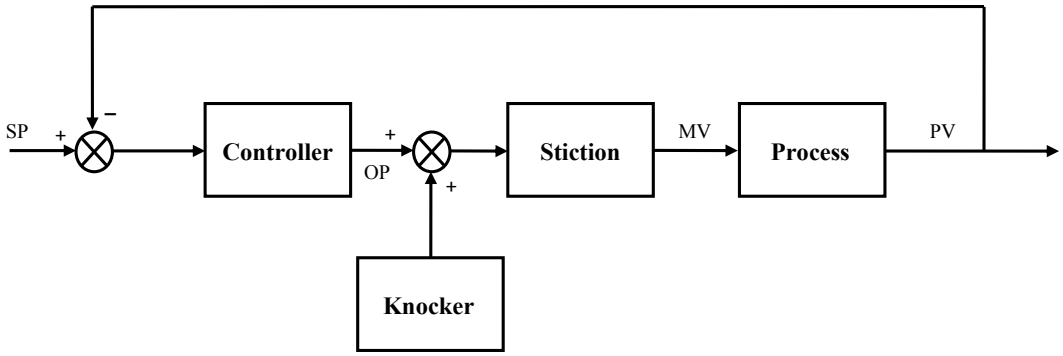

Figure 1.11: Block diagram of the control loop with a knocker.

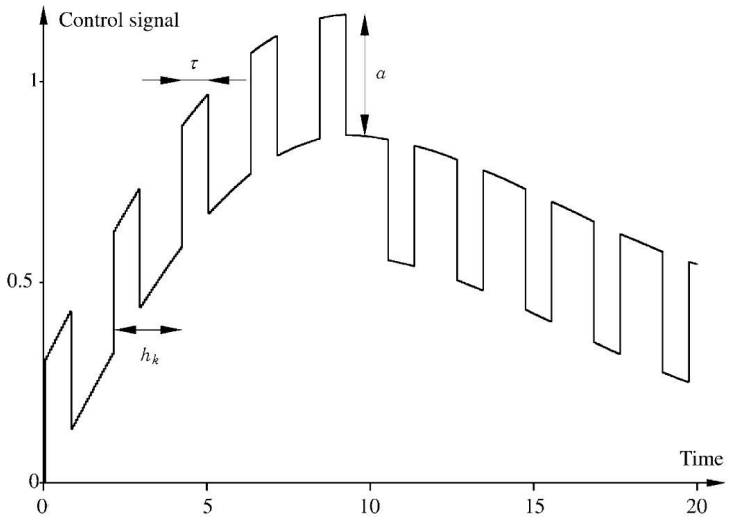

Figure 1.12: Control command after adding the knocker signal [15].

utilizes knocker to compensate the stiction.

This compensator can successfully remove stiction-induced oscillations from the process output. This achievement is gained by making the valve stem move faster and even wider than before, because the algorithm only increases the controller output in terms of magnitude for some sampling intervals. This extra movement of the valve will increase the rate of mechanical damage, considering the significant friction force which exists between the valve stem and the sealing packing. Regardless, the mentioned method can be considered as a short-term solution to the stiction problem.

Constant Reinforcement

This method was presented by [22]. The main idea is similar to that of the knocker, except that the additive signal is not of pulse form. The authors suggest that the

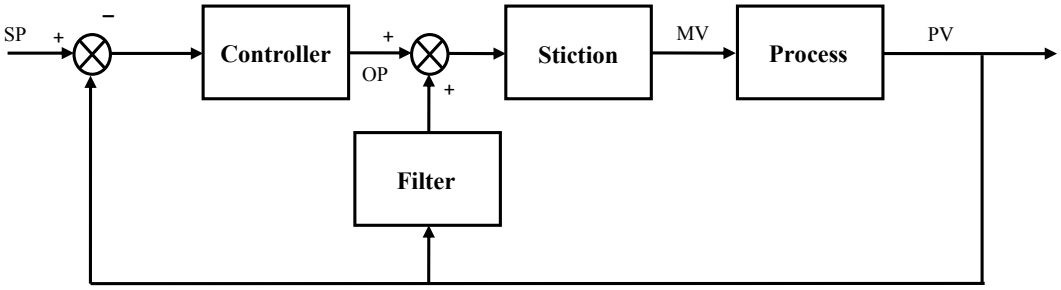

Figure 1.13: Block diagram of the control loop with the filtered feedback compensator.

compensating signal should have a constant value. This value can be calculated using Equation 1.3, in which only the value of a_{cr} is to be chosen.

$$\alpha_k = a_{cr} \times sign(\Delta u) \tag{1.3}$$

Similar to the previous method, this method also cannot decrease extra movements of the valve. As a matter of fact, this method is useful only for time intervals when the valve does not move in response to the controller output changes, and generally ignores extra movements.

Filtered Feedback Signal

The block diagram shown in Figure 1.13, illustrates the basic idea of the method introduced by [16]. Although the structure and order of the filter has not been elaborated by the authors, they claim this method can effectively reduce oscillations up to 75%.

Two-move Compensator

This approach, which was introduced in [43], is different from the other mentioned methods. Its main focus is on maintaining the valve at its steady state position. In order to achieve this goal, at least two moves in opposite direction are required for the valve stem, because even after setting the controller output (OP) at the steady state value, there is no guarantee that the valve is located at the desired position. The signals which produce such movements should have magnitudes large enough to overcome the friction force and make the stem move, but not too large to saturate the valve.

Although the idea is new and to some extent effective, there are still some limitations for this method. For instance, we know that the setpoint of the control loop may change during operation and information (correct value of OP) about the new steady states of the system with sticky valve may not be available. This method

does not consider these variations, and as a result it cannot be automated to track the setpoint. Another disadvantage is the use of Stenman's one-parameters stiction model, which decreases the accuracy of the method.

1.3 Thesis Organization and Contributions

The goal of this thesis is to address the problem caused by static friction in control valves, which directly affects the performance of the control system. Diverse aspects of this phenomenon have been studied in different chapters. In Chapter 2, a novel qualitative approach to detect the stiction problem in multi-loop control systems is proposed. The fact that there is no isolated single-loop system in practice has been ignored in the derivation of most of the existing detection algorithms. The proposed method uses routine operating data from a plant, and is capable of detecting multiple sticky valves in the entire system. This method is successfully validated using simulation and industrial data.

Chapter 3 focuses on frequency analysis of the stiction phenomenon. A mathematical condition for the occurrence of nonlinearity-induced oscillation in a multi-loop control system is derived in this chapter. It has been shown by simulation and experiment that satisfaction of this condition leads the system to continuous oscillation. Variations of the frequencies and magnitudes of the oscillations due to the changes in the process dynamics can be predicted by the proposed analysis. The derived condition only requires dynamics of the system, including the process and the controller, and the severity of the stiction, determined by the detection and quantification algorithms.

A new model-based compensation methodology is proposed Chapter 4. This method of oscillation removal is designed for systems where the stiction-induced oscillations are not removable by changing the tunings of the controllers only. Getting a non-oscillatory output without forcing the valve stem to move faster and wider than normal is the most important characteristic of this algorithm. By using a two-parameter stiction model, which predicts the behavior of a sticky valve more precisely, this method does not need extensive prior information about the process and the controller. This method can also be automated to track setpoint changes during the operation. The simulation results are reported and the ability of the method to handle uncertainties in the estimation of the process model and stiction severity is discussed.

In the last chapter, The condition derived in Chapter 3 is used as a tool to provide a stiction compensation scheme for single-loop, as well as multi-loop processes. The objective in Chapter 5 is to find the best tuning for the controllers with regards to the presence of stiction in the control valve, in order to eliminate

or reduce oscillations. Different combinations of the processes and controllers have been studied and suggestions to eliminate (if possible) the stiction-induced oscillations have been made. When the oscillation cannot be removed, the method will minimize the frequency and magnitude of oscillation. This compensation framework has also been validated using two different pilot-scale experiments on level and temperature-control systems with sticky valves and an industrial level-control system.

The contributions of this work can be summarized as follows:

- Existing data-driven stiction models will be compared with real pilot-scale data. The most commonly used data-driven models, including one and two-parameter models, will be studied in this work and the accuracy of their predictions will be discussed.

- A qualitative method for stiction detection in multi-loop control systems will be introduced. This new method will use shape fitting and surrogate analysis and will be able to detect multiple sticky valves in a system.

- A general condition for occurrence of nonlinearity-induced oscillations in multi-loop systems will be derived and validated through experimental study. This analysis will enable the prediction of variations in frequencies and magnitudes of oscillations due to changes in the system dynamics.

- A model-based compensation methodology will be introduced for stiction-induced oscillation removal from systems in which the effects of this nonlinearity cannot be eliminated by only changing the controller tuning. The accuracy of this method with regards to uncertainties in stiction and/or process modeling are investigated by simulation studies.

- A framework to compensate stiction in single- and multi-loop control systems is elaborated, which will be based on changing the controller tunings only. The proposed method will use the condition explained above, and will give qualitative suggestions to remove or reduce stiction-induced oscillations in a system.

Chapter 2

Detection of Stiction in Multi-Loop Control Systems

2.1 Limit Cycles in Nonlinear Systems and Describing Function

Almost all processes exhibit certain nonlinearities. Unlike linear processes, the behavior of nonlinear ones cannot be simply expressed as complex or real exponential functions. This fact makes the control-related analyses more complicated. One of the common problems with nonlinearity in practice is the dependence of their responses to the initial condition or input properties. In some cases, this dependance leads to a continuing oscillation in the system. The features of these oscillations, also called limit cycles, depend on the dynamics of the system and the initial condition of the input [14].

Linearization is a known approach to ease the study of nonlinear systems. This method is valid for a limited range of operating conditions. In addition to linearization, there exists another approach in which the properties of the linearized systems are maintained, while the result is dependent on certain features of the input to the system. This method of approximation is called quasi-linearization, which leads to the definition of "describing function". The describing function (DF) is defined to explain the relation between the response of the nonlinear system and its dynamics (e.g., parameters S and J for stiction) or the properties of the input.

In an oscillating system, two characteristics of the signals should be studied: frequency and magnitude. Therefore, frequency analysis, which is defined for linear systems, is useful in studying and predicting the frequency response (FR) of systems. Similarly, for a nonlinear system, DF analysis may be used. The value of DF is a complex number and represents a pair of frequency and magnitude. In spite of the similarity between DF and FR in terms of the values, there are differences between them. The FR of a linear system is only a function of the frequency of the harmonic

input to the system, while DF may be a function of some other properties as well as the frequency. In some cases, DF can even be defined independent of the frequency. The DF for stiction nonlinearity is proposed by [7] with the following formulae.

$$
\begin{aligned}
N_{(A)} &= -\frac{1}{\pi A}(P_{real} - jP_{im}) \\
P_{real} &= \frac{A}{2}\sin 2\varphi - 2A\sin\varphi + 2(S-J)\cos\varphi \\
P_{im} &= -\frac{3A}{2} + \frac{A}{2}\cos 2\varphi + 2A\sin\varphi - 2(S-J)\sin\varphi \\
\varphi &= \sin^{-1}(\frac{A-S}{A})
\end{aligned}
$$

where A is the magnitude of the harmonic input, S and J are stiction parameters used in Choudhury's two-parameter model. The value of the proposed DF depends on magnitude of the harmonic input only and not on its frequency. This will simplify the future analyses.

Due to the approximate nature of the DF technique, there will be some inaccuracies such as: (1) the amplitude and frequency of the predicted limit cycle are not accurate, (2) a predicted limit cycle may not actually exist, (c) an existing limit cycle may not be properly predicted [41]. The reason for these possible discrepancies between the predictions and observations are the assumptions usually made during the derivation of DF. One of these assumptions is considering the harmonic input in the nonlinear system purely sinusoidal. As mentioned in Section 1.2.2, the oscillations induced by stiction nonlinearity are not necessarily sinusoidal.

This chapter has focused on the detection of stiction in multi-loop control systems as a probable cause for oscillations.

2.2 Plant-wide Oscillation

When a control loop is oscillating due to any possible cause, the oscillation will be propagated to its neighboring loops because of the interactions between the loops. In such situations, identifying the source of the problem will be difficult, since many loops appear to be oscillating. However, when the source of the oscillations is nonlinear by nature, secondary oscillations have a lower nonlinearity due to filtering effects of the processes through which the oscillation has passed. Such linear dynamics may alter the phase coherence of the signals and change them to ones with smoother time trends and less harmonics [48].

There are numerous methods to detect the root cause of plant-wide oscillations. these causes can originate from linear sources (external disturbances, poor tuning of the controller, etc.) or nonlinear sources (valve problems, sensor failures, etc.). The

methods to detect nonlinear sources have been classified by [49] as: (1) nonlinear time series analysis, (2) limit cycle methods, (3) valve diagnosis methods. Some of these methods which specifically focus on the detection of stiction as the main cause for the oscillations were briefly introduced in Section 1.2.2. In this chapter, one of the nonlinearity detection method, named "surrogate testing", will be used to identify the nonlinear elements of the system.

2.3 Proposed Method

As mentioned in the previous chapter, most of the stiction detection methods are specifically designed for single-loop control systems. In the case of plant-wide oscillations, use of such methods is extremely limited. Methods which rely on the study of the shapes of harmonic signals can be considered as the easiest and a first stiction detection approach. Different types of monitoring softwares, used in almost all process plants, enable visual detection of oscillations in a time series. But, it is not easy to be certain wether or not the cause of oscillations is stiction, especially for multi-loop processes with multiple controllers.

In this work, a novel method for detection of stiction will be proposed, which uses only OP and PV time series, and is designed for multi-loop control systems. In the development of this detection algorithm, both qualitative shape-based approach and surrogate nonlinearity analysis will be used. Before elaborating the proposed algorithm, the system which will be studied is introduced and two sections for shape and phase analyses of the stiction-induced oscillations in multi-loop systems will be presented.

2.3.1 Multi-loop Control System Under Study

The standard multivariate process, which will be studied, can be presented by Equation 2.1.

$$Y_{(s)} = \begin{bmatrix} Y_1 \\ \vdots \\ Y_n \end{bmatrix} = \begin{bmatrix} g_{11} & \cdots & g_{1n} \\ \vdots & \ddots & \vdots \\ g_{n1} & \cdots & g_{nn} \end{bmatrix} \begin{bmatrix} U_1 \\ \vdots \\ U_n \end{bmatrix} = G_{(s)}U_{(s)} \tag{2.1}$$

In such systems, each output is formed by the summation of n different values, each representing the dynamics from one of the n inputs. This fact causes the resulting signals to have more complicated shapes than triangular or square oscillations, as studied in the existing methods for single-loop systems. In other words, n different oscillating signals with different harmonic shapes and phases are contributing to each of the outputs of the process. For instance, Equation 2.2 shows the ith output of this process.

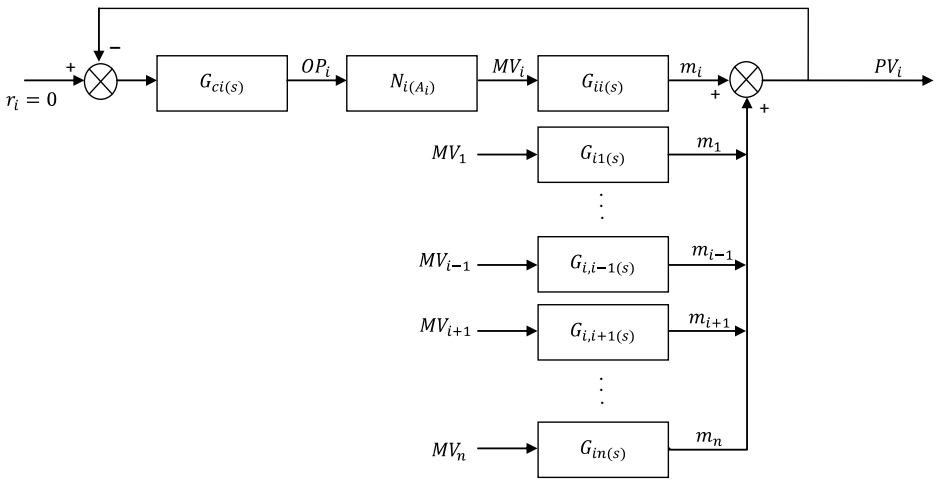

Figure 2.1: Standard block diagram of one of the loops in a multi-loop control system with stiction.

$$Y_{i(s)} = \sum_{j=1}^{n} g_{ij(s)} U_{j(s)} \qquad 1 \leq i, j \leq n \tag{2.2}$$

Figure 2.1 illustrates how each output signal is made by n values, called m_i $(i = 1, ..., n)$. One of the strategies to control such processes is to pair each output with one of the inputs which has the most contributing value to this output and use a controller to regulate each input-output combination. Some guidelines to find the best pairing and tuning for the controllers exist in the literature, for instance [31]. This work specifically studies this type of control systems.

2.3.2 Assumptions of the Method

For multi-loop systems which are intended to be diagnosed by this method, it is assumed that:

1. Oscillation is already detected in the system.
2. Processes are stable and have low-pass filtering action, i.e. the magnitude of the frequency responses are finite for small values of frequency ($\omega \to 0$) and decreasing for large values ($\omega \to \infty$).
3. All controllers are proportional-integral (PI).

2.3.3 Shape Analysis

There is a fact about the behavior of a sticky valve with regards to the harmonic inputs in this nonlinear medium. Regardless of what kind of oscillating signal (sinusoidal, triangular, square, etc.) leaves the controller and enters the sticky valve,

output of the sticky valve changes as a square shape. In other words, the position of the valve (MV) changes discretely and step-wise in both directions. This can be interpreted as a sharpening effect of the stiction element on the shape of the control signal (OP). All other elements of the system (process, controller and sensor) smoothen the shape of the signals due to low-pass filtering actions. This fact helps us predict the shapes of PVs and OPs in a system.

Observed Shapes of Stiction-induced Harmonics in Single-loop Systems

Because of the sharpening effect of stiction on the control signal, the step-response of a single-loop process will play the biggest role in specifying the shape of the oscillations. Oscillating signals commonly observed in cases where stiction exists in control valves are square-shaped (a sequence of steps) for fast self-regulating processes, smooth triangle-shaped for slow self-regulating processes, and sharp triangular (can be stated in terms of a ramp signal) for processes with a dominant integral action. This observation can also be mathematically investigated. Consider a case in which we have an integrating process (e.g., a level-control loop) and because of a sticky valve, the process input is a harmonic signal with a square-shaped oscillation. This signal can be represented by a sequence of step changes. Therefore, the output of the process can be calculated by Equation 2.3.

$$Y_{(s)} = G_{(s)}U_{(s)} = \frac{K}{s} \times \frac{1}{s} = \frac{K}{s^2} \tag{2.3}$$

Taking a inverse Laplace transform from the result will yield the following:

$$y_{(t)} = Kt \tag{2.4}$$

which is known as a ramp. A sequence of increasing and decreasing ramps forms a sharp triangular signal. Hence, an integrating process which is being manipulated by a sticky valve will show a sharp triangular oscillation in its output. Using a similar approach to analyze other feasible dynamics, Table 2.1 can be developed.

Similar to the above approach, it is possible to find the shapes of OP signals. Table 2.2 shows the possible shapes of the harmonic signals for combinations of processes with different controllers with sticky control valves.

A simpler version of Table 2.2 exists in [44], which has been reported as a summary of experimental observations. It is noteworthy to mention that the provided tables are specifically developed for control systems with single feedback loops and do not apply to multi-loop systems.

Table 2.1: Observed shapes in the output of different dynamic processes considering different inputs.

Dynamic	Input Shape	Output Shape
Stiction	Square Smooth Triangle Sharp Triangle	Square
Integrating	Square Smooth Triangle Sharp Triangle	Sharp Triangle
Fast Self-Regulating	Square Smooth Triangle Sharp Triangle	Square (Smoother) Smooth Triangle Smooth Triangle
Slow Self-Regulating	Square Smooth Triangle Sharp Triangle	Sharp Triangle Smooth Triangle Sharp Triangle

Table 2.2: Possible shapes of PV and OP signals in single-loop systems with stiction.

Process	Controller	OP	PV
Integrating	P	Sharp Triangle	Sharp Triangle
Integrating	PI	Smooth Triangle (Parabolic)	Sharp Triangle
Fast Self-regulating	P	Smooth Square	Smooth Square
Fast Self-regulating	PI	Triangle	Smooth Square
Slow Self-regulating	P	Sharp Triangle	Sharp Triangle
Slow Self-regulating	PI	Smooth Triangle (Parabolic)	Sharp Triangle

Generalization to Multi-loop Cases

It is well known that in a multi-loop control system, in case of oscillation due to any root cause, the entire system will oscillate with the same frequency. In other words, signals m_i in Figure 2.1, are harmonics with equal frequency but different shapes and magnitudes. Before using the frequency domain analysis to investigate the changes in the shapes of the oscillations, it is worth to mention that m_i cannot be treated as sinusoidal harmonics, since each of them represents a group of sinusoidal oscillations with different frequencies. That is, using Fourier transform, the oscillating signals which may have square or triangular shapes, can decompose to their base oscillations with different frequencies.

Figure 2.2 shows bode plots (magnitude ratio) of a hypothetical self-regulating process with a PI controller. Consider ω_{pr} and ω_{co} as the cut-off frequencies of the process and the controller transfer functions, respectively.

First, the effect of PI controller on oscillating signals will be studied. If the loop

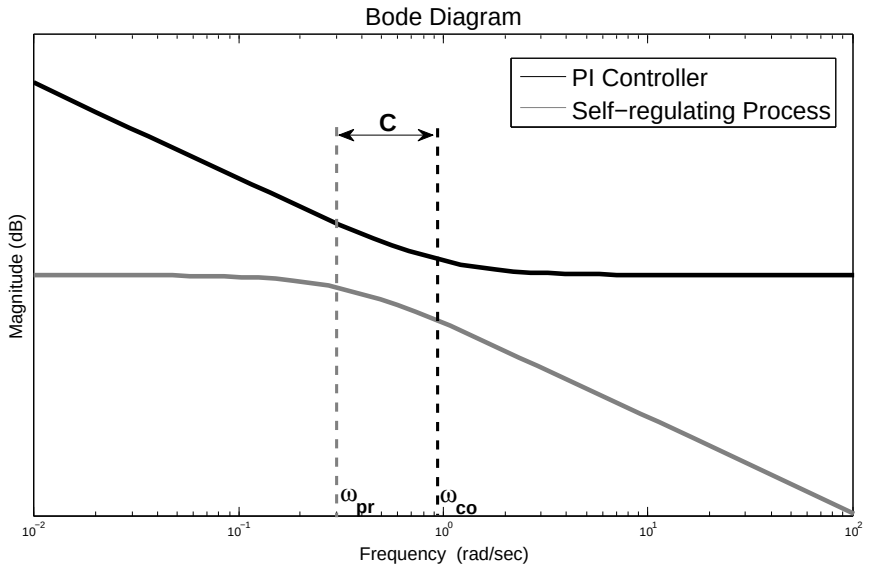

Figure 2.2: Examples for the magnitude of responses of PI controller and a low-pass process to different frequencies.

is not externally excited, control error is equal to $SP_i - PV_i$, where SP_i represents the constant setpoint of the ith loop. As shown in Figure 2.2, when an oscillating signal is passing through a PI controller, the magnitude of the components with lower frequencies is amplified, while compared to the first group, no change in that of high frequency components will be observed. In other words, the PI controller will smoothen the shape of the control error signal. Hence, the shape of OP will be similar to PV, with the exception that high-frequency oscillations are damped.

If the process acts as a low-pass filter (as assumed), the high frequency components of the inputs will be eliminated in practice. The parameter C in Figure 2.2 is a constant of which smaller values will lead to more accurate detection. As the width of the interval between ω_{pr} and ω_{co} decreases (smaller value of C), the controller filters out a wider band of high-frequency components. If there is no stiction in the valve, the control signal will directly enter the process and will be filtered. As a result, the signal m in loops without stiction can be considered to have a smoother (sinusoidal) shape.

The final value of the outputs are obtained from the summation of signals m_i. The shape of m_i can be considered as square or triangular in the case of stiction and sinusoidal otherwise. Thus, the phase differences between these contributing signals must be investigated, which the following section is dedicated to.

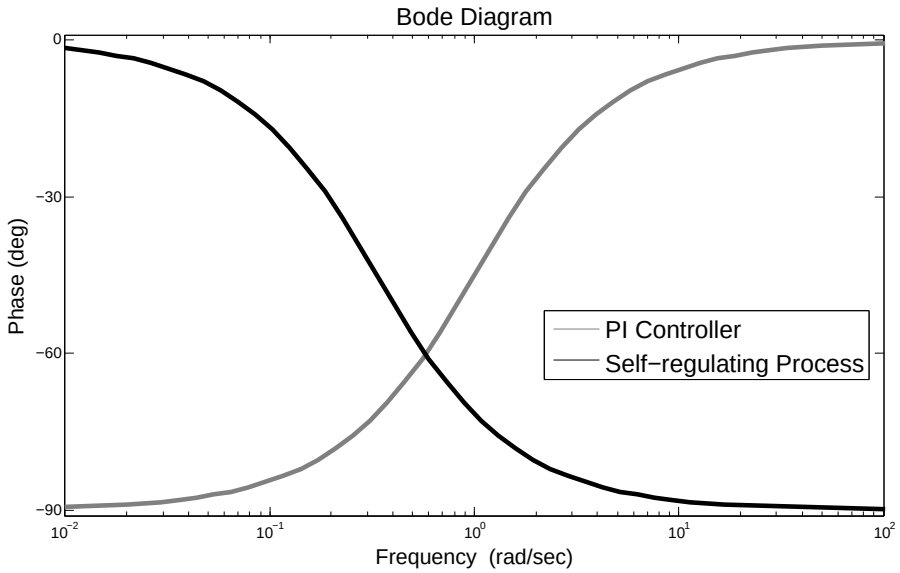

Figure 2.3: Example of phase shifts introduced in the responses of PI controller and a low-pass process for different frequencies.

2.3.4 Phase Analysis

The dynamics of the processes and the controllers shift the phases of the harmonic outputs from that of the inputs (see Figure 2.3). In addition to this, the stiction nonlinearity will also introduce phase delay in the system.

Using the describing function of stiction nonlinearity, explained in Section 2.1, the phase delay can be calculated between the OP and MV. Figure 2.4 illustrates the resulting phase delay by a sticky valve with stick-band parameter (S) equal to 6 and different values for the slip-jump parameter (J). The absolute value of the phase tends to go to zero as the magnitude of the input (A) increases.

Finally, since PV_i is the summation of n different signals, it is clear that the resulting appearance of the oscillations will not be of the known forms of square, triangle, etc. This is because shape and phase of all n signals are different. An example of the mentioned "unknown" pattern can be observed in Figure 2.5, which is plotted for a hypothetical double-loop system with one sticky valve.

2.3.5 Detection Algorithm

Based on what was concluded in previous discussions, an algorithm to detect stiction in a multi-loop system can now be introduced. The algorithm can be described in two main parts: (1) structure decomposition and (2) locating the sticky valves in the system. In the first part, the total number of sticky valves (k) in the entire system will be determined by decomposition of each PV to its n constructors. In the second

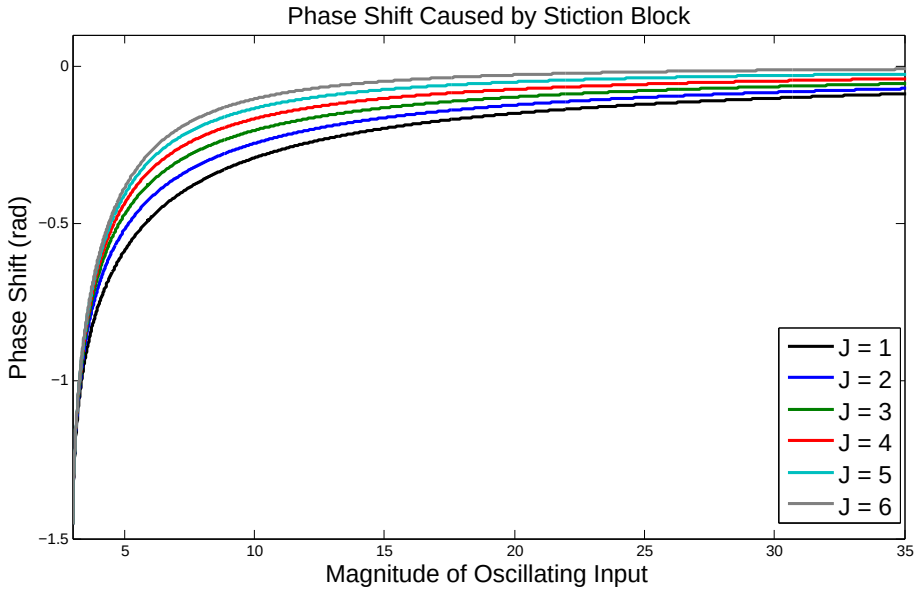

Figure 2.4: Phase shift caused by stiction for inputs with different magnitudes ($S = 6$).

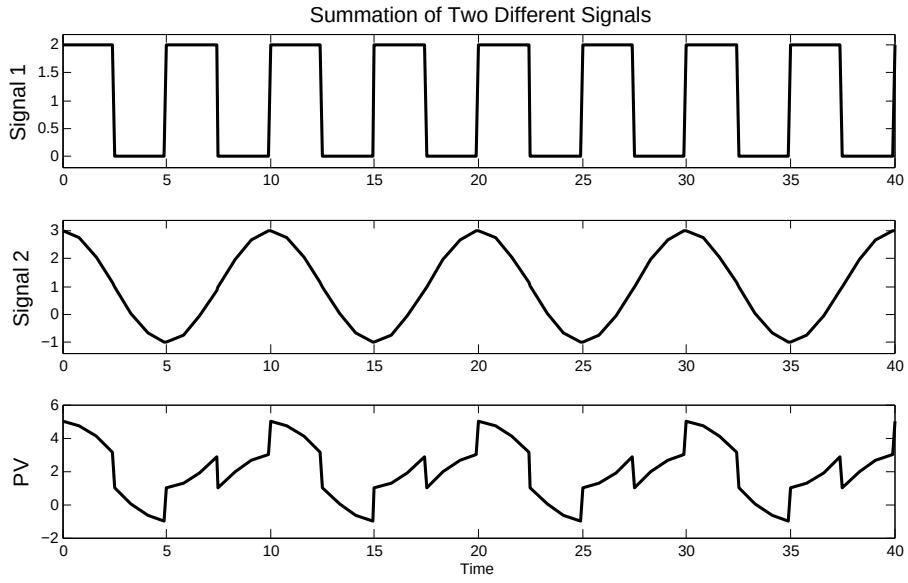

Figure 2.5: Summation of two signals with different shapes and phases to form one of the outputs in a double-loop system.

part, k_{opt} sticky valves will be identified and also ranked according to the nonlinearity index introduced by the surrogate method in [48]. Another technique which can be used for the second part of the algorithm is the Hammerstein nonlinear identification approach. This identification approach for the multi-loop processes may not be the first choice, since it is computationally more expensive than surrogate method.

There are three steps in the algorithm. First two steps are related to part one, and the third is for part two of the detection algorithm. It is noteworthy that the term "known" in the next few paragraphs refers to conventional structures of signals which have been seen before in single-loop cases and also exist in Table 2.1, while the term "unknown" points to the any possible structure resulting from the combination of all known shapes similar to what is introduced in Figure 2.5.

Step 1. Obtain n outputs (PV_i) and all related OPs.

Step 2. Produce a structure containing k known patterns (square and/or triangles) representing faulty loops and $n-k$ sinusoidal oscillations as contributing signals from healthy loops. All the produced signals have the same frequency, but different bias terms, magnitudes, and phases. For the next attempt, increase k in the range of $\{1, ..., n\}$ to reach the best fit for the produced structures to all PVs. After finding the best structure, k_{opt} is determined, i.e., we know k_{opt} out of a total of n valves have stiction problem.

Remark 1: As it can be observed from Figure 2.6, for each fitting process we need to estimate one geometric parameter for sinusoidal signals and two for triangular or square. Also we consider a time window with the length equivalent to the frequency of oscillations. By moving the time window across the oscillation patterns, the relative phases of signals can be determined in the fitting procedure. The bias terms are considered along with other parameters.

Remark 2: Choosing between square and triangle structures for the output of faulty loops is subject to some observations, i.e., the shape of the outputs can give ideas about the structure to be used. By using only one structure for all faulty signals, the fitting process will be simplified, but the quality will also be affected.

Remark 3: Fitting is only performed on one cycle for oscillations with regular shapes. In cases where there are cycles with dissimilar shapes, the procedure can be repeated for several cycles to confirm the results.

Step 3. In this step, all nonlinearities in the system (stiction problems) will be ranked in terms of severity, using surrogate testing method. After ranking, the first k_{opt} nonlinear elements of the entire system are assumed to be the

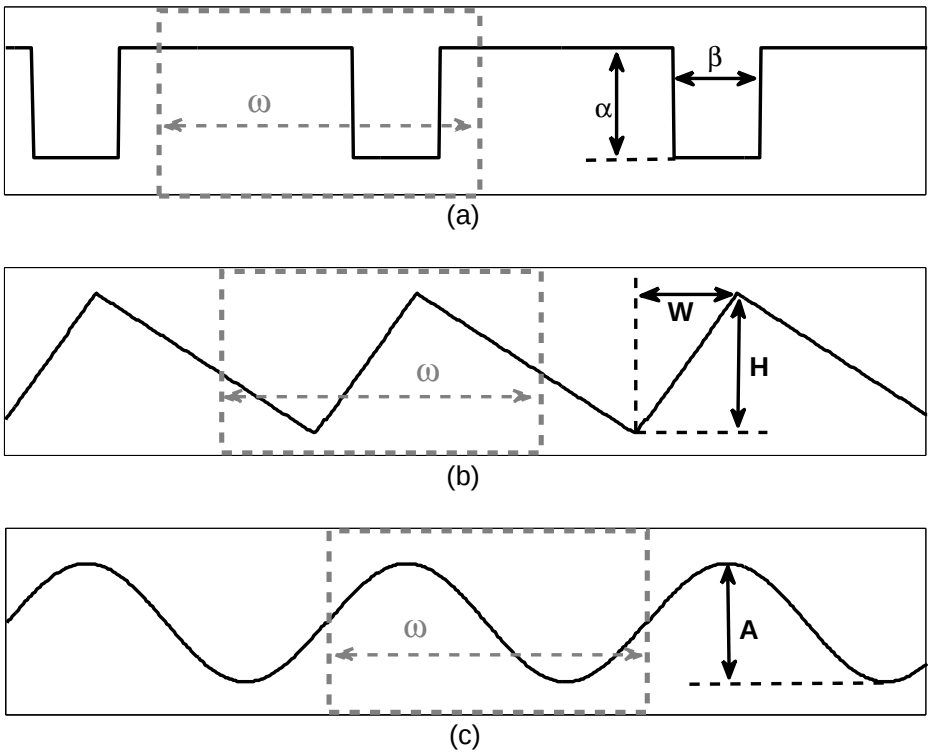

Figure 2.6: Geometry of different structures: (a) square, (b) triangular, (C) sinusoidal.

valves suffering from stiction. In order to create surrogates of OP and PV signals, first an embedded matrix Y_{emb} is produced using each time series.

$$Y_{emb} = \begin{bmatrix} y_{(1)} & y_{(2)} & \cdots & y_{(E)} \\ y_{(2)} & y_{(3)} & \cdots & y_{(E+1)} \\ \vdots & \vdots & & \vdots \\ y_{(l-E+1)} & y_{(l-E+2)} & \cdots & y_{(l)} \end{bmatrix} \tag{2.5}$$

where l is the length of the time series and E is the number of columns of Y_{emb}, representing the length of the time window to be predicted. It is worth mentioning that each time series should be processed before the construction of the the embedded matrix. Data are re-sampled to include S_n samples per cycle. The integer value of S_n should be chosen to be minimum, subject to maintaining all parts of the shape of the time trends. Each time series should also be end-matched, i.e., there are exact number of cycles in each row of Y_{emb}.

In the next step, for each row y_i of the embedded matrix, K nearest neighbors, having smallest value of $\|y_j - y_i\|$ must be found. It is suggested in [48] that the first neighbor y_j can be chosen which satisfies $|j - i| > \frac{E}{2}$. Then, the sum of squared prediction errors for H steps ahead should be calculated as shown in Equation 2.6.

$$\Gamma_{test} = \sum_{i=1}^{l-H} \left[y_{(i+H)} - \frac{1}{k} \sum_{j=1}^{K} y_{(j+H)} \right]^2 \tag{2.6}$$

The above mentioned steps should be carried out on the generated surrogates. To get better results, it is suggested to construct M surrogates for each time series and calculate $\bar{\Gamma}_{surr}$ by averaging the prediction errors. Assume F_i is the Fourier transform of signal F in the frequency channel i. To create the surrogate of the signal, a value ϕ_i is added to the phase of F_i.

$$F_i = |F_{(j\omega_i)}| e^{[j\angle F_{(j\omega_i)}]} \tag{2.7}$$

$$F_{surr,i} = |F_{(j\omega_i)}| e^{[j\angle F_{(j\omega_i)} + \phi_i]} \tag{2.8}$$

the selected phase ϕ_i in Equation 2.8 has uniform random distribution in the range $-\pi < \phi_i \leq \pi$. The new frequency channels above the Nyquist sampling frequency ($l/2+1$ for even, and $ceil(l/2)+1$ for odd value of l) will add phases with opposite signs. If l is even,

$\phi_1 = 0$, $\phi_{\frac{l}{2}+1} = 0$, and $\phi_{l-i+2} = -\phi_i$, for $i = 2, ..., \frac{l}{2}$,

and if l is odd,

$\phi_1 = 0$, and $\phi_{l-i+2} = -\phi_i$, for $i = 2, ..., ceil(\frac{l}{2})$.

By taking inverse of the Fourier transform from F_{surr}, we can create the surrogate in the time domain. The nonlinearity index is calculated in Equation 2.9, of which value more than one indicates that the test time series is nonlinear.

$$NI = \frac{\bar{\Gamma}_{surr} - \Gamma_{test}}{3\sigma_{\Gamma_{surr}}} \tag{2.9}$$

Remark 4: It has been stated in [48] that some small negative values are possible for NI, because of the stochastic nature of the test. But, results giving $NI < -1$ will not be observed because surrogates are always less predictable, i.e., $\bar{\Gamma}_{surr} > \Gamma_{test}$.

Remark 5: Although it has been suggested in [48] that the default number of samples per cycle can be chosen in the range of $7 \leq S_n \leq 25$, due to the complexity of the shape of the oscillations in multi-loop systems, it is more reasonable to pick values greater than 30. Other suggested defaults values for parameters used in surrogate method are acceptable ($S = E = H$, $K = 8$, $M = 50$, for a data set consisting of more than 12 cycles in the time domain).

2.4 Detection of Stiction in a Simulated System

The simulated multi-loop system, introduced by [31] for a pilot-scale binary distillation column used to separate ethanol and water, has the following dynamics.

$$\begin{bmatrix} Y_1 \\ Y_2 \\ Y_3 \end{bmatrix} = \begin{bmatrix} \frac{0.66e^{-2.6s}}{6.7s+1} & \frac{-0.61e^{-3.5s}}{8.64s+1} & \frac{-0.0049e^{-s}}{9.06s+1} \\ \frac{1.11e^{-6.5s}}{3.25s+1} & \frac{-2.36e^{-3s}}{5s+1} & \frac{-0.012e^{-1.2s}}{7.09s+1} \\ \frac{-33.68e^{-9.2s}}{8.15s+1} & \frac{46.2e^{-9.4s}}{10.9s+1} & \frac{0.87(11.61s+1)e^{-s}}{(3.89s+1)(18.8s+1)} \end{bmatrix} \begin{bmatrix} U_1 \\ U_2 \\ U_3 \end{bmatrix} \tag{2.10}$$

The controllers used to control this system are tuned according to Equations 2.11 to 2.13.

$$G_{c1(s)} = 0.65 + \frac{0.09}{s} \tag{2.11}$$

$$G_{c2(s)} = -0.157 + \frac{-0.031}{s} \tag{2.12}$$

$$G_{c3(s)} = 0.675 + \frac{0.61}{s} \tag{2.13}$$

The simulation of the oscillatory system is done using the stiction parameters shown in Table 2.3 for three sticky valves in the system. The stiction model used in this simulation is introduced by [17]. Also, three noise series with a mean value of zero and a variance of 0.01 were added to each loop. Three different scenarios were studied based on the existence of one, two, and three sticky valves. Figure 2.7 show the simulated outputs and the oscillations in each case.

Table 2.3: Stiction parameters for three faulty valves in the simulated system.

f_{s1}	f_{d1}	f_{s2}	f_{d2}	f_{s3}	f_{d3}
4.5	1.5	3.0	1.0	4.0	1.0

For the first step, PV signals have to be decomposed into three signals. Figure 2.8 shows the flowchart of the decomposition procedure. Mean square error (MSE) has been used to compare the accuracies of the different fittings and n is the total number of OPs contributing to each PV (for this simulated system, $n = 3$ for all PVs).

Both triangular- and square-shaped structures were used as representatives of faulty loops in this particular system. The results of the decomposition step determine the total number of sticky valves in the system. Tables 2.4 to 2.6 indicate the detailed information of these results. Note that scenarios A, B and C respectively, refer to situations in which we assume there is one, two, or three sticky valves in the system.

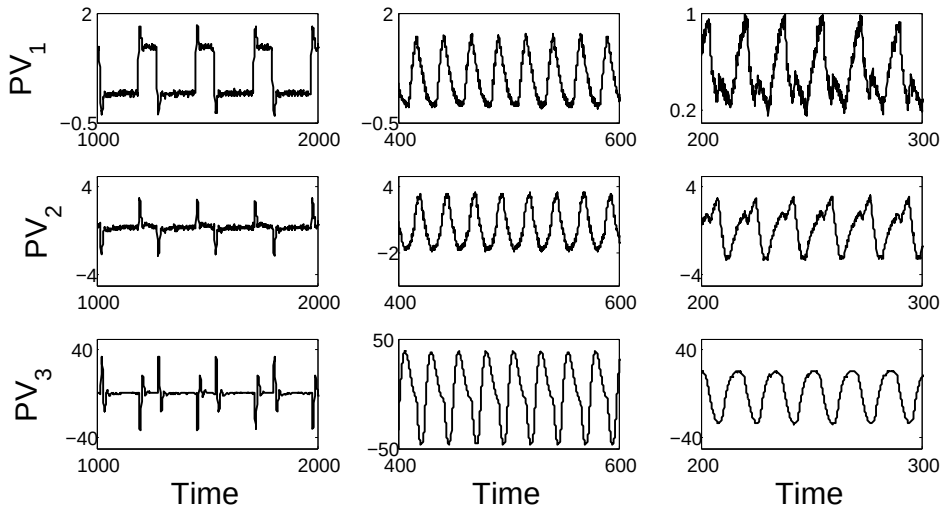

Figure 2.7: The outputs of a three-loop simulated system with one (left), two (middle), and three (right) sticky valves in the system.

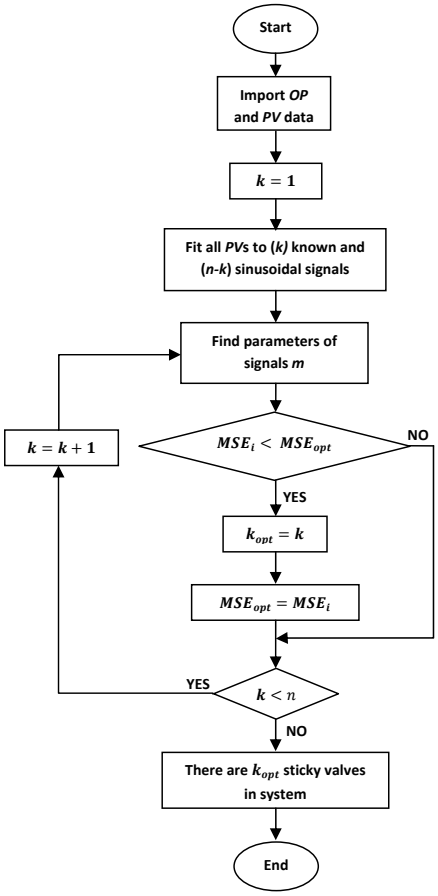

Figure 2.8: Algorithm of the first part of the proposed detection method; Finding the total number of sticky valves in the system.

Table 2.4: The results of the fitting procedure for PV signals when there is only one sticky valve present in the system.

Scenario	$MSE_{PV_1} \times 10^{-4}$	$MSE_{PV_2} \times 10^{-4}$	$MSE_{PV_3} \times 10^{-4}$
A	0.0002	0.0051	1.2981
B	0.0011	0.0037	1.1350
C	0.0014	0.0065	1.4887

Table 2.5: The results of the fitting procedure for PV signals when there are two sticky valves present in the system.

Scenario	$MSE_{PV_1} \times 10^{-5}$	$MSE_{PV_2} \times 10^{-5}$	$MSE_{PV_3} \times 10^{-5}$
A	0.0001	0.0006	1.4960
B	0.0001	0.0002	0.2450
C	0.0006	0.0003	0.8707

In all cases, the algorithm correctly determined the number of sticky valves in the system, as shown in Tables 2.4 to 2.6. The best structure for each output is reported in Table 2.7. Figure 2.9 shows the components of one of the outputs after implementation of the first part of the algorithm.

After the first step was carried out and the total number of faulty valves in each case was determined, the surrogate analysis was used to rank the nonlinearities of the system. Table 2.8 shows the results related to this step. Some values for the parameters used to calculate the nonlinearity indices are in accordance to what was suggested in Section 2.3.5.

The following remarks can be made:

1. All nonlinearity indices, even when only one sticky valve is present in the system, have values greater than one. This indicates existence of nonlinearity in the signals.

2. Ranking the nonlinear elements of the system based on the indices of PV signals can help locate sticky valves.

3. The indices of OP signals are usually within or close to the range $N < 1$.

2.5 Experimental Validation

The proposed detection methodology was implemented on the data obtained from an industrial case. The studied plant is a diluent recovery unit and has been addressed by [27, 29]. In this process, there are a total of 8 outputs which are controlled by 5 manipulated variables. Figure 2.10 illustrates the schematic of this process. Also,

Table 2.6: The results of the fitting procedure for PV signals when there are three sticky valves present in the system.

Scenario	$MSE_{PV_1} \times 10^{-4}$	$MSE_{PV_2} \times 10^{-4}$	$MSE_{PV_3} \times 10^{-4}$
A	0.0001	0.0007	1.9160
B	0.0005	0.0047	0.5854
C	0.0002	0.0006	0.5007

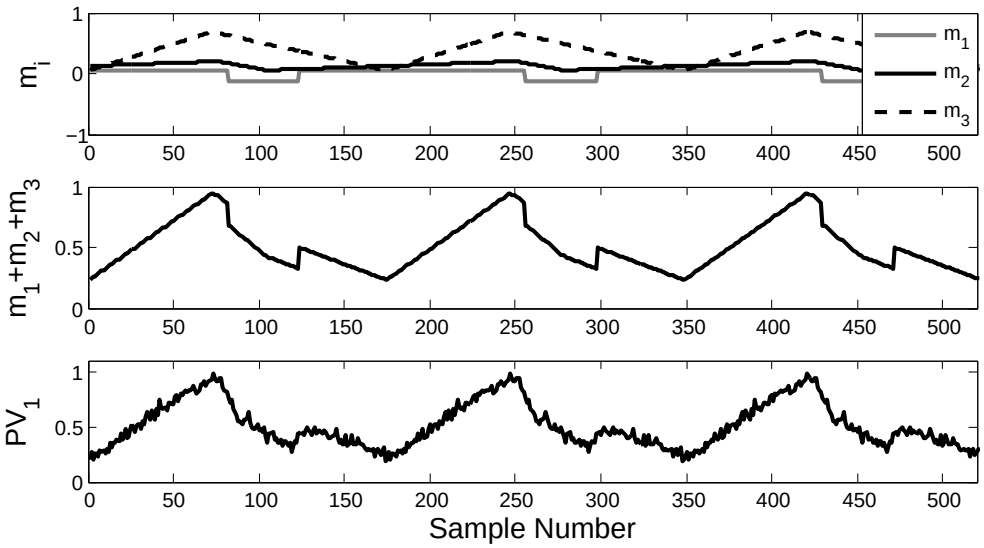

Figure 2.9: PV_1 and its components after the decomposition process.

the descriptions of all 13 monitored variables in the system are mentioned in Table 2.9. The gain matrix for this highly interacting multi-loop process is known and given in Equation 2.14.

$$\begin{bmatrix} PV_1 \\ PV_2 \\ PV_3 \\ PV_4 \\ PV_5 \\ PV_6 \\ PV_7 \\ PV_8 \end{bmatrix} = \begin{bmatrix} -0.57 & 0.23 & -0.102 & 0.436 & -0.159 \\ -1.13 & -1.56 & 0.39 & 0.2 & 0 \\ -1.46 & -1.42 & 0.66 & 0.28 & 2.92 \\ -16.3 & 0 & 0 & 2.79 & 0 \\ -0.55 & 0.49 & 0.181 & 0 & 0 \\ -4.16 & 0.49 & 0.181 & 0 & 0 \\ 0 & 0 & 0 & -2.38 & -2.37 \\ -0.595 & -1.15 & 0.125 & 0 & 0 \end{bmatrix} \begin{bmatrix} MV_1 \\ MV_2 \\ MV_3 \\ MV_4 \\ MV_5 \end{bmatrix} \tag{2.14}$$

The registered data by the monitoring system for a certain period of time is shown in Figure 2.11. It is clear that there are oscillations in the outputs of loops 3, 4 and 6. Therefore, in order to enhance the performance of the system, it should be tested for different possible causes of oscillation, i.e., external disturbances, aggressive tuning of the controllers, and stiction in control valves. The proposed methodology will be implemented on the oscillatory loops to find the possible sticky

Table 2.7: The best structures fitted to each signal in the simulated system.

Scenario	PV_1	PV_2	PV_3
A	tri*+ sin+ sin*	tri+ sin+ sin	tri+ sin+ sin
B	tri+ tri+ sin	tri+ squ*+ sin	tri+ tri+ sin
C	tri+ tri+ squ	tri+ tri+ squ	tri+ tri+ squ

**tri= triangular, sin= sinusoidal, squ= square.*

Table 2.8: The nonlinearity indices calculated for each signal for all simulated scenarios.

Scenario	OP_1	OP_2	OP_3	PV_1	PV_2	PV_3
A	1.4478	0.1150	1.4499	11.0361	7.2391	8.2083
B	1.013	-0.8190	-0.2103	12.3109	9.4891	7.4260
C	-0.2138	0.2513	0.9936	9.3172	6.3321	9.0021

valves in the plant.

The first part of the detection algorithm was carried out for two cycles of each oscillatory signal. As can be observed from Figure 2.12, both cycles of PV_4 were decomposed to two triangular-shaped components. This fact can be interpreted as existence of two sticky valves in the plant. On the other hand, according to Figure 2.13, PV_6 is formed by the summation of one triangular and two sinusoidal cycles, which indicates the presence of only one sticky valve. This controversy can be solved by implementing the fitting procedure on PV_3. The least value of fitting MSE for the combinations of one triangular plus four sinusoidal or two triangular plus three sinusoidal will indicate the final number of the sticky valves in the entire system.

According to Table 2.10, the first pattern (one triangular plus 4 sinusoidal) has the least value of MSE which indicates the best fit. The result of fitting this pattern to PV_3 is shown in Figure 2.14. This result confirms the existence of only one sticky valve in the system. To locate this faulty valve, the second part of the method will be implemented on all outputs.

In the second part of the detection task, nonlinearity indices of all PVs have been calculated based on the analysis used in [48]. According to the results reported in Table 2.11, the output of loop 4 shows the most nonlinearity relative to the others. Although this fact implies the presence of stiction in the control valve of loop 4, checking the valve in loop 1 as well, may help improve the performance of the system.

Another procedure for detection of stiction in this plant using the exact same data set has been done by [29], which confirms the correctness of this prediction. In the mentioned work, the authors have used the Hammerstein nonlinear identification technique for the purpose of detection and quantification of stiction in the system.

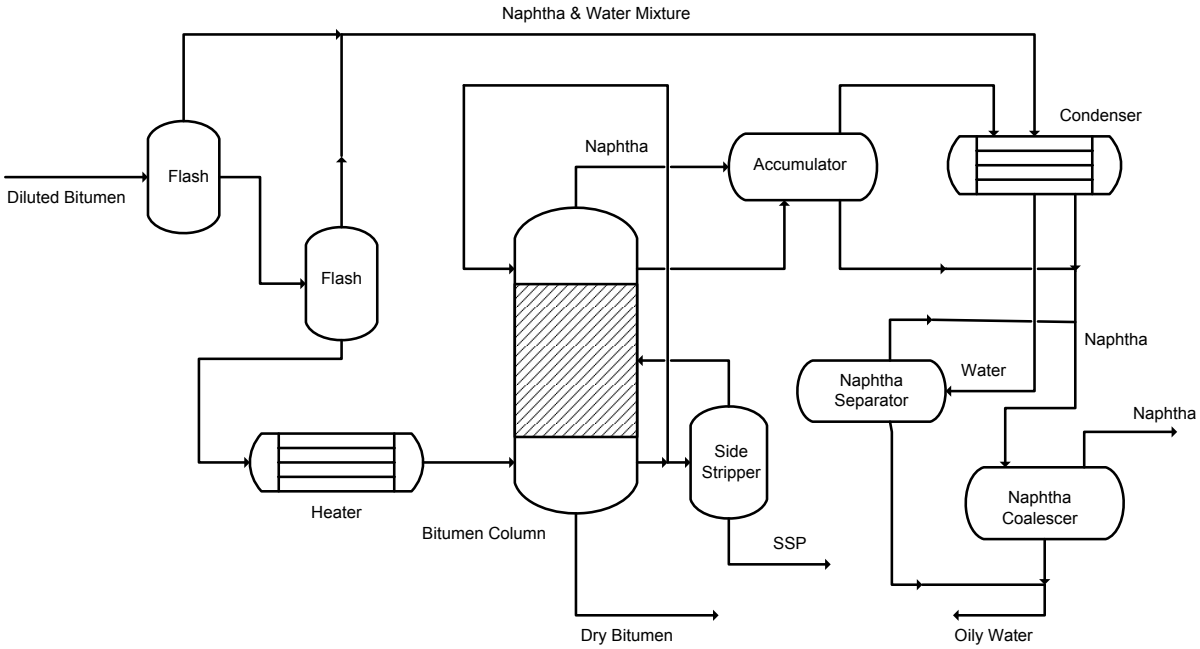

Figure 2.10: Schematic representation of the studied diluent recovery process.

2.6 Conclusion

In this chapter, a novel method for detecting stiction in multi-loop systems was introduced. This method mainly uses process output measurement (PV) and the controller output signal (OP) in order to predict the existence of stiction in control valves. First, an analysis was performed for possible signal shapes of a faulty multi-loop system. Then, the effects of the dynamics of the process, controller and stiction nonlinearity on the phases of the signals were discussed. Finally, a three-step algorithm for detection of stiction was proposed, which is able to handle multi-loop processes. The method was validated using simulation of a three-loop control system considering different number of sticky valves, in addition to a data set obtained from an industrial plant.

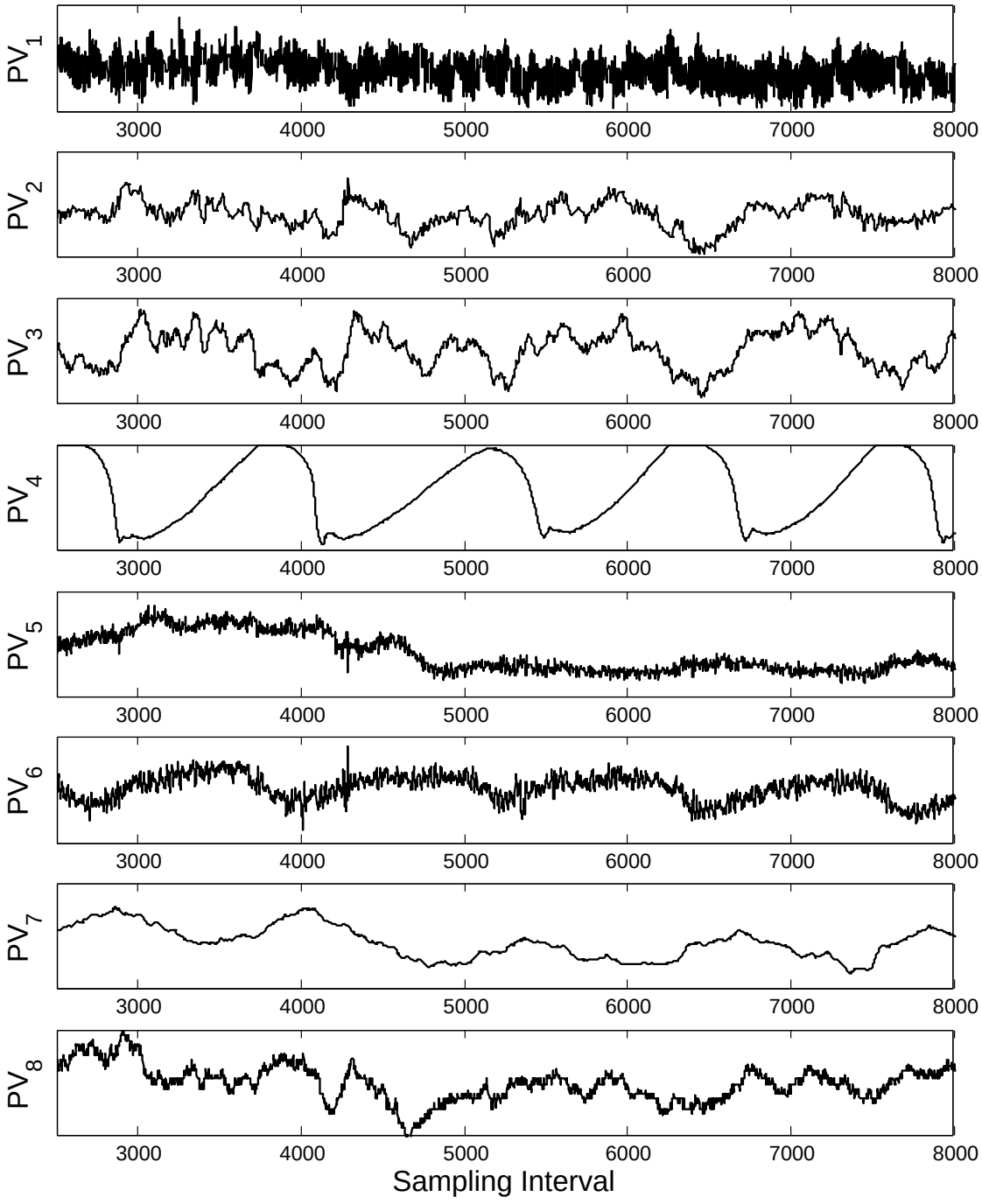

Figure 2.11: Time trends of the outputs of the diluent recovery plant.

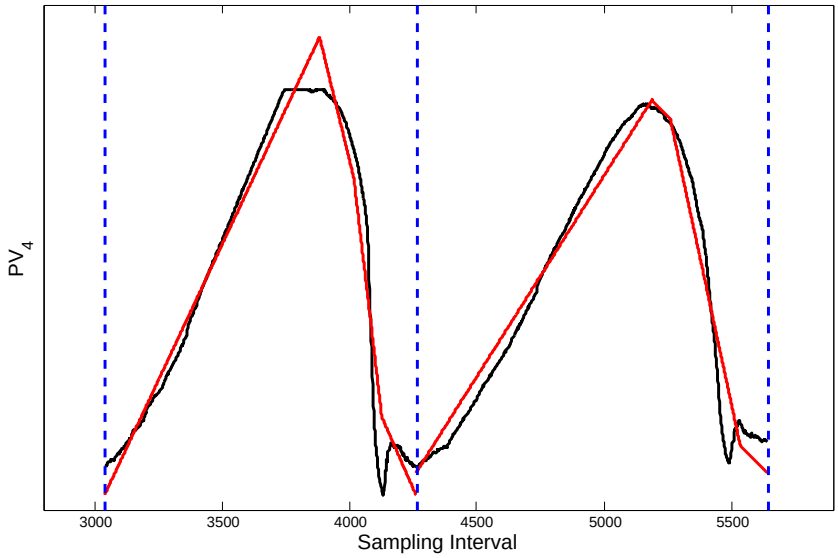

Figure 2.12: Two cycles of PV_4, fitted to the summation of two triangular patterns.

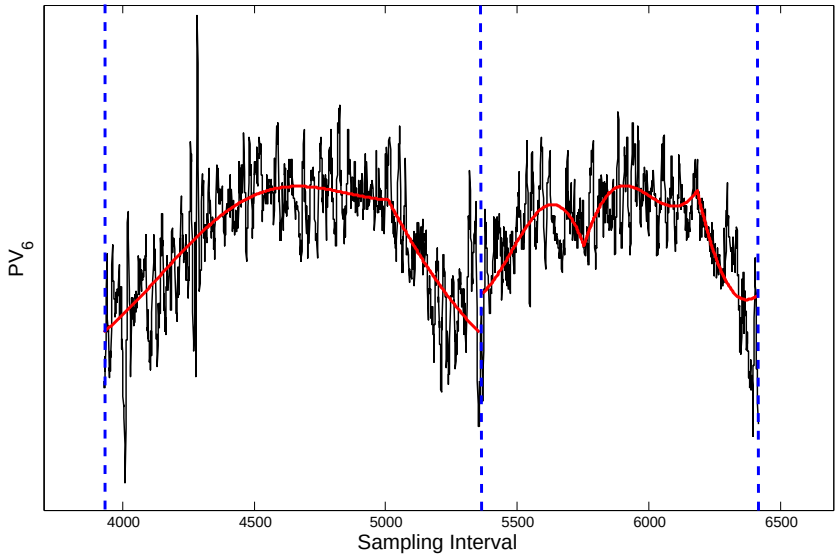

Figure 2.13: Two cycles of PV_6, fitted to the summation of one triangular and two sinusoidal patterns.

Table 2.9: Description of the registered variables for the studied industrial plant [29].

PV/MV	Description
PV_1	Side stripper Product
PV_2	Naphtha 95% point calculation
PV_3	SSP 5% point calculation
PV_4	Naphtha coalescer water boot level
PV_5	Bitumen column flooding maximum
PV_6	Pressure compensated reflux temperature
PV_7	Naphtha reflux temperature
PV_8	Bitumen column overhead temperature
MV_1	Bitumen column overhead pressure
MV_2	Naphtha reflux flow to bitumen column
MV_3	Pump around return temperature
MV_4	Steam to bitumen column
MV_5	Steam to side stripper

Table 2.10: Mean square error for fitting of two different patterns to PV_3.

Pattern	Cycle 1	Cycle 2
1× tri+ 4 × sin	57.0498	60.6555
2× tri+ 3 × sin	9.9303×10^2	1.0081×10^2

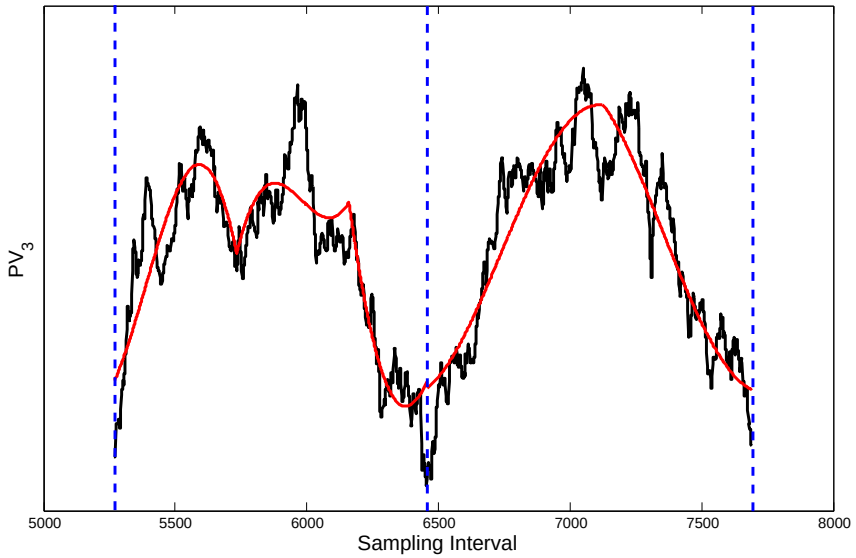

Figure 2.14: Two cycles of PV_3, fitted to the summation of one triangular and four sinusoidal patterns.

Table 2.11: Mean square error for fitting of two different patterns to PV_3.

Time Series	PV_1	PV_2	PV_3	PV_4	PV_5	PV_6	PV_7	PV_8
Nonlinearity Index	12.3432	8.2652	6.5963	14.3326	6.5061	4.3307	5.6333	9.9754

Chapter 3

Frequency Analysis and Experimental Validation of Stiction Phenomenon in Multi-loop Processes†

3.1 Oscillations Induced By Nonlinearities

Static friction, also called stiction, is one of the most frequently observed faults in control systems which affects their stability. Generally, the properties of all oscillations caused by nonlinearities depend on the dynamics of the entire system. In other words, in a standard control loop, not only the process transfer function, but also the type and tuning of the controller directly affect the frequency and magnitude of the nonlinearity-induced oscillations [6]. This chapter focuses on derivation and validation of a condition, under which nonlinearity-induced oscillations occur in a multi-loop system. This condition is derived in the frequency domain and enables the prediction of oscillations in a process and comparing them under different situations.

In next sections, a general condition for occurrence of nonlinearity-induced oscillations in multi-loop systems will be discussed. Then, the proposed condition will be validated by simulation and experiment on multi-loop systems. Stiction will specifically be studied as the only existing nonlinearity in the control system. In the end, the results of theoretical calculations, simulations and experimental studies will be presented and compared.

† This Chapter has been accepted for publication as **M. Alemohammad**, B. Huang, Frequency Analysis and Experimental Validation for Stiction Phenomenon in Multi-loop Processes, Journal of Process Control.

3.2 Condition for Oscillation Occurrence

In general, regardless of any root cause, there are two main features for an oscillating signal: frequency and magnitude. Frequency analysis is a strong tool to study and predict the behavior of linear systems. In addition, for nonlinear systems, Describing Function (DF) is defined. The DF output, similar to the frequency response (FR) of a linear system, is a complex number. Each complex number represents a magnitude and frequency. The FR or DF output, represented by complex numbers, can be shown in different ways depending on the application, as shown in following equations. Equation 3.3 is also called "Phasor" representation of C [10].

$$C = \alpha + j\beta \tag{3.1}$$

$$|C| = \sqrt{\alpha^2 + \beta^2}, \quad \measuredangle C = \theta = \arctan(\frac{\beta}{\alpha}) \tag{3.2}$$

$$C = |C|e^{j\theta} = |C|(\cos\theta + j\sin\theta) \tag{3.3}$$

There is a major difference between FR and DF. As it is obvious from the name, FR of a linear system is a function mapping from frequency, which is a real domain, to a complex space. But, DF may use other inputs beside frequency, or even have no functionality of frequency [14]. For the stiction nonlinearity, DF is a function of three parameters: 1) stickband (S), 2) slip-jump band (J) and 3) magnitude of the oscillating input (A). The first two are known as stiction parameters, used in data-driven models introduced in [24, 7, 17]. DF of stiction is proposed by [7], shown in Equation 3.4.

$$N_{(A)} = -\frac{1}{\pi A}(P_{real} - jP_{im}) \tag{3.4}$$

$$P_{real} = \frac{A}{2}\sin 2\varphi - 2A\sin\varphi + 2(S-J)\cos\varphi$$

$$P_{im} = -\frac{3A}{2} + \frac{A}{2}\cos 2\varphi + 2A\sin\varphi - 2(S-J)\sin\varphi$$

$$\varphi = \sin^{-1}(\frac{A-S}{A})$$

where A is the magnitude of the harmonic input, and S and J are the stiction parameters described above. The value of the proposed DF does not depend on frequency. This will simplify the future analyses.

3.2.1 Multi-loop Control Systems

A standard multi-loop system with m inputs and n outputs can be presented by Equation 3.5.

$$G = \begin{bmatrix} g_{11} & g_{12} & \cdots & g_{1m} \\ g_{21} & g_{22} & \cdots & g_{2m} \\ \vdots & & \ddots & \vdots \\ g_{n1} & g_{n2} & \cdots & g_{nm} \end{bmatrix}_{n \times m} \tag{3.5}$$

where g_{ij} is the transfer function from j^{th} input to i^{th} output. Based on the number of inputs and outputs, a system can be: underdefined ($m < n$), overdefined ($m > n$), or square ($m = n$) [31].

Underdefined Systems

This situation happens when outputs of the system need to be controlled using less number of inputs. In such cases, based on economics, safety and stability or any other considerations, m outputs should be picked out of total n, in order to be controlled by m inputs in a multiloop control setting. The remaining $n - m$ less important outputs may not be controlled.

After reducing the dimension of G, the new square ($m \times m$) system can now be controlled by m controllers. In order to pair outputs with suitable inputs for each controller, Relative Gain Array (RGA) can be used. The RGA is a matrix showing the extent of the influence of inputs on the system outputs. Equation 3.6 shows the definition of RGA.

$$\Lambda = \begin{bmatrix} \lambda_{11} & \lambda_{12} & \cdots & \lambda_{1m} \\ \lambda_{21} & \lambda_{22} & \cdots & \lambda_{2m} \\ \vdots & & \ddots & \vdots \\ \lambda_{m1} & \lambda_{m2} & \cdots & \lambda_{mm} \end{bmatrix}_{m \times m} \tag{3.6}$$

where λ_{ij} is the relative gain between output i and input j, with the definition mentioned in [31]. Equation 3.7 represents this definition.

$$\begin{aligned} \lambda_{ij} &= \frac{\left(\frac{\partial y_i}{\partial u_j}\right)_{all\ loops\ open}}{\left(\frac{\partial y_i}{\partial u_j}\right)_{loop\ m_j\ open; all\ other\ loops\ closed\ with\ perfect\ control}} \\ &= \left(\frac{open\ loop\ gain}{closed\ loop\ gain}\right)_{for\ loop\ i\ under\ the\ control\ of\ m_j} \end{aligned} \tag{3.7}$$

Overdefined Systems

These type of systems are more challenging to deal with, since there are more than one way to control each output. In fact, in order to make them square, $m-n$ inputs should be ignored. As suggested in [31], RGA can help us pick the best square $(n \times n)$ subsystem of G to control n outputs. The challenging part of this control strategy is picking one out of $\begin{pmatrix} m \\ n \end{pmatrix} = \frac{m!}{n!(m-n)!}$ possible subsystems. According to [31], some guidelines to compare different subsystems based on their RGA are:

1. It is better if all elements of Λ are positive.
2. Pairings which cause $0 < \lambda_{ij} \leq 0.5$ should be avoided.
3. λ_{ij} should be as close as possible to 1.

Square Systems

After the original system has been reduced , G is a square matrix (e.g., $n \times n$) representing the dynamics of the system. Suppose this system is controlled by n controllers $(g_{c1}, ..., g_{cn})$. Then, the following equations hold for this system in the frequency domain.

$$\begin{cases} y_1 = g_{11}u_1 + g_{12}u_2 + ... + g_{1n}u_n \\ y_2 = g_{21}u_1 + g_{22}u_2 + ... + g_{2n}u_n \\ \vdots \\ y_n = g_{n1}u_1 + g_{n2}u_2 + ... + g_{nn}u_n \end{cases} \tag{3.8}$$

Considering no external excitation ($SP_i = 0$), the relation between output and input in the i^{th} loop can be written as Equation 3.9.

$$u_i = -g_{c1(j\omega)}N_{i(A_i)}y_i \tag{3.9}$$

where $N_{i(A_i)}$ represents DF of the stiction nonlinearity in loop i and A_i is the magnitude of the harmonic input to this sticky valve. The assumption here is that all loops contain nonlinearity, however, $N_i = 1$ can be considered for valves without stiction.

Substituting equation 3.9 in 3.8, for u_1 to u_n, gives a new set of equations.

$$\begin{cases} [1 + g_{11(j\omega)}g_{c1(j\omega)}N_{1(A_1)}]y_1 + [g_{12(j\omega)}g_{c2(j\omega)}N_{2(A_2)}]y_2 + ... + [g_{1n(j\omega)}g_{cn(j\omega)}N_{n(A_n)}]y_n = 0 \\ [g_{21(j\omega)}g_{c1(j\omega)}N_{1(A_1)}]y_1 + [1 + g_{22(j\omega)}g_{c2(j\omega)}N_{2(A_2)}]y_2 + ... + [g_{2n(j\omega)}g_{cn(j\omega)}N_{n(A_n)}]y_n = 0 \\ \vdots \\ [g_{n1(j\omega)}g_{c1(j\omega)}N_{1(A_1)}]y_1 + [g_{n2(j\omega)}g_{c2(j\omega)}N_{2(A_2)})]y_2 + ... + [1 + g_{nn(j\omega)}g_{cn(j\omega)}N_{n(A_n)}]y_n = 0 \end{cases} \tag{3.10}$$

The set of Equations 3.10 can be re-written in matrix form to ease future analyses.

$$\mathcal{H}Y = \emptyset_{n\times 1} \tag{3.11}$$

$$\mathcal{H} = \begin{bmatrix} 1 + g_{11(j\omega)}g_{c1(j\omega)}N_{1(A_1)} & g_{12(j\omega)}g_{c2(j\omega)}N_{2(A_2)} & \cdots & g_{1n(j\omega)}g_{cn(j\omega)}N_{n(A_n)} \\ g_{21(j\omega)}g_{c1(j\omega)}N_{1(A_1)} & 1 + g_{22(j\omega)}g_{c2(j\omega)}N_{2(A_2)} & \cdots & g_{2n(j\omega)}g_{cn(j\omega)}N_{n(A_n)} \\ \vdots & & \ddots & \vdots \\ g_{n1(j\omega)}g_{c1(j\omega)}N_{1(A_1)} & g_{n2(j\omega)}g_{c2(j\omega)}N_{2(A_2)}) & \cdots & 1 + g_{nn(j\omega)}g_{cn(j\omega)}N_{n(A_n)} \end{bmatrix} \tag{3.12}$$

$$Y = \begin{bmatrix} y_1 \\ y_2 \\ \vdots \\ y_n \end{bmatrix} \tag{3.13}$$

It is noteworthy that Equation 3.11 does not hold in Laplace or real domain. This equation is only valid in a new space formed by the frequency of oscillation (ω), and at least one (maximum n) magnitude ($A_1, ..., A_p\ ,\ p \leq n$). Because Y is non-zero, there will be only one situation that Equation 3.11 holds: the matrix $\mathcal{H}$ is not full rank, i.e., its determinant is zero.

$$det(\mathcal{H}) = 0 \tag{3.14}$$

Under this condition, the system will oscillate with the frequency of ω and magnitudes of $A_1, ..., A_p$ ($p \leq n$), observable in controller output signals. But, due to the inaccurate nature of DF analysis, the exact value of real frequency and magnitudes may differ from analytically calculated ones. This condition is useful in predicting the occurrence of nonlinearity-induced oscillation in a system, rather than calculating and comparing numerical values of the oscillation properties.

3.2.2 Existence of an Answer for the Proposed Oscillation Condition

Finding the answer to Equation 3.11, which maps variables from multi-dimensional real domain to complex space, can be considered as the most challenging part of the analysis. In this section, some guidelines for solving this equation are presented based on the processes (single or multi-loop) and number of the faulty valves.

Single-loop Process

For a single-loop process, the matrix of the proposed condition will be reduced to a scalar. Therefore, the first diagonal element of $\mathcal{H}$ is put equal to zero.

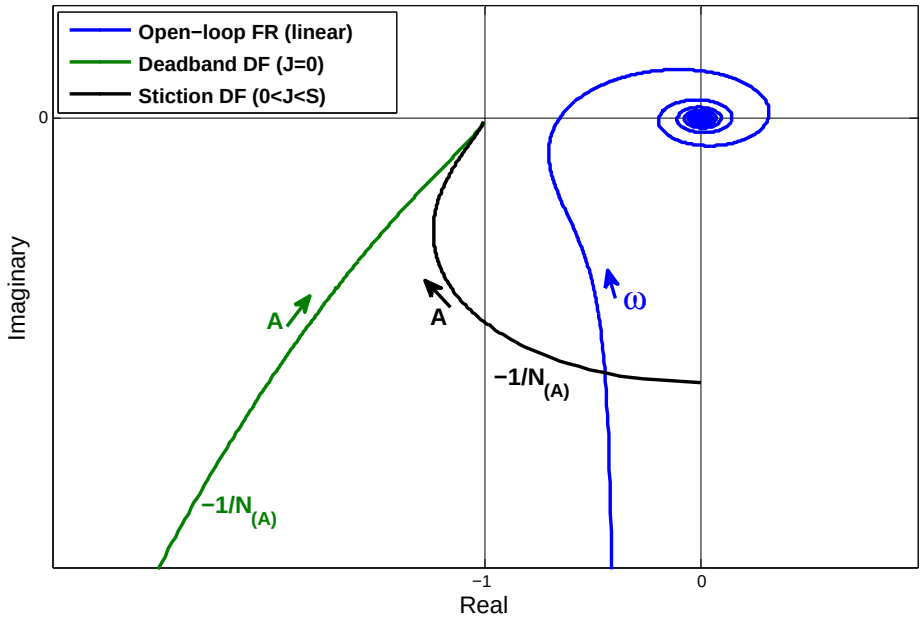

Figure 3.1: An example of using the graphical method to examine the existence of an answer for Equation 3.14.

$$1 + g_{(j\omega)} g_{c(j\omega)} N_{(A)} = 0 \tag{3.15}$$

which can be re-arranged as

$$g_{(j\omega)} g_{c(j\omega)} = \frac{-1}{N_{(A)}} \tag{3.16}$$

The simplicity of this problem enables the equation to be separated into two parts: 1) the open-loop FR of the linear process ($g_{(j\omega)} g_{c(j\omega)}$) and 2) the representation of the DF for the nonlinearity ($\frac{-1}{N_{(A)}}$). It has been clarified that both sides of this equation have complex values. Also, each side of Equation 3.16 contains an independent unknown variable from that of the other side (ω and A). Given the dynamics of the process, the exact value of the solution can be calculated analytically or numerically. But, since the discussion is about the existence of an answer to this equation, the graphical method may be the most beneficial.

In order to detect the existence of an answer graphically, the trajectories created by both sides of the equation for positive values of ω and A will be plotted in one complex plane. Independency of the unknown variables from each other guarantees the independency of the two trajectories. Obviously, the point at which the curve of the nonlinear side in Equation 3.16 intersects that of its linear side represents the solution.

Figure 3.1 illustrates an example of using the graphical method to examine the existence of a solution. The trajectories produced for stiction and deadband are

based on the describing function cited in Section 3.2. This figure confirms that this hypothetical system will oscillate in the presence of stiction in the control valve, but not for deadband.

Multi-loop Process with One Sticky Valve

For a process with more than one control loop, an analytical solution can be found when only one faulty valve exists. Due to an increase in the dimension of the problem, the use of graphical method will also be limited. Assuming the only sticky valve in the process is present in the i^{th} loop, the matrix $\mathcal{H}$ will be of the following form. In current section, the notation $g_{(j\omega)}$ for linear process FRs will be reduced to g to ease following the discussion for readers.

$$\mathcal{H} = \begin{bmatrix} 1+g_{11}g_{c1} & \cdots & g_{1i}g_{ci}N_i & \cdots & g_{1n}g_{cn} \\ g_{21}g_{c1} & \cdots & g_{2i}g_{ci}N_i & \cdots & g_{2n}g_{cn} \\ \vdots & \ddots & \vdots & & \vdots \\ g_{i1}g_{c1} & \cdots & 1+g_{ii}g_{ci}N_i & \cdots & g_{in}g_{cn} \\ \vdots & & \vdots & \ddots & \vdots \\ g_{n1}g_{c1} & \cdots & g_{ni}g_{ci}N_i & \cdots & 1+g_{nn}g_{cn} \end{bmatrix}$$

Now, matrix $\mathcal{H}'$ is defined similar to $\mathcal{H}$, except the i^{th} column is divided by N_i.

$$\mathcal{H}' = \begin{bmatrix} 1+g_{11}g_{c1} & \cdots & g_{1i}g_{ci} & \cdots & g_{1n}g_{cn} \\ \vdots & \ddots & \vdots & & \vdots \\ g_{i1}g_{c1} & \cdots & \frac{1}{N_i}+g_{ii}g_{ci} & \cdots & g_{in}g_{cn} \\ \vdots & & \vdots & \ddots & \vdots \\ g_{n1}g_{c1} & \cdots & g_{ni}g_{ci} & \cdots & 1+g_{nn}g_{cn} \end{bmatrix}$$

Then, $\overline{\mathcal{H}}_{hk}$ is defined as the matrix resulting from the elimination of the h^{th} row and k^{th} column of $\mathcal{H}$. Similarly, $\overline{\mathcal{H}}'_{hk}$ is derived from $\mathcal{H}'$. Based on the definition, the determinant of $\mathcal{H}$ can be expanded using its i^{th} row.

$$\begin{aligned} |\mathcal{H}| =& (-1)^{i+1}g_{i1}g_{c1}|\overline{\mathcal{H}}_{i1}| + (-1)^{i+2}g_{i2}g_{c2}|\overline{\mathcal{H}}_{i2}| + \cdots + \\ & (-1)^{2i}(1+g_{ii}g_{ci}N_i)|\overline{\mathcal{H}}_{ii}| + \cdots + (-1)^{i+n}g_{in}g_{cn}|\overline{\mathcal{H}}_{in}| = 0 \end{aligned} \tag{3.17}$$

In addition, if all the elements of a column of $\overline{\mathcal{H}}_{hk}$ are multiplied by N_i, the matrix $\overline{\mathcal{H}}'_{hk}$ will be produced. Based on this fact, the following equation will hold for their determinants.

$$|\overline{\mathcal{H}}_{hk}| = \begin{cases} |\overline{\mathcal{H}}'_{hk}| & k = i \\ N_i|\overline{\mathcal{H}}'_{hk}| & otherwise \end{cases} \tag{3.18}$$

The following can be concluded from substituting Equation 3.18 in Equation 3.17.

$$\begin{aligned}|\mathcal{H}| =&(-1)^{i+1}g_{i1}g_{c1}N_i|\overline{\mathcal{H}}'_{i1}| + (-1)^{i+2}g_{i2}g_{c2}N_i|\overline{\mathcal{H}}'_{i2}| + \cdots \\ &+ (-1)^{2i}(1 + g_{ii}g_{ci}N_i)|\overline{\mathcal{H}}'_{ii}| + \cdots + (-1)^{i+n}g_{in}g_{cn}N_i|\overline{\mathcal{H}}'_{in}| = 0 \end{aligned} \tag{3.19}$$

Equation 3.19 can be re-arranged as shown bellow, considering $(-1)^{2i} = 1$.

$$\begin{aligned}\frac{-1}{N_i} =&(-1)^{i+1}g_{i1}g_{c1}\frac{|\overline{\mathcal{H}}'_{i1}|}{|\overline{\mathcal{H}}'_{ii}|} + (-1)^{i+2}g_{i2}g_{c2}\frac{|\overline{\mathcal{H}}'_{i2}|}{|\overline{\mathcal{H}}'_{ii}|} + \cdots \\ &+ g_{ii}g_{ci} + \cdots + (-1)^{i+n}g_{in}g_{cn}\frac{|\overline{\mathcal{H}}'_{in}|}{|\overline{\mathcal{H}}'_{ii}|} \end{aligned} \tag{3.20}$$

Similar to the previously studied case, each side of Equation 3.20 is a function of an unknown variable independent of that of the other side (ω and A_i). Likewise, the existence of a solution to this equation can be investigated graphically, although the trajectory of the linear part may be more complicated.

Multi-loop Process with Multiple Sticky Valves

For the case of Multi-loop process, general form of the matrix $\mathcal{H}$ is presented in Equation 3.12. Similar to the previously studied case, a new matrix ($\mathcal{H}''$) can be defined as follows.

$$\mathcal{H}'' = \begin{bmatrix} \frac{1}{N_1} + g_{11}g_{c1} & \cdots & g_{1i}g_{ci} & \cdots & g_{1n}g_{cn} \\ \vdots & \ddots & \vdots & & \vdots \\ g_{i1}g_{c1} & \cdots & \frac{1}{N_i} + g_{ii}g_{ci} & \cdots & g_{in}g_{cn} \\ \vdots & & \vdots & \ddots & \vdots \\ g_{n1}g_{c1} & \cdots & g_{ni}g_{ci} & \cdots & \frac{1}{N_n} + g_{nn}g_{cn} \end{bmatrix}$$

Likewise, $\overline{\mathcal{H}}''_{hk}$ can be defined as the matrix resulting from the elimination of the h^{th} row and k^{th} column of $\mathcal{H}''$. Therefore, Equation 3.21 shows the relation between the determinants of $\overline{\mathcal{H}}''_{hk}$ and $\overline{\mathcal{H}}_{hk}$, of which definition is the same as explained before.

$$|\overline{\mathcal{H}}_{hk}| = \frac{N_T}{N_k}|\overline{\mathcal{H}}''_{hk}| \tag{3.21}$$

where N_T is the product of values of stiction DFs for all different loops.

$$N_T = \prod_{p=1}^{n} N_p \tag{3.22}$$

Finally, determinant of $\mathcal{H}$ can be written based on defined matrices.

$$\begin{aligned}|\mathcal{H}| =&(-1)^{i+1}g_{i1}g_{c1}\frac{N_T}{N_1}|\overline{\mathcal{H}}''_{i1}| + (-1)^{i+2}g_{i2}g_{c2}\frac{N_T}{N_2}|\overline{\mathcal{H}}''_{i2}| + \cdots \\ &+ (-1)^{2i}(1+g_{ii}g_{ci}N_i)\frac{N_T}{N_i}|\overline{\mathcal{H}}''_{ii}| + \cdots + (-1)^{i+n}g_{in}g_{cn}\frac{N_T}{N_n}|\overline{\mathcal{H}}''_{in}| = 0 \end{aligned} \quad (3.23)$$

As observable in implicit Equation 3.23, the expression of the oscillation condition for the case with multiple loops and faulty valves can not be presented by simple equations. Also, it can not be explicitly divided into independent parts considering all unknown variables (ω, A_1, $\cdots$, A_p, where $1 \leq p \leq n$). In the absence of analytical solutions, numerical methods can be used.

3.3 Simulation of a Multi-loop Process

The multi-loop system introduced by [31] for a pilot scale binary distillation column used to separate ethanol and water, has been simulated. The matrix of dynamics of this process is shown in Equation 3.24.

$$\begin{bmatrix} Y_{1(s)} \\ Y_{2(s)} \\ Y_{3(s)} \end{bmatrix} = \begin{bmatrix} \frac{0.66e^{-2.6s}}{6.7s+1} & \frac{-0.61e^{-3.5s}}{8.64s+1} & \frac{-0.0049e^{-s}}{9.06s+1} \\ \frac{1.11e^{-6.5s}}{3.25s+1} & \frac{-2.36e^{-3s}}{5s+1} & \frac{-0.012e^{-1.2s}}{7.09s+1} \\ \frac{-33.68e^{-9.2s}}{8.15s+1} & \frac{46.2e^{-9.4s}}{10.9s+1} & \frac{0.87(11.61s+1)e^{-s}}{(3.89s+1)(18.8s+1)} \end{bmatrix} \begin{bmatrix} U_{1(s)} \\ U_{2(s)} \\ U_{3(s)} \end{bmatrix} \quad (3.24)$$

It is to say that for a hypothetical variable x, the notation $X_{(s)}$ represents transformation of $x_{(t)}$ into the Laplace domain. For simplicity, all variables in time domain will be shown without subscript of time (t). Also, the steady state value of variable x will be noted as $\bar{x}$ in future formulae.

The outputs y_1, y_2 and y_3 are paired with the inputs u_1, u_2 and u_3, respectively. All the controllers are proportional-integral (PI). The initial tunings for three controllers used to control this process are as follows.

$$\begin{aligned} g_{c1(s)} &= 0.65 + \frac{0.09}{s} \\ g_{c2(s)} &= -0.157 + \frac{-0.031}{s} \\ g_{c3(s)} &= 0.675 + \frac{0.61}{s} \end{aligned} \quad (3.25)$$

It has been assumed that the control valves in loops 2 and 3 have stiction problem. The stiction parameters for these two valves are reported in Table 3.1. The valve in loop 1 is assumed to work perfectly. In current section, He's model [17] is used to simulate sticky valves.

Table 3.1: Stiction parameters for the simulated system.

S_2	J_2	S_3	J_3
4.0	2.0	6.0	3.0

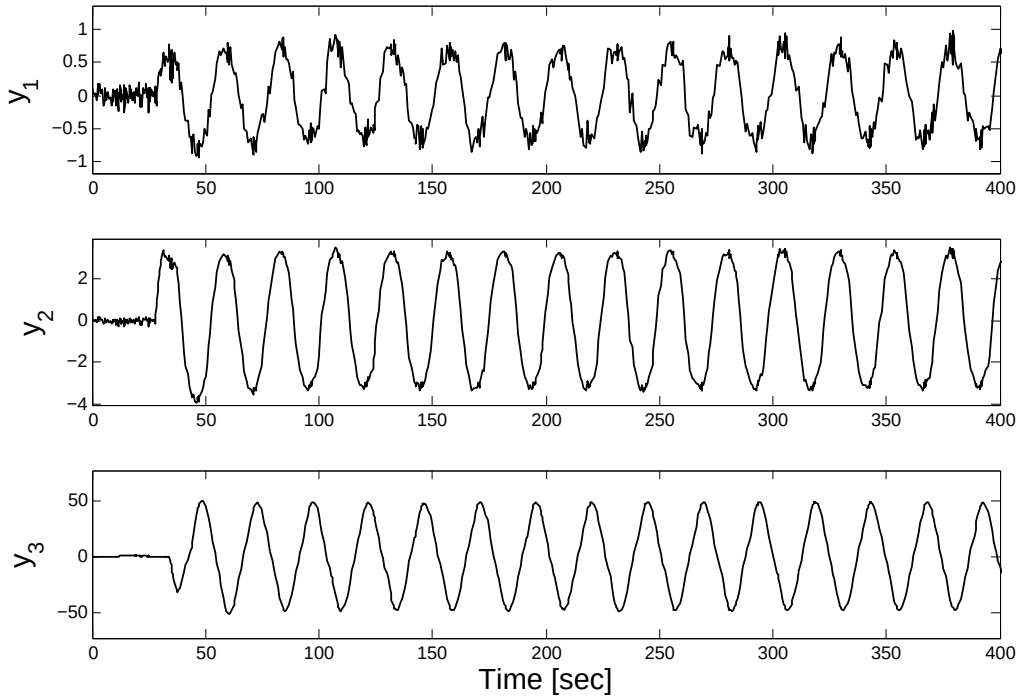

Figure 3.2: Simulation results using the first set of tunings for the controllers.

Simulations show that by using these controllers, all loops of the system will oscillate with the same frequency, but different shapes and magnitudes. Figure 3.2 illustrates these oscillations.

For the second attempt, different tunings were considered for the controllers. All other dynamics are kept the same as the previous state. Transfer functions of the controllers are represented by Equation 3.26.

$$\begin{aligned} g_{c1(s)} &= 2 + \frac{0.05}{s} \\ g_{c2(s)} &= -1 + \frac{-0.031}{s} \\ g_{c3(s)} &= 2 + \frac{0.61}{s} \end{aligned} \tag{3.26}$$

As expected, the system response changed to what can be seen in Figure 3.3. It can be observed that the oscillations in all loops still have equal frequencies, but the values of these frequencies are different from the first run.

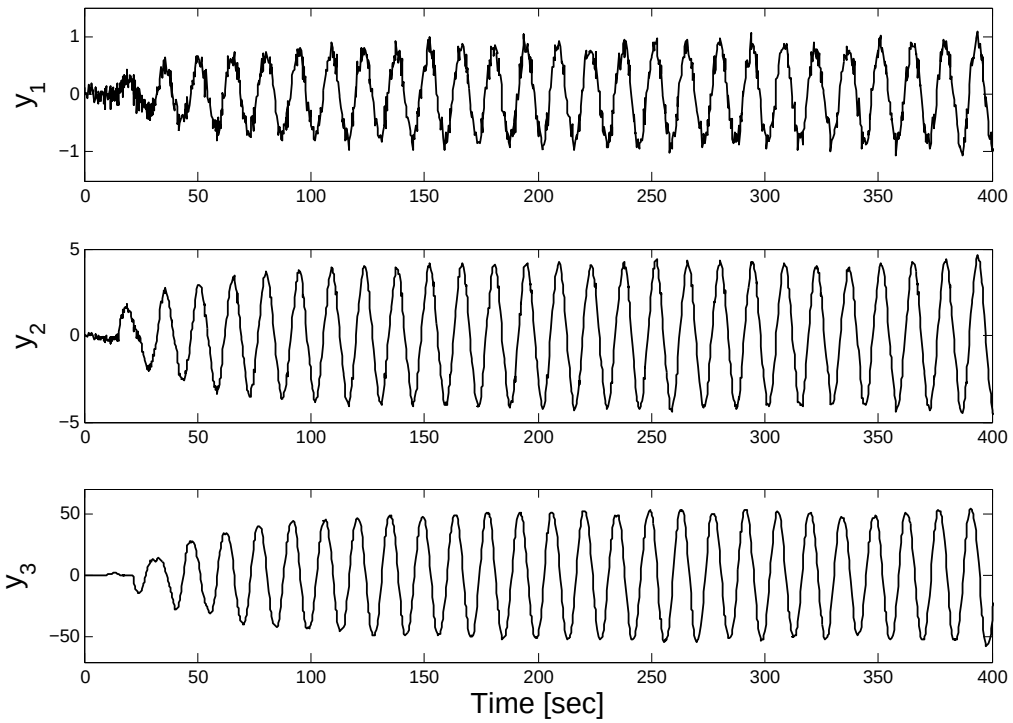

Figure 3.3: Simulation results using the second set of tunings for the controllers.

3.3.1 Theoretical Study of the Simulated System

The matrix $\mathcal{H}$ in Equation 3.11 for the simulated system can be written as follows.

$$\mathcal{H} = \begin{bmatrix} 1 + g_{11(j\omega)}g_{c1(j\omega)} & g_{12(j\omega)}g_{c2(j\omega)}N_{2(A_2)} & g_{13(j\omega)}g_{c3(j\omega)}N_{3(A_3)} \\ g_{21(j\omega)}g_{c1(j\omega)} & 1 + g_{22(j\omega)}g_{c2(j\omega)}N_{2(A_2)} & g_{23(j\omega)}g_{c3(j\omega)}N_{3(A_3)} \\ g_{31(j\omega)}g_{c1(j\omega)} & g_{32(j\omega)}g_{32(j\omega)}N_{2(A_2)}) & 1 + g_{33(j\omega)}g_{c3(j\omega)}N_{3(A_3)} \end{bmatrix} \tag{3.27}$$

Since the control valve of loop 1 has no stiction, the value of DF for this loop is considered to be 1 in all calculations ($N_{1(A_1)} = 1$). Equation 3.14 for this system needs to be solved for 3 unknowns: ω, A_2 and A_3. The solutions to this equation for both sets of tunings are summarized in Table 3.2.

Table 3.2: Theoretically calculated values for the oscillation frequencies and magnitudes.

Tuning	ω	A_2	A_3
First	0.16	3.35	3.30
Second	0.46	2.95	3.05

According to theoretical calculations, the frequency of the oscillations in the second run is greater than that of the first. This corresponds to the simulation

results shown in Figures 3.2 and 3.3. The magnitudes of the oscillations remain almost the same after changing the tunings.

It is clear that calculated values for the magnitudes and frequencies, reported in Table 3.2, are not equal to that of the oscillations observed in the above mentioned figures. According to [41], this type of discrepancies is the most common one in DF analysis. The reason behind this fact can be inaccurate nature of the DF analysis, i.e., unrealistic assumptions used to derive DF for nonlinear systems. One of the basic assumptions which enables us to analytically derive a mathematical expression for DF is that the input to the nonlinear system is a sinusoidal signal [14], which rarely happens in reality.

In the next section, an experimental case will be studied to show the reliability of this analysis.

3.4 An Experiment With Multi-loop Control System and Multiple Sticky Valves Setting

After studying the proposed condition stated in Equations 3.11 and 3.14 by simulation, an experiment was carried out. In this experiment, which is related to a multi-loop control system, two different states were studied. Only tunings of the controller parameters differentiate these two situations.

3.4.1 Experimental System Setup

In order to investigate the effect of stiction on a system in presence of interaction between loops, a three-input-three-output process was designed. Figure 3.4 shows the schematic of the process and configuration of the control loops.

This setup consists of two tanks in series. In the first tank (top), the level (h_1) and temperature (T) are being controlled. Inputs to this tank are cold water with flowrate of f_c and saturated steam with flowrate of f_s traveling through a heating coil inside the tank. The outlet stream of the first tank, together with a stream of hot water (f_h), flow into the next tank (bottom). In this tank only the level (h_2) is being controlled. The whole process is being controlled by three PI controllers. Each output is paired with one of the inputs, i.e., flowrates of cold water, hot water and steam are manipulated variables to control the level of the top tank, level of bottom tank and the temperature, respectively. Also, there is a cascade loop for each flowrate.

Therefore, the dynamics of this process will be of the form shown in Equation 5.55:

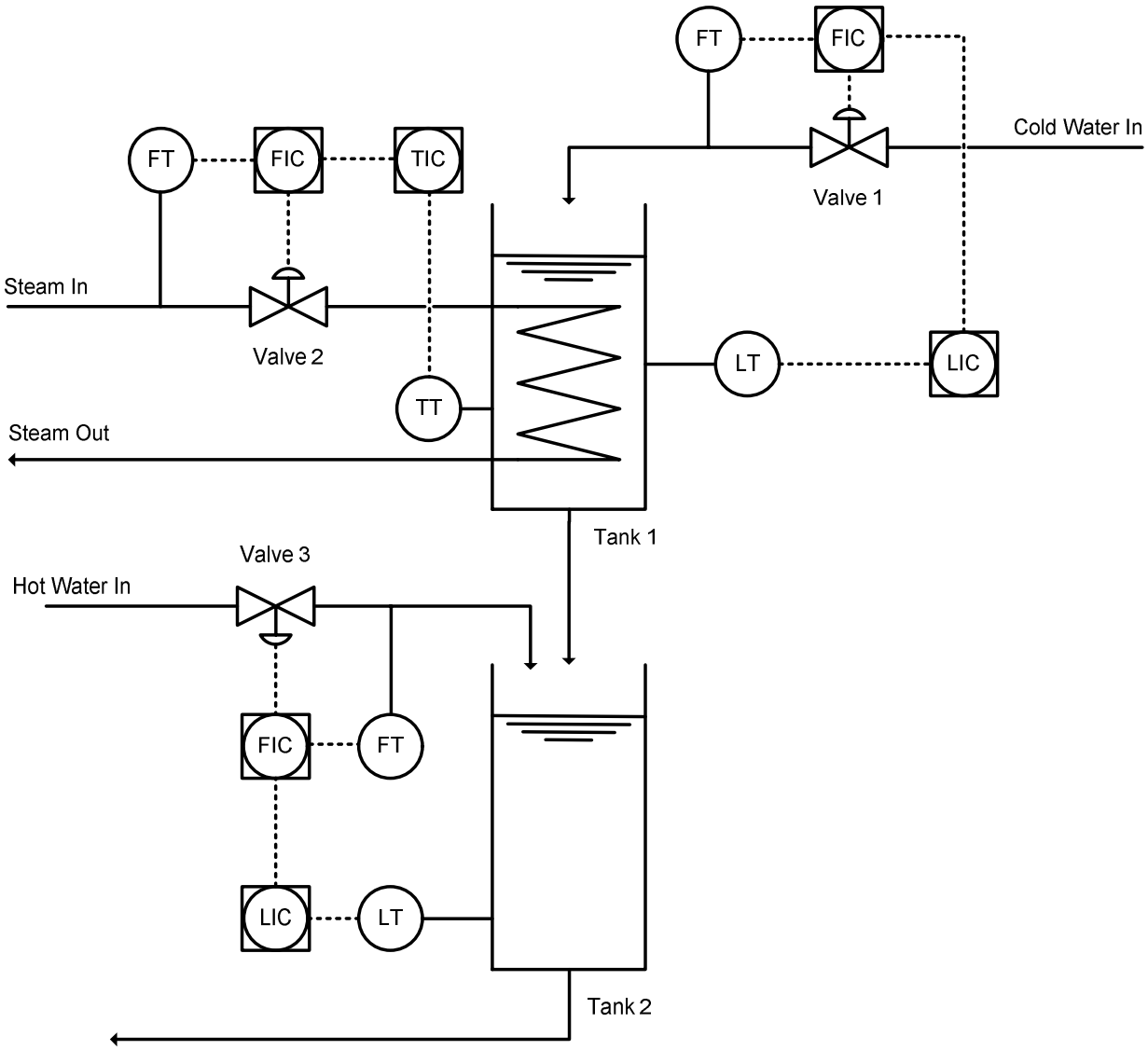

Figure 3.4: Schematic of the studied 3×3 process used for the experiment.

$$\begin{bmatrix} H_{1(s)} \\ H_{2(s)} \\ T_{(s)} \end{bmatrix} = G_{(s)} \begin{bmatrix} F_{c(s)} \\ F_{h(s)} \\ F_{s(s)} \end{bmatrix} \tag{3.28}$$

where $G_{(s)}$ is a 3×3 matrix. The elements of $G_{(s)}$ show the dynamics from the inputs to the outputs of the process.

3.4.2 Valve Characterization

In chemical processes, most of manipulated variables are in terms of flowrates and control valve converts the control signal to flowrate. Likewise, in the current process we have three control valves to change values of inputs F_c, F_h and F_s. Before any further implementations we need to know about the existence of possible nonlinearities in the valves. One of the simplest and most common methods of observing faults in a valve is "valve characterization" or also called "open-loop testing". In this simple procedure, the valve is opened and closed manually by the operator. This will lead to a closed cyclic path in the output-input plot of the valve. The paths which the valve passes while being opened and closed can give useful information about faults in the valve. Some definitions of valve nonlinearities are presented by [37] and schematically summarized in Figure 1.5.

The characterization procedure was performed on three different valves with gradual changes in the valve position with size of 1% and maximum lift of 50%, i.e., each valve travels from fully closed to half-open position by step-size of 1% of the entire stem travel length and then returns to its fully closed position. For each valve, the values for maximum and step-size of changes have been selected based on operating conditions, severity of stiction at different positions of the valve stem and safety issues. According to Figure 3.5, preliminary studies indicate that when two of the valves are at positions lower than 50%, they show more nonlinear responses.

It is noteworthy that, because the actual valve position (MV) could be measured in this particular experiment, graphs in Figure 3.5 can be generated. Cascade loops in the control system enable us to back-calculate the position of the valves, given their manufacturing specifications are in hand. This is also a method for stiction detection and quantification [24]. Based on this method, stiction parameters used in two-parameter models [24, 7] were calculated for this system as follows.

$$\begin{cases} Cold\ Water\ Valve: & S_1 = 5, \quad J_1 = 1.4 \\ Hot\ Water\ Valve: & S_2 = 6, \quad J_2 = 1.3 \end{cases} \tag{3.29}$$

According to Figure 3.5, the control valve on the steam line is working reasonably good and stiction only exists in valves 1 and 2. The values shown in Equation 3.29

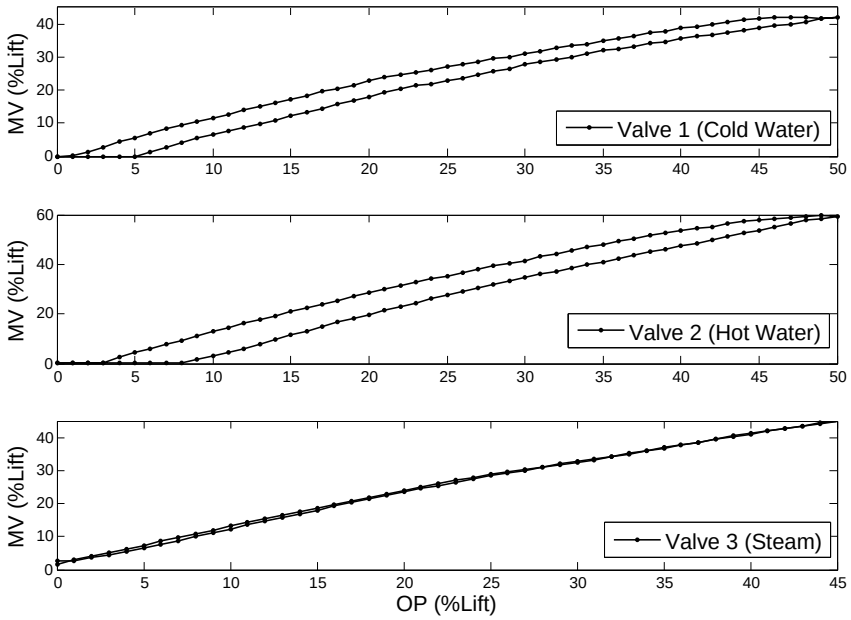

Figure 3.5: Results of characterization of the valves; actual valve position (MV) vs. expected valve position (OP).

will be used in future analyses. Although severity of stiction varies from one position of valve to another, because of local oscillations in faulty valves, these values can be considered constant. The calculated parameters belong to cold and hot water valves when oscillating near the steady state positions of 30% and 18%, respectively.

3.4.3 Process Model

In order to model this multivariate process, two mass balance equations (for two tank levels) and one energy balance equation (for temperature) are needed. The resulting differential equations governing the system are stated in Equations 3.30 to 3.32.

$$\rho_{(T)} A_1 \frac{dh_1}{dt} = f_c - \frac{h_1}{R_1} \tag{3.30}$$

$$\rho_{(T)} A_2 \frac{dh_2}{dt} = \frac{h_1}{R_1} + f_h - \frac{h_2}{R_2} \tag{3.31}$$

$$(f_c - \frac{h_1}{R_1}) C_{p(T)} \frac{dT}{dt} = f_c C_{p(T_c)} [T_c - T_{ref}] - \frac{h_1}{R_1} C_{p(T)} [T - T_{ref}] + k f_s (\Delta \hat{H}) \tag{3.32}$$

where all parameters and variables used in these formulae have been presented in Table 3.3. It is obvious that the derivatives of all outputs ($\frac{dh_1}{dt}, \frac{dh_2}{dt}, \frac{dT}{dt}$) are nonlinear functions of the inputs (f_c, f_h, f_s) and outputs (h_1, h_2, T).

$$\frac{dh_1}{dt} = \mathcal{F}(f_c, h_1, T) \tag{3.33}$$

$$\frac{dh_2}{dt} = \mathcal{G}(f_h, h_1, h_2, T) \tag{3.34}$$

$$\frac{dT}{dt} = \mathcal{N}(f_c, h_1, f_s, T) \tag{3.35}$$

Table 3.3: Parameters and variable used in modeling of the process.

Parameter/Variable	Symbol	Unit	Value (Steady State)
Level of tank 1	h_1	m	0.2
Level of tank 2	h_2	m	0.3
Temperature of tank 1	T	$^\circ C$	45
Cold water flowrate	f_c	Kg/min	4.4
Hot water flowrate	f_h	Kg/min	2
Steam flowrate	f_s	Kg/hr	11
Cross section area of tank 1	A_1	m^2	0.016
Cross section area of tank 2	A_2	m^2	0.016
Resistance of outlet from tank 1	R_1	$m.s/Kg$	3.2488
Resistance of outlet from tank 2	R_2	$m.s/Kg$	8.8433
Heat transfer fraction from coil	k	N/A	0.97
Temperature of inlet to tank 1	T_c	$^\circ C$	24.6
Reference temperature	T_{ref}	$^\circ C$	0
Specific enthalpy of steam[§]	$\Delta\hat{H}$	J/Kg	1994737

§ *Calculated for saturated steam (*150 *psig) fully condensed, and subject to* T_{ref}.

Therefore, liniarization is needed for functions $\mathcal{F}$, $\mathcal{G}$, and $\mathcal{N}$, in local neighborhood of the steady state ($\bar{f}_c$,$\bar{f}_h$,$\bar{f}_s$,$\bar{h_1}$,$\bar{h_2}$ and $\bar{T}$). After liniarization and substitution of numerical values for the parameters stated in Table 3.3, the governing equations have the form shown in Equations 3.36 to 3.38.

$$\frac{dh_1}{dt} \simeq 7.4296 \times 10^{-4} + 0.0011(f_c - \bar{f}_c) - 0.0194(h_1 - \bar{h_1}) - 3.1523 \times 10^{-6}(T - \bar{T}) \tag{3.36}$$

$$\frac{dh_2}{dt} \simeq 0.0038 + 0.0194(h_1 - \bar{h_1}) - 0.0071(h_2 - \bar{h_2}) + 0.0011(f_h - \bar{f}_h) + 1.5173 \times 10^{-6}(T - \bar{T}) \tag{3.37}$$

$$\frac{dT}{dt} \simeq 38.0394 - 181.9993(h_1 - \bar{h_1}) - 44.8299(f_c - \bar{f}_c) + 10.9199(f_s - \bar{f}_s) - 5.2463(T - \bar{T}) \tag{3.38}$$

In the calculation of above functions, the high order polynomials presented in Equations 3.39 and 3.40 were used to describe heat capacity ($C_{p(T)}$) and density of water ($\rho_{(T)}$) as functions of temperature. These functions are valid in the range of $40°C \leq T \leq 60°C$. The steady state values of $C_{p(\bar{T})}$, $\rho_{(\bar{T})}$, and their derivatives are listed in Equations 3.41 and 3.42.

$$\rho_{(T)} = -0.003\,T^2 - 0.1205\,T + 1001.18 \tag{3.39}$$

$$C_{p(T)} = 2.564 \times 10^{-6}\,T^5 - 5.175 \times 10^{-4}\,T^4 + 0.0401\,T^3 - 1.471\,T^2 + 25.19\,T + 4022 \tag{3.40}$$

$$C_{p(\bar{T})} = 4181\ [\frac{J}{Kg°C}], \quad \rho_{(\bar{T})} = 990.3025\ [\frac{Kg}{m^3}] \tag{3.41}$$

$$\frac{dC_{p(T)}}{dt}\Big|_{\bar{T}} = 0.2588\ [\frac{J}{s.Kg°C}], \quad \frac{d\rho_{(T)}}{dt}\Big|_{\bar{T}} = -0.3905\ [\frac{Kg}{s.m^3}] \tag{3.42}$$

Finally, Equations 3.36 to 3.38 will be transported to the Laplace domain in order to perform the required analyses. These equations are rearranged as shown below. All parameters are introduced in Table 3.4.

Table 3.4: Parameters used in Equations 3.46 to 3.51.

b_1	c_1	d_1	b_2	c_2	d_2
0.001	-0.0194	3.1523×10^{-6}	0.0194	-0.0071	0.0011
e_2	b_3	c_3	d_3	e_3	
1.5173×10^{-6}	-44.8299	-181.9993	10.9199	-5.2463	

$$H_{1(s)} = \alpha F_{c(s)} + \beta F_{s(s)} \tag{3.43}$$

$$H_{2(s)} = \mu F_{c(s)} + \nu F_{s(s)} + \eta F_{h(s)} \tag{3.44}$$

$$T_{(s)} = \gamma F_{c(s)} + \lambda F_{s(s)} \tag{3.45}$$

where

$$\alpha = \frac{b_1(s-e_3)+d_1b_3}{(s-e_3)(s-c_1)-c_3d_1} \tag{3.46}$$

$$\beta = \frac{d_1d_3}{(s-e_3)(s-c_1)-c_3d_1} \tag{3.47}$$

$$\gamma = \frac{\alpha c_3+b_3}{s-e_3} \tag{3.48}$$

$$\lambda = \frac{\beta c_3+d_3}{s-e_3} \tag{3.49}$$

$$\mu = \frac{\alpha b_2+\gamma e_2}{s-c_2} \tag{3.50}$$

$$\nu = \frac{\beta b_2+\lambda e_2}{s-c_2} \tag{3.51}$$

Experiments were carried out to calculate time lags of transfer functions. As expected, there were only delays for dynamics from $F_{c(s)}$ and $F_{s(s)}$ (inputs) to T (output). Thus, the actual transfer functions can be rewritten as:

$$\frac{T_{(s)}}{F_{c(s)}} = \gamma e^{-22s} \tag{3.52}$$

$$\frac{T_{(s)}}{F_{s(s)}} = \lambda e^{-10s} \tag{3.53}$$

No significant delay was detected in other transfer functions. In the next sections, the model will be used to study oscillations induced by stiction, based on the methodology proposed in Section 3.2.

3.4.4 Results of the Experiment

The experiment was run for 7000 seconds under steady state, with sampling time of 1 second. As mentioned in Section 3.4.1, each loop is equipped with one controller (i.e., g_{c1},g_{c2} and g_{c3}). In order to observe the effect of controller tunings on the performance of the system, the parameters of g_{c1} and g_{c2} were changed at sampling step 8700. The original and new values of the controller gain (K_c) and the integral time (τ_I) are reported in Tables 3.5 and 3.6, respectively. It is noteworthy that τ_I and K_c are used in the transfer function of PI controllers with the configuration shown in Equation 3.54.

$$g_{c(s)} = K_c(1+\frac{1}{\tau_I s}) \tag{3.54}$$

Figure 3.6 illustrates the performance of the control system. In this figure, time trends of three process outputs have been plotted. The dotted line in the middle of each graph separates two time intervals when the process was under control with different controller tunings. The following points can be inferred from this figure:

Table 3.5: Original values of the control parameters (sample no. < 8700).

	$g_{c1(s)}$	$g_{c2(s)}$	$g_{c3(s)}$
K_c	127.77 $[\frac{Kg}{min.m}]$	51.11 $[\frac{Kg}{min.m}]$	1.26 $[\frac{Kg}{hr.m}]$
τ_I [sec]	30	40	41

Table 3.6: New values of the control parameters (sample no. ≥ 8700).

	$g_{c1(s)}$	$g_{c2(s)}$	$g_{c3(s)}$
K_c	25.55 $[\frac{Kg}{min.m}]$	51.11 $[\frac{Kg}{min.m}]$	1.26 $[\frac{Kg}{hr.m}]$
τ_I [sec]	20	30	41

1. Oscillations can be clearly observed in all outputs.
2. The frequency of the oscillations observed in loops 1 and 3 are similar to each other, while loop 2 oscillates with a completely different frequency.
3. After the tunings changed (sample no. $= 8700$), the steady state oscillations in all outputs varied in terms of frequency and magnitude.

In the next section, theoretical analysis of these observations will be presented.

3.4.5 Theoretical Study of the Experiment Results

Once the stiction parameters and the process model are specified, the next steps of the analysis can be carried out. The dynamics of this multi-variable process can be stated in matrix form as shown in Equation 3.55.

$$G_{(s)} = \begin{bmatrix} g_{11} & 0 & g_{13} \\ g_{21} & g_{22} & g_{23} \\ g_{31} & 0 & g_{33} \end{bmatrix}_{3\times 3} = \begin{bmatrix} \alpha & 0 & \beta \\ \mu & \eta & \nu \\ \gamma e^{-22s} & 0 & \lambda e^{-10s} \end{bmatrix} \tag{3.55}$$

Matrix $\mathcal{H}$ in Equation 3.14 can be calculated, once the process model, S and J are known. It has to be mentioned that, since the steam control valve has no stiction, in the next derivations $N_{3(A_3)} = 1$ will be applied.

$$\mathcal{H} = \begin{bmatrix} 1 + g_{11(j\omega)}g_{c1(j\omega)}N_{1(A_1)} & 0 & g_{13(j\omega)}g_{c3(j\omega)} \\ g_{21(j\omega)}g_{c1(j\omega)}N_{1(A_1)} & 1 + g_{22(j\omega)}g_{c2(j\omega)}N_{2(A_2)} & g_{23(j\omega)}g_{c3(j\omega)} \\ g_{31(j\omega)}g_{c1(j\omega)}N_{1(A_1)} & 0 & 1 + g_{33(j\omega)}g_{c3(j\omega)} \end{bmatrix} \tag{3.56}$$

Because of the special structure of $\mathcal{H}$, its determinant can be written in a simple form and then equated to zero.

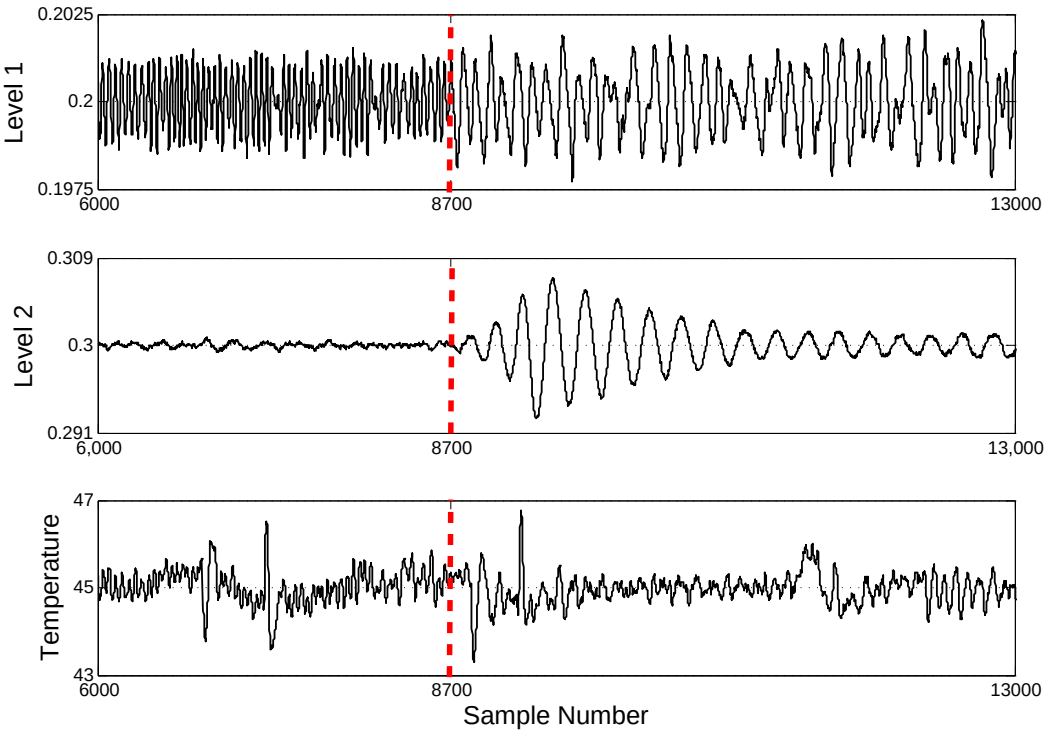

Figure 3.6: Results obtained from running the experiment under two different sets of control parameters.

$$det(\mathcal{H}) = (1 + g_{11(j\omega)}g_{c1(j\omega)}N_{1(A_1)})(1 + g_{22(j\omega)}g_{c2(j\omega)}N_{2(A_2)})(1 + g_{33(j\omega)}g_{c3(j\omega)}) - (g_{13(j\omega)}g_{c3(j\omega)})(1 + g_{22(j\omega)}g_{c2(j\omega)}N_{2(A_2)})(g_{31(j\omega)}g_{c1(j\omega)}N_{1(A_1)}) = 0 \quad (3.57)$$

which can be rearranged as

$$(1 + g_{22(j\omega)}g_{c2(j\omega)}N_{2(A_2)})\Big[(1 + g_{11(j\omega)}g_{c1(j\omega)}N_{1(A_1)})(1 + g_{33(j\omega)}g_{c3(j\omega)}) - (g_{13(j\omega)}g_{c3(j\omega)})(g_{31(j\omega)}g_{c1(j\omega)}N_{1(A_1)})\Big] = 0 \quad (3.58)$$

Equation 3.58 can be divided into two simpler equations, each involving one magnitude and one frequency. If either of these two equations (or both) hold, the oscillation will be predicted to occur in the entire system due to stiction.

$$\frac{-1}{N_{2(A_2)}} = g_{22(j\omega)}g_{c2(j\omega)} \quad (3.59)$$

or

$$\frac{-1}{N_{1(A_1)}} = \frac{g_{11(j\omega)}g_{c1(j\omega)} + g_{11(j\omega)}g_{c1(j\omega)}g_{33(j\omega)}g_{c3(j\omega)} - g_{13(j\omega)}g_{31(j\omega)}g_{c1(j\omega)}g_{c3(j\omega)}}{1 + g_{33(j\omega)}g_{c3(j\omega)}} \quad (3.60)$$

Existence of solutions for Equations 3.59 and 3.60 can be investigated by graphical methods. Figure 3.7 illustrates that two different solutions exist for these equations. It can be justified by stability analysis of the limit cycles, considering weak interactions between two sub-systems. According to the criterion stated in Section **??**, points I and II represent stable limit cycles for sub-systems of Equations 3.59 and 3.60 respectively (see Figure 3.7). According to extended Nyquist criterion, presented by [41], the point II is an unstable state for the sub-system of loops 1 and 3. Therefore, this sub-system will oscillate in limit cycle shown by point I. On the other hand, sub-system of loop 2 can stably oscillate in both points, depending on initial and operating condition (in this experiment, this loop is located at point II). Because of the weak interactions, obviously explained by nature of the multi-loop process in Section 3.4.1, two subsystems cannot affect stable oscillations of each other. As the result, each sub-system remains at its own stable limit cycle.

All remarks stated in Section 3.4.4 can be justified by Figure 3.7 as follows:

1. Points I and II represent answers to Equations 3.59 and 3.60, respectively. Thus, oscillation takes place in all loops.

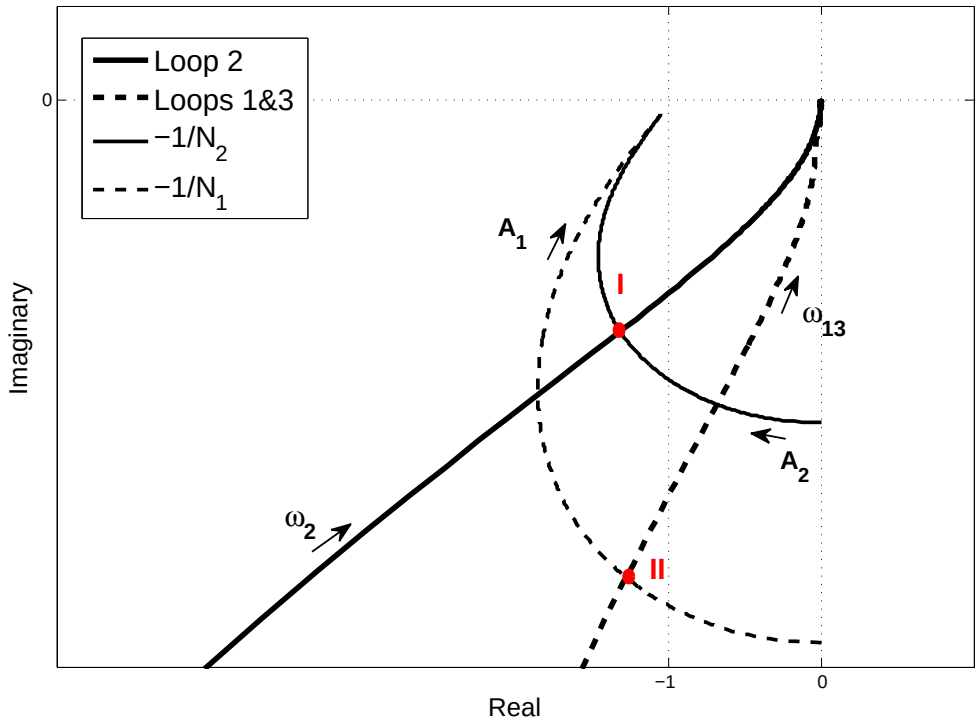

Figure 3.7: Graphical solution to Equations 3.59 and 3.60.

2. There is a unique answer (pair of ω and A) for each equation, indicating that the frequency of oscillation in loop 2 is different from the other loops. The frequencies of loops 1 and 3 are equal and noted as ω_{13}.

3. With change in controller tuning, the path of frequency responses will definitely change. So, Equations 3.59 and 3.60 will hold for different points, i.e., the resulting frequencies and magnitudes of the oscillations will change.

3.4.6 Comparison of Theoretical and Experimental Results

Equations 3.59 and 3.60 can also be solved by numerical methods. Table 3.7 reports the results of numerical solutions for these equations.

Table 3.7: Numerical solutions to Equations 3.59 and 3.60 under control with two different tunings.

	ω_2	A_2	ω_{13}	A_1
Tuning 1	0.0265	4.575	0.0335	3.225
Tuning 2	0.0315	4.5650	0.0125	3.365

Despite what can be observed on Table 3.2, in this experiment two frequencies can be calculated, since the special structure of the system allows separation of the

key condition ($det(\mathcal{H}) = 0$) to two equations. According to Table 3.7, it is implied that:

1. After changing the tunings in loop 2, the frequency of oscillation slightly grows, while an increase in the magnitude is sensible.

2. The magnitudes of oscillations in loops 1 and 3 remain almost the same, but the frequency decreases significantly.

3. Before changing the tuning $\omega_2 < \omega_{13}$ is valid, and afterwards this changes to $\omega_2 > \omega_{13}$.

As observable in Figure 3.6, all but the last remark mentioned above agree with experimental results. During the experiment and under both tunings, ω_2 is always less than ω_{13}. Possible reasons for this discrepancy can be: (1) Inaccuracies of describing function analysis, due to its basic assumptions [41], (2) Approximation of stiction by only two time-invariant parameters, even for different locations of the stem, and (3) mismatches between the dynamics of the real setup and the first-principle model developed for this experiment.

3.5 Conclusion

In this chapter, the condition under which nonlinearity-induced oscillations occur in control systems has been mathematically derived. This condition, utilizing frequency responses and describing functions of nonlinearities, can predict possible oscillations in multi-loop and single-loop systems. To validate the performance of this analysis, a multi-loop process experiment was designed and the results confirmed the theoretical calculations.

Chapter 4

Model-based Approach to Compensate Stiction in Control Loops

4.1 Stiction Compensation

There exist hundreds to thousands control loops in a normal industrial plant. Performance of each loop is closely related to safety, product quality, and energy consumption. Almost one third of poor performed loops are caused by nonlinearities of the control valves, one of which is static friction [9]. The effect of this fault is usually observed as oscillations in process output. Since industrial plants include numerous interacting loops, the oscillations will be propagated to the entire system. Many methods have been proposed in the literature aiming at detection oscillations and their root causes. Doubtlessly, scheduling the faulty valves to be repaired is the definite solution to this problem. But, because shutting down the process to isolate the faulty valve for maintenance purposes is not economical, this solution does not count as the primary one. There should be a method to compensate the destructive effect of the stiction phenomenon on the control valve and quality of the product, especially when maintenance is not available. This chapter focuses on existing compensation issues, followed by a proposal of a new model-based compensation approach for this nonlinearity.

4.2 New Methodology to Compensate for Stiction

Some of the existing algorithms for compensation of stiction in control systems have been explained in Section 1.2.4. Similar to the methods developed for detection of stiction, compensation methods are not without some limitations. The proposed method has focused on overcoming some of the remaining issues which previous

methods are facing. These problems are addressed here:

Geometry of the compensating signal and stiction model: It was concluded from studying "Knocker" and "Constant Reinforcement" methods that geometry features of the compensator signal is related to the oscillations observed in OP and PV signals. It is required to find an compensating signal which can effectively remove all or some parts of the oscillations from the system.

Forcing OP to have constant value: This idea is practical as long as the steady state condition of the process does not change over time, i.e., if the setpoint is changing, it is not wise to fix OP at an unsuitable value. Existence of an algorithm which is able to learn new steady states conditions during the operation is necessary in order to pursue this idea.

Improvement of two-move approach: Although looks simple, two-move method is the most effective approach to change the position of the stem of a sticky valve. This fact is a motivation for the following work. For instance, using two-parameter stiction models [24, 7, 17] instead of the one-parameter model [46] can increase the accuracy of its performance.

4.2.1 General Idea and Assumptions of the Method

Without doubt, control valves are not the first examples of effect of stiction on mechanical instruments. Many publications can be found which have tried to model, detect, and compensate for this phenomenon. For example, one of the simplest methods to attack such a problem is to vibrate the sticky surfaces with high frequency. It is similar to the idea of "Knocker" method, and does not use any specific friction model. But if a good model is available, there is an alternative. The friction force can be estimated using the model, and then an equal force in the opposite direction can compensate the effect of friction [33]. Effective application of this idea to a system with stiction, needs some assumptions:

1. The plant is stable and completely controlled in absence of stiction.
2. Plant model is known.
3. Stiction parameters have been quantified accurately.

The proposed methodology consists of three parts: (1) learning the steady state, (2) holding the controller output at its steady state value (OP_{ss}) and (3) regulating the position of the valve stem. Automation of this algorithm will help compensation for stiction, even for the case of changing setpoint. In the next few sections, each of the above mentioned steps will be discussed in detail.

4.2.2 Learning the Steady State

In order to keep the valve stem at a proper position (MV_{ss}), the first thing to find is the position for the system which is already oscillating due to stiction nonlinearity. In some cases, there exists some prior information about the steady state of the system, such as numerical values of controller output (OP_{ss}), valve position (MV_{ss}), and process output (PV_{ss}). It is obvious that they are all equivalent and depend on the setpoint (SP). If the setpoint changes, the information will no longer be useful.

There are some simple facts about a control loop with stiction which will be stated shortly. Note that all numerical values should have the same units, e.g., percentage of the valve travel length. Otherwise, the term "equality" will be meaningless. The conversion of units can be done using look-up table of the valve. This table, being provided by the manufacturer, assigns a valve percentage to each value of controller output signal.

1. When there is no stiction in control valve, because OP and MV are always equivalent, the system will eventually reach its steady state.

2. If the valve suffers from stiction, at each time step t, controller output and valve position are different ($OP_t \neq MV_t$).

3. In presence of stiction, because of the feedback, the control error (e_t) has a value inequivalent to OP_t for all time steps. Therefore, the system will not settle and continues to oscillate.

Among all mentioned facts, only the second requires further illustration. It is known that OP/MV plot (also called valve signature) for a sticky valve has the shape of parallelogram instead of straight line. The mentioned difference is observable in Figure 4.1, where MV_t is the desirable position and equivalent to OP_t, and MV_{up} and MV_{down} are representing the situations when the sticky valve is moving upwards and downwards, respectively.

The difference between required and actual positions of the valve is representative of friction force. Considering this point and above stated facts, the solution to the problem appears to be removal of this difference by opposing the friction with an equal force.

Consider a standard control loop with a compensator block similar to Figure 4.2. For each time step t, we can find the proper position of the valve ($\widehat{MV}_t$) which is equivalent to OP_t, using look-up table of the valve.

$$\widehat{MV}_t = OP_t \tag{4.1}$$

It is also known that the actual position of the valve (MV_t) is different from $\widehat{MV}_t$.

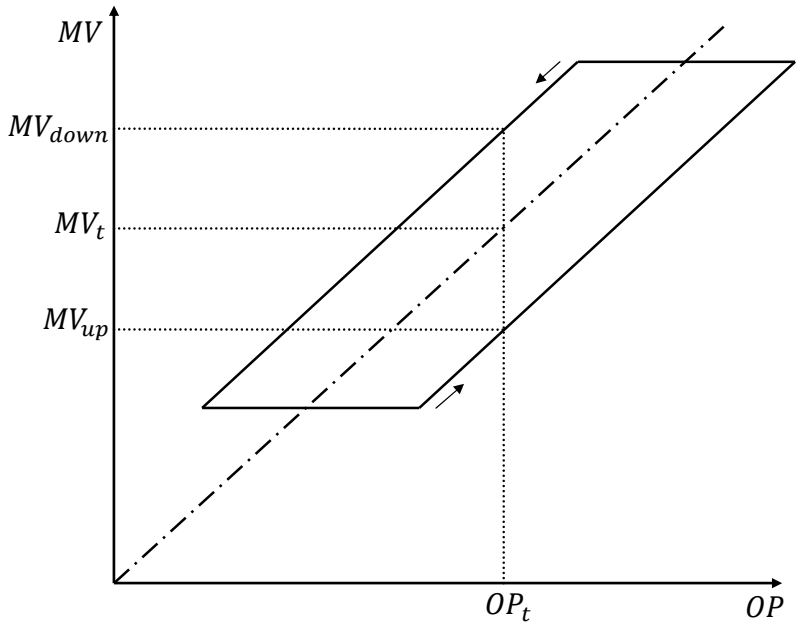

Figure 4.1: Signature of a control valve with stiction (simplified).

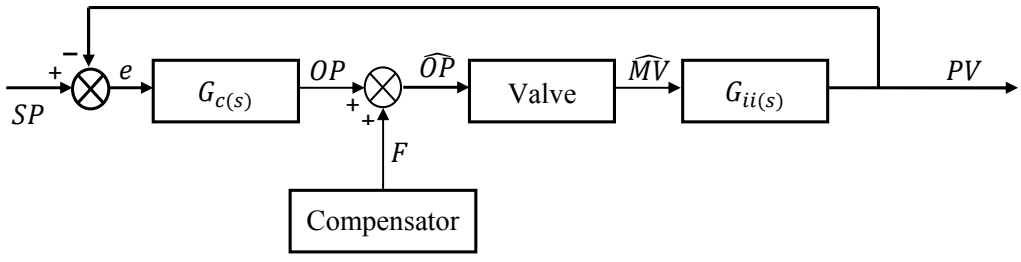

Figure 4.2: Block diagram of a standard control loop and position of the compensator block.

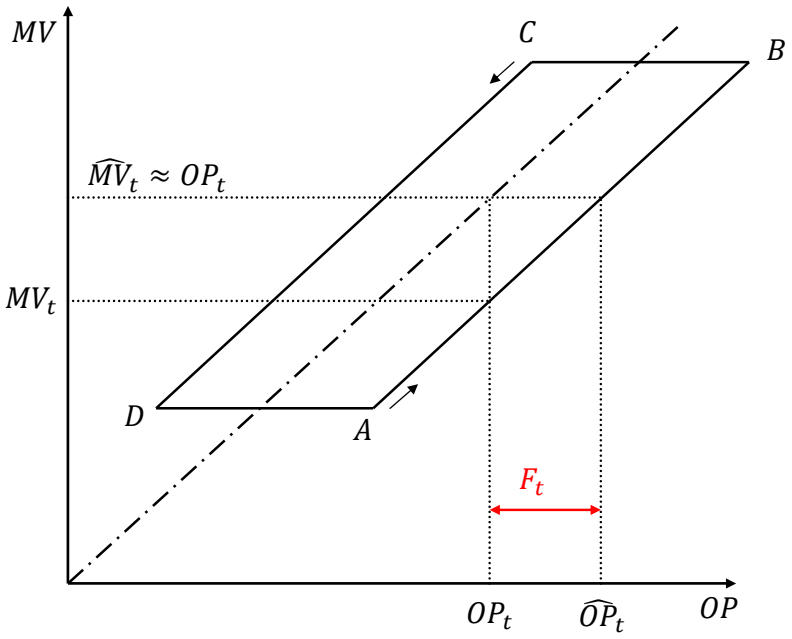

Figure 4.3: Calculation of F_t Using the Valve Signature.

$$MV_t = \mathcal{S}(OP_t, MV_{t-1}, f_s, f_d) \tag{4.2}$$

where $\mathcal{S}$ represents the stiction model, and f_s and f_d are parameters used in He's two-parameter stiction model. The position of a sticky valve at each time step depends on the value of the control command at the current time, previous position of the valve, and severity of stiction. Suppose we can calculate $\widehat{OP}_t$ for which the valve settles at $\widehat{MV}_t$.

$$\widehat{OP}_t = \mathcal{S}^{-1}(\widehat{MV}_t, MV_{t-1}, f_s, f_d) \tag{4.3}$$

Therefore we can calculate the force (F_t) which is required to remove the difference between MV_t and $\widehat{MV}_t$.

$$F_t = \widehat{OP}_t - OP_t \tag{4.4}$$

This force (or its equivalent) will be added to OP_t at each time step, shown in Figure 4.2. As a result, OP_t and new valve position ($\widehat{MV}_t$) will be (or approximately) equal. Hence, the problem changes to: How can $\widehat{OP}_t$ be calculated? To answer this question, a precise model is required for stiction. Once a model is accessible, the behavior of the valve (valve signature) can be predicted. Figure 4.3 shows how $\widehat{OP}_t$ is calculated using the signature of a valve.

It is indicated in Figure 4.3 that

$$\widehat{MV}_t \approx OP_t \tag{4.5}$$

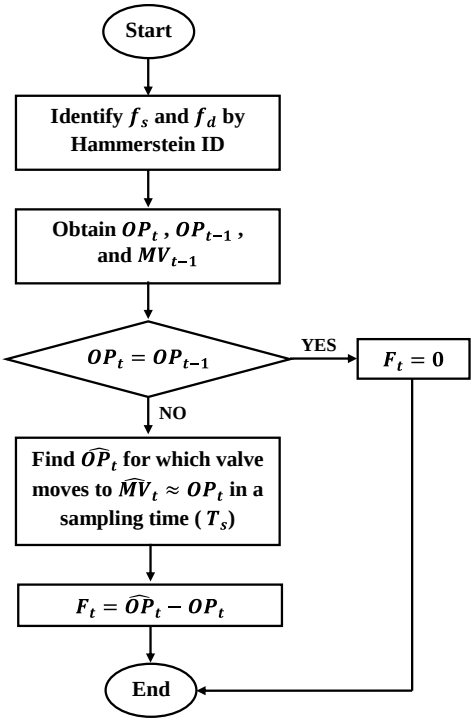

Figure 4.4: Algorithm of Finding Steady State of the System.

This is due to the fact that in the signature of a sticky valve, two long sides of the parallelogram are not straight lines, but have step-wise changes, i.e., lines $\overline{AB}$ and $\overline{CD}$ are formed by sequences of steps. Therefore, in practice, possible values of the valve position on the vertical axis are discrete, while controller output can have continuous values. Equation 4.5 emphasizes that when there is no $\widehat{MV}_t$ which is exactly equal to OP_t, its closest value should be picked for further calculations.

To automate calculation of the compensator signal, the flowchart in Figure 4.4 can be used. This flowchart shows the procedure of calculation of F_t for one time step.

After implementation of this procedure, controller output is settled at its steady state value (OP_{ss}). But due to small deviations of $\widehat{MV}_t$ and OP_t, still there may be slight oscillations in the system around steady state.

Finally, after running the algorithm between time t_1 and t_2, OP_{ss} can be calculated by taking average of OP_t over time.

$$OP_{ss} = \frac{\sum_{t_1}^{t_2} OP_t}{t_2 - t_1} \tag{4.6}$$

This algorithm, called "learning", has the ability to find OP_{ss} for a process with variable setpoint, using stiction model and routine process information. The system is now ready to be stabilized by keeping OP at its steady state value, calculated using Equation 4.6.

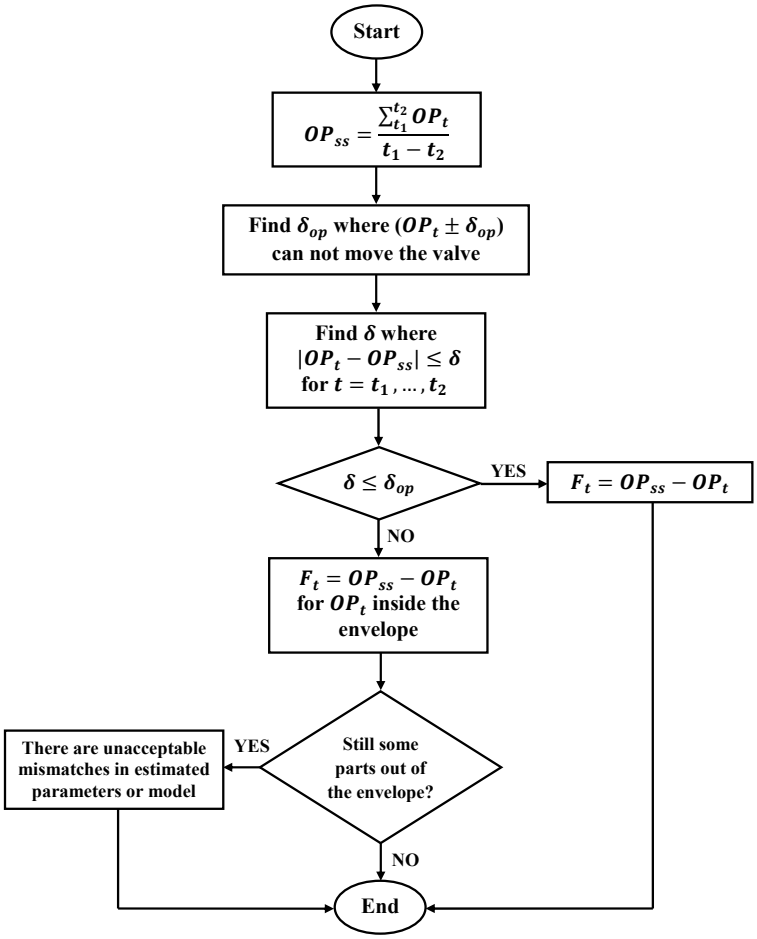

Figure 4.5: Algorithm of Maintaining Controller Output at OP_{ss}.

4.2.3 Holding the Control Command at OP_{ss}

It was mentioned in Section 4.2.2 that because of the discrete positions of the valve, OP will slightly oscillate around OP_{ss}. Suppose these fluctuations can be located in an envelope with 2δ of width. Also, there always exists another envelope, $2\delta_{op}$ wide, so that all changes of OP inside this envelope will not change the position of the valve, i.e., it cannot overcome the static friction force. The value of δ_{op} depends on severity of stiction in the valve. The case $\delta > \delta_{op}$ means while implementing learning algorithm, OP can change significantly enough to make the valve move. These movements cause OP not to settle, hence calculation of OP_{ss} will be affected. The cause of this problem is incorrect predictions of the stiction model, in other words, poor estimation of stiction parameters.

Figure 4.5 shows flowchart of the procedure for fixing OP at OP_{ss}. This procedure is required to be run after learning step, to effectively keep the valve from destructive movements. In the next sections, the latter explained action will be addressed as "holding" step.

4.2.4 Regulating the Position of the Valve Stem (MV_{ss})

After running previous steps, the oscillation has been removed from the system and the valve stem has no extra movements. But, a new problem will be observed: Fixing the controller output signal at OP_{ss} in a random time, does not guarantee that the process output converges to its desirable value (setpoint).

To illustrate this observation, suppose at time t, OP is forced to remain at OP_{ss}, i.e., initiating holding phase. Considering that the learning procedure is finished at time $t-1$, the following equations hold.

$$\begin{aligned} F_{t-1} &\neq 0 \\ F_t = 0 &\Rightarrow \widehat{OP}_t = OP_t \\ \widehat{MV}_{t-1} &= OP_{t-1} \end{aligned} \tag{4.7}$$

The new position of the valve can be calculated as

$$\widehat{MV}_t = \mathcal{S}(OP_{ss}, \widehat{MV}_{t-1}, f_s, f_d) \tag{4.8}$$

Equation 4.8 can be rewritten using Equation 4.7as follows.

$$\widehat{MV}_t = \mathcal{S}(OP_{ss}, OP_{t-1}, f_s, f_d) \tag{4.9}$$

According to the definition of δ_{op}, explained in Section 4.2.3, the valve will not move if accumulative control signal is not large enough,i.e.

$$|OP_{ss} - OP_{t-1}| < \delta_{op} \Rightarrow \widehat{MV}_t = OP_{t-1} = \widehat{MV}_{t-1} \tag{4.10}$$

While the learning algorithm is being run, the difference between OP_{t-1} and OP_{ss} is insignificant if quantification of stiction parameters is accurate. In other words, in case of use of an accurate stiction model and depending on the time of initiation of the holding algorithm, the valve remains in the same position as of the previous time step. Therefore, the process output will be different from the expectation.

The solution to this problem is discussed in [43], which developed the two-move compensation approach. As stated in Section 4.2, this method can be improved using two-parameter models. These two moves of the valve stem, can be made by manipulation of OP. For a valve stuck in the wrong place, it is known that

$$\begin{aligned} MV_{ss} &= OP_{ss} \\ \widehat{MV}_t &\neq MV_{ss} \end{aligned}$$

In two-moves framework, the two moves should be large enough to overcome the friction force and move the valve stem, but not too large to make the valve saturated. Suppose that the value of the controller output signal increases from OP_{ss} to OP_{mid} in the first move. Then the intermediate position of the valve ($\widehat{MV}_{mid}$) is

$$\widehat{MV}_{mid} = \mathcal{S}(OP_{mid}, \widehat{MV}_t, f_s, f_d) \tag{4.11}$$

where $\widehat{MV}_t$ is the wrong position of the valve before enforcing it by two moves. For the second move, the controller output will change from OP_{mid} to OP_{end}, in order to bring the valve stem to its final position $\widehat{MV}_{end}$.

$$\widehat{MV}_{end} = \mathcal{S}(OP_{end}, \widehat{MV}_{mid}, f_s, f_d) \tag{4.12}$$

Now the problem changes to finding OP_{mid} and OP_{end} such that Equation 4.13 holds.

$$\widehat{MV}_{end} = MV_{ss} = OP_{ss} \tag{4.13}$$

It is not difficult to find suitable values for these two moves, because based on nature of stiction there are only two simple conditions to be satisfied.

$$|OP_{ss} - OP_{mid}| > \frac{f_s + f_d}{2}$$
$$|OP_{mid} - OP_{end}| > \frac{f_s + f_d}{2}$$

where f_s and f_d are the stiction parameters used in He's stiction model [17]. It can also be replaced by S, where S is one of the other commonly used parameters in two-parameter models [24, 7]. The only remaining unknown point of the design procedure is the value of $\widehat{MV}_t$ which is not always accessible. Unfortunately, measurement of this quantity is impossible for majority of control valves in practice. In cases when exact value of $\widehat{MV}_t$ is unknown, the process model is used to estimate it.

$$PV = G_p\widehat{MV} \Rightarrow \widehat{MV} = G_p^{-1}PV \tag{4.14}$$

where both PV and $\widehat{MV}$ are stabilized. It is obvious that there may be inaccuracy in estimation of $\widehat{MV}$ because of process model mismatch. The effect of uncertainty on performance of the method will be discussed later. Figure 4.6 shows the regulation step done for a sticky valve, when the actual location of the valve stem is higher than its expected value ($\widehat{MV}_t > OP_{ss}$).

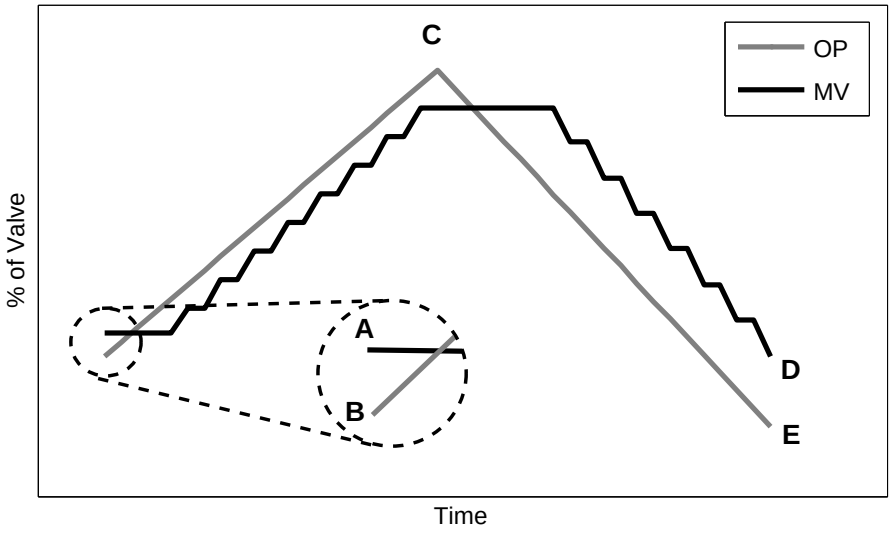

Figure 4.6: Regulation of MV using two changes in OP.

Table 4.1: Corresponding values for the points shown in Figure 4.6.

Point	A	B	C	D	E
Value	$\widehat{MV}_t$	OP_{ss}	OP_{mid}	OP_{ss}	OP_{end}

The numerical values of points A to E, shown in Figure 4.6, are stated in Table 4.1. It is noteworthy that, the objective of this section can be summarized as moving from point A to D.

Remark: Obviously, directions of two moves are opposite. But it is possible to use both upward and downward directions for the first move. Based on experiences, it is more effective to use upward direction for the first move when the valve is needed to be slightly closed, i.e. $\widehat{MV}_t > OP_{ss}$, and downwards for opening the valve.

4.3 Simulation Results

The simulated system includes a First Order Plus Dead Time (FOPDT) process which is controlled by Proportional-Integral (PI) controller. The two-parameter model proposed by He et. al. is used to simulate behavior of sticky valve.

$$G_p = \frac{0.66}{6.7s+1}e^{-2.6s}$$
$$G_c = 0.1 + \frac{0.09}{s}$$
$$f_s = 3.0$$
$$f_d = 2.0$$

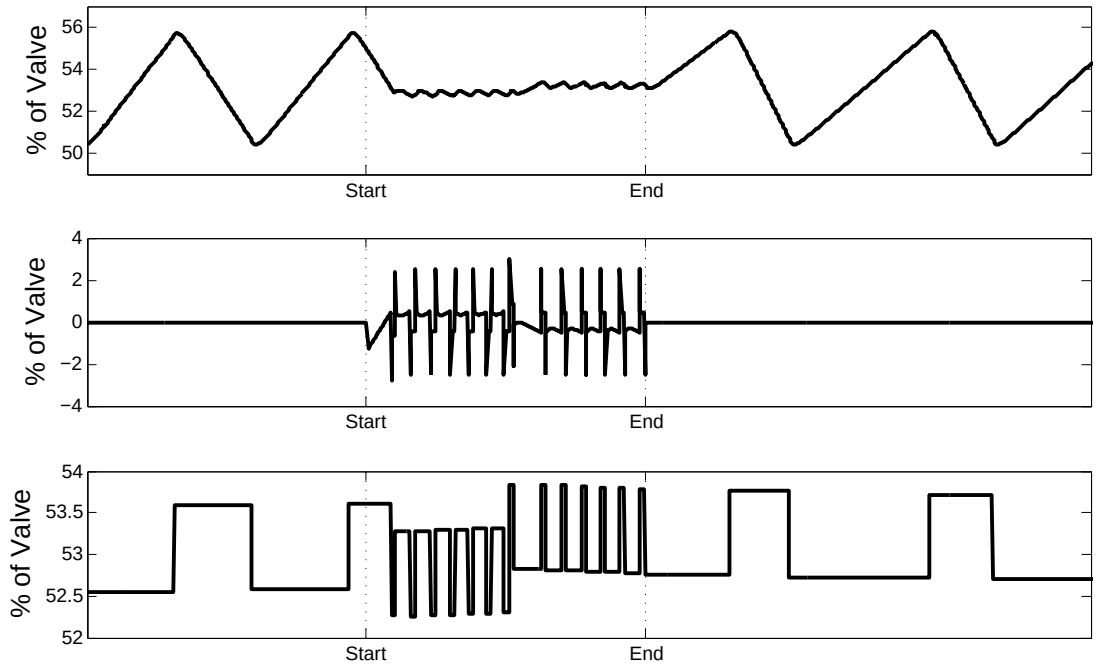

Figure 4.7: Results of the learning phase; controller output (up), compensating signal (middle), and valve position (bottom).

The system is controlled in absence of stiction, and oscillates significantly in its presence. The value of setpoint for this system is fixed at $SP = 2$.

4.3.1 Learning Phase

In this phase, the objective is to find steady state value of controller output. Detailed algorithm is explained in Section 4.2.2. Figure 4.7 shows the result of implementation of this phase. learning algorithm is run from 1000 to 1500 seconds.

It can be observed in Figure 4.7 that OP is almost stabilized in this phase. Also, the geometry of added signal is different from that of other methods, such as knocker and constant reinforcement. The valve still has aggressive movements which is not desirable. In the next step, OP will be fixed at the calculated value of $OP_{ss} = 53.0\%$.

4.3.2 Holding Phase

In this phase, the controller output signal will be fixed. To show the problem described in Section 4.2.4, two simulations have been done. In these simulations, holding phase is initiated in two different time steps, to show the dependency of final position of the valve, which is wrong, on time of initiation. Figures 4.8 and 4.9 illustrate the results.

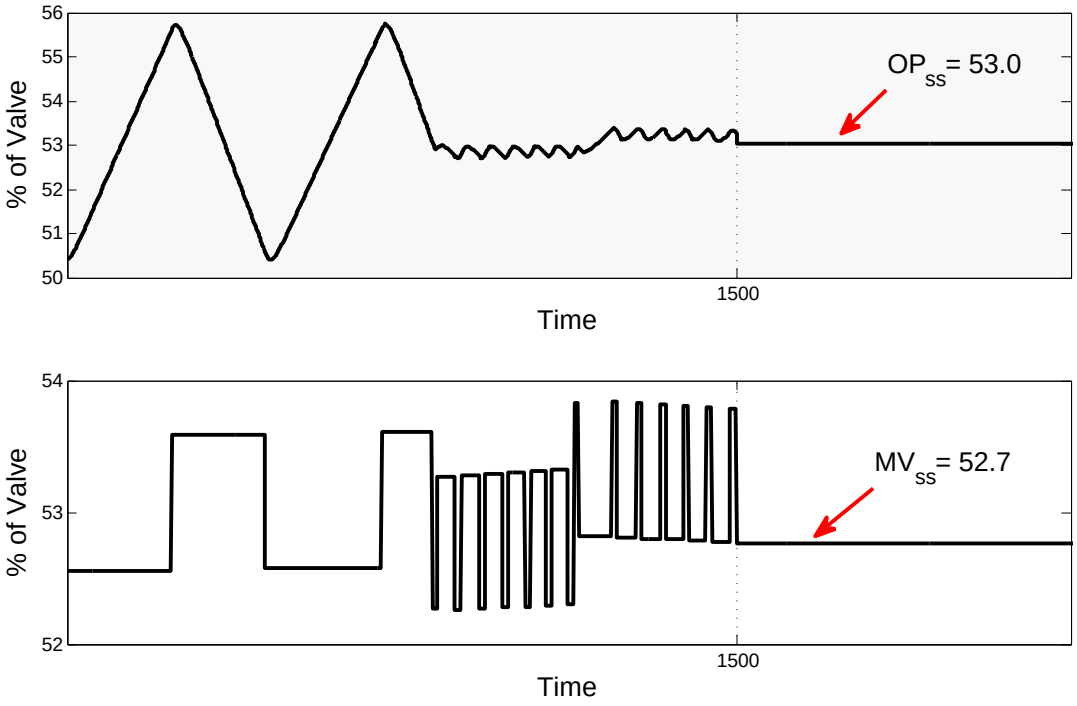

Figure 4.8: Results of the holding phase, initiation time= 1500 s; Controller output (up), valve position (bottom).

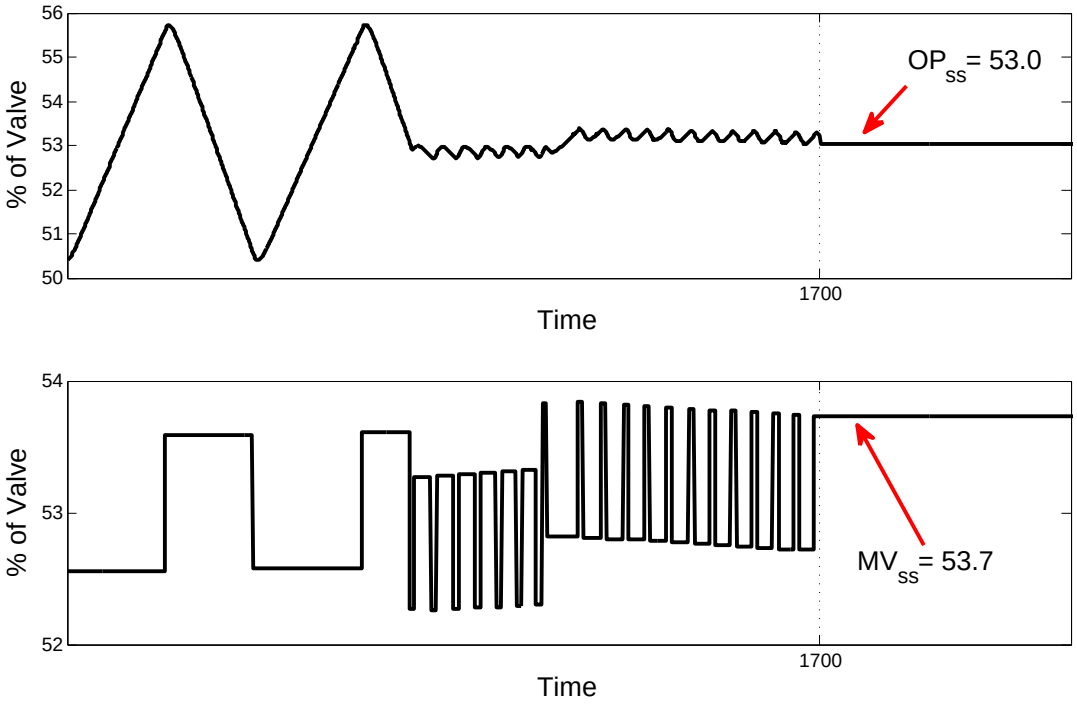

Figure 4.9: Results of the holding phase, initiation time= 1700 s; Controller output (up), valve position (bottom).

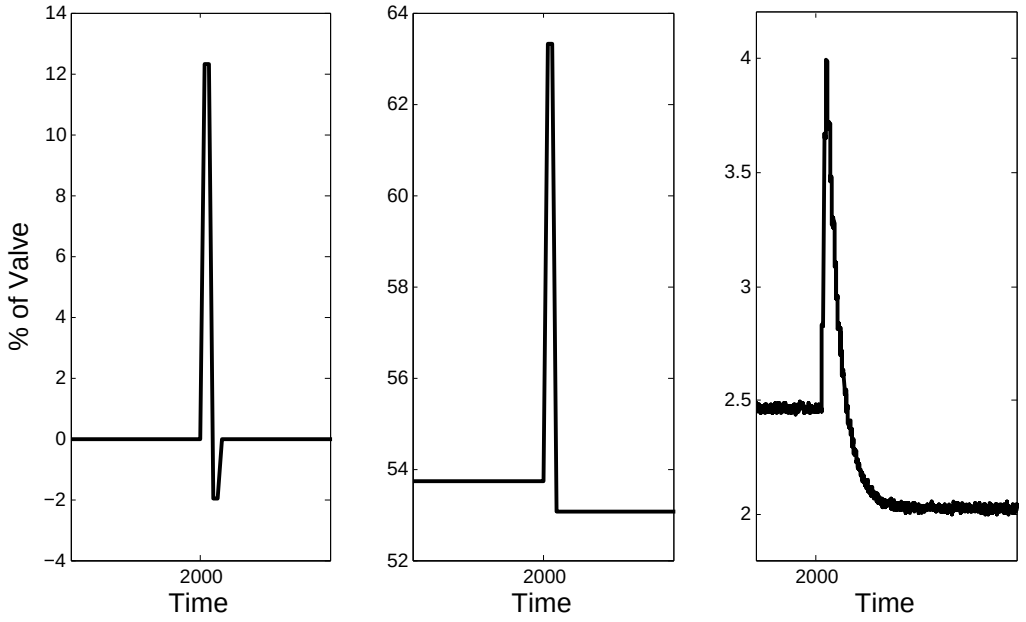

Figure 4.10: Regulation phase; Compensating moves (left), valve position (middle), and process output (right).

4.3.3 Regulation Phase

In order to illustrate the performance of the regulation phase, the second simulated case is used, when the holding is started at $t = 1700\ s$ and the wrong position of the valve is as expected. Table 4.2 shows the calculated values of the added signals to create two moves. They are equivalent to friction forces in each move. The negative value of f_2 shows its downwards direction.

Table 4.2: Calculated forces for the regulation phase.

OP_{ss}	$f_1(OP_{mid})$	$f_2(OP_{end})$	PV_{ss}
53.0	12.3	-14.25	2.00

Figure 4.10 shows two designed changes in the compensator signal, along with variations of the valve position and process output. The procedure of regulation was performed at $t = 2000\ s$.

Finally, the whole plot of the proposed compensation method implemented on a FOPDT system, including all three parts, is shown in Figure 4.11.

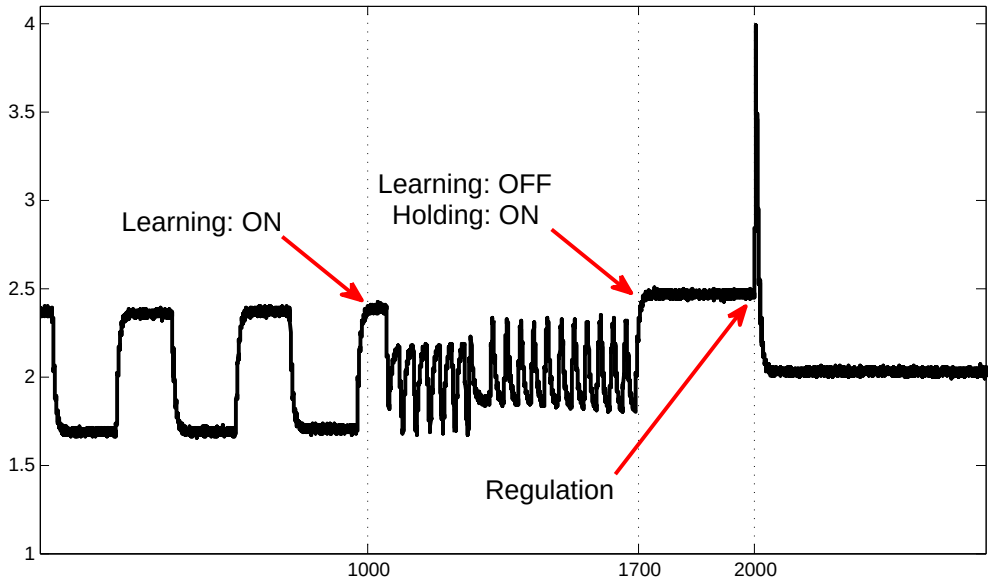

Figure 4.11: The entire procedure of compensation for the simulated system.

4.4 Effect of Uncertainty in Estimation of Model and Stiction Parameters

One of the basic assumptions of the developed method is the accurate estimation of the plant model and stiction parameters. The achieved estimations for model parameters can deviate from their actual values. In this section, sensitivity of performance of the method to these mismatches is illustrated by an example.

4.4.1 Stiction Parameters (f_s and f_d)

According to the algorithm of compensation, it is predictable that the main effect of inaccuracy in estimation of stiction parameters can be seen in the part related to determination of OP_{ss}. Incorrect estimation of OP_{ss} causes variations in the final value of the process output.

Consider $\hat{f}_s$ and $\hat{f}_d$ as estimated values of stiction parameters. The same system has been used as in Section 4.3. Simulations are done for diverse scenarios based on numerical values of stiction parameters. Table 4.3 shows the results.

4.4.2 Model Parameters (K, τ, and θ)

Among three parameters of FOPDT system, the process gain (K) has the most severe effect on performance of the method. Table 4.4 shows the results of this study, for different values of k and corresponding outputs. The different values of θ and τ do not change the final value of PV significantly.

Table 4.3: Uncertainty in estimation of the stiction parameters.

$\hat{f}_s$	$\hat{f}_d$	$\hat{OP}_{ss}$	$f_1(OP_{mid})$	$f_2(OP_{end})$	PV_{ss}
3	1.5	52.99	15.5	-17.6	1.97
3	2.5	53.04	7.9	-10	2.01
2.5	2	53.16	12.2	-14.1	2.08
3.5	2	53.17	13.8	-15.65	2.08

Table 4.4: Uncertainty in estimation of the process gain (K).

Relative Error (%)	$\hat{OP}_{ss}$	PV_{ss}
-20	53.8	2.006
-15	53.6	2.019
-10	53.4	2.019
-5	53.2	2.006
5	52.9	2.009
10	52.8	2.032
15	52.6	1.973
20	52.5	1.98

4.5 Conclusion

In this chapter, a model-based approach for stiction compensation was proposed. Achieving a non-oscillatory output without forcing the valve stem to move faster and wider than normal, is the most important characteristic of this algorithm. Using two-parameter stiction model, which predicts the behavior of a sticky valve more precisely, this method does not need extensive prior information about the process and the controller, and also can be automated to track setpoint changes during operation. The simulation results are illustrated, and ability of the method to handle uncertainties in estimation of the process model and stiction severity is discussed.

Chapter 5

Compensation For Stiction Using Controller Tunings

5.1 Process/Controller Pairings and Dynamics

Static friction, also called stiction, is one of the most frequently observed faults of control systems. Generally, the properties of oscillations caused by nonlinearities depend on dynamics of the entire system. In other words, in a standard control loop, not only the process transfer function, but also type of the controller, and tunings of its parameters have direct effect on frequency and magnitude of the nonlinear-induced oscillations [6]. This chapter focuses on study of the relations between numerical values of parameters of Proportional-only (P-only) and Proportional-Integral (PI) controllers, and characteristics of the oscillations observed in first order self-regulating and integrating processes. Selected controllers and process types are the most commonly used systems in chemical industries, for the purpose of modeling, control, and optimization. In the next sections, using the general condition of occurrence of nonlinearity-induced oscillations in multi-loop systems, proposed in Chapter 3, related analysis of single-loop first order systems will be presented. In all cases, the objective is to find the optimum tuning of the controller parameters, for which the frequency and magnitude of oscillations are reduced, or permanently eliminated if possible.

5.2 Aggressive Tuning of Controller for Systems With Stiction

The common root causes of oscillations in control loops can be classified as external or internal, according to [49]. Aggressive tuning of controllers and valve nonlinearities are known as internal causes. In most of the oscillating systems, distinguishing between these two possible sources is a tricky task, as stability analysis of nonlinear

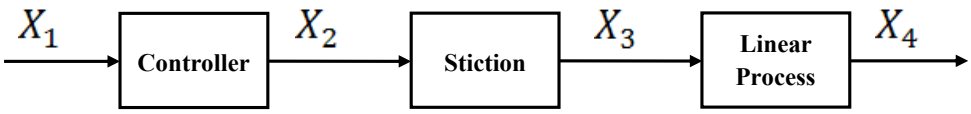

Figure 5.1: Open-loop configuration of a process with controller and sticky control valve.

system is complicated. Some simple approaches to discriminate linear and nonlinear causes have been proposed in [55] and [52]. This work will adopt the Nyquist stability criteria for stability analysis. As mentioned in Section 2.1, describing function represents an approximation similar to linearization with dependency on operating and initial conditions and some special parameters (like S and J for stiction).

Consider Figure 5.1 for an open-loop configuration of a process. For a sinusoidal input $X_1 = \sin(\omega t)$ to the system, the frequency response X_2 can be determined as follows:

$$X_2 = A_2 \sin(\omega t + \phi_2) \tag{5.1}$$
$$A_2 = |G_{c(j\omega)}| \tag{5.2}$$
$$\phi_2 = \measuredangle G_{c(j\omega)} \tag{5.3}$$

where $G_{c(j\omega)}$ is frequency response of the controller. For stiction, of which DF is shown by N, the output will have the same frequency but different magnitude and phase from those of X_2:

$$X_3 = N_{(S,J,A_2)} = \alpha + \beta j \tag{5.4}$$
$$A_3 = \sqrt{\alpha^2 + \beta^2} \tag{5.5}$$
$$\phi_3 = \phi_2 + \arctan(\frac{\beta}{\alpha}) \tag{5.6}$$

Finally, the response (X_4) of the process ($G_{p(j\omega)}$) can be determined as follows:

$$A_4 = \sqrt{\alpha^2 + \beta^2}|G_{p(j\omega)}| \tag{5.7}$$
$$\phi_4 = \phi_3 + \measuredangle G_{p(j\omega)} \tag{5.8}$$

In this procedure, X_4 represents the response of the open-loop system to a sinusoidal input with frequency of ω. The same task can be done for inputs with different frequencies and then the trajectory of frequency response can be generated in the complex plane. According to Nyquist criteria, if the point (-1,0) is not enclosed by this trajectory, the controller is tuned well. This statement can be made

due to this fact that most of the process control problems are open-loop stable and have no unstable pole-zero cancelation [39], i.e., Nyquist stability criterion will be limited to number of encirclements of the critical point by the FR curve. Hence, the other possible source, i.e. stiction, can induce oscillation.

5.3 First Order Self-regulating Process

Generally, the term "First Order Process" is referred to the processes, of which dynamics between inputs and outputs can be described by a first order differential equation in time domain. Transformation of such differential equation to Laplace domain results in a transfer function with power of one for the variable s in denominator. The mostly used model for chemical processes with self-regulating behavior is shown by Equation 5.9.

$$G_{(s)} = \frac{Y_{(s)}}{U_{(s)}} = \frac{K}{\tau s + 1} e^{-\theta s} \tag{5.9}$$

where $Y_{(s)}$ and $U_{(s)}$ are laplace transforms of the output and the input of the system respectively, and the parameters K, τ and θ are gain, time constant (or rise time) and time delay (or dead time) of the process. The dynamics of a first order self-regulating process can be completely determined by these three parameters.

Along with the process, the controller is another basic element of a control loop. Proportional-integral (PI) controller is one of the mostly used controllers in chemical industries. As obvious in name, its dynamics include two parts. Equation 5.10 shows the standard form of dynamics of PI controller from the control error ($E_{(s)}$) to the control signal ($OP_{(s)}$).

$$G_{c(s)} = \frac{OP_{(s)}}{E_{(s)}} = K_c(1 + \frac{1}{\tau_I s}) \tag{5.10}$$

where K_c and τ_I are refereed to as proportional gain and integral time constant. As a matter of fact, different numeric values for this two parameters, also known as controller tuning, specifies the quality of the control action in a loop. The proportional-only (P-only) controller is a special format of this controller, when the integral term ($\frac{1}{\tau_I s}$) is zero.

5.3.1 Process Without Time Delay ($\theta = 0$)

In this section, a fast first order self-regulating process will be considered in a single-loop control system. The controller can be PI or P-only. According to the proposed condition in Section 3.2.1, existence of solution for Equation 5.11 confirms occurrence of oscillation in the system because of the stiction in control valve.

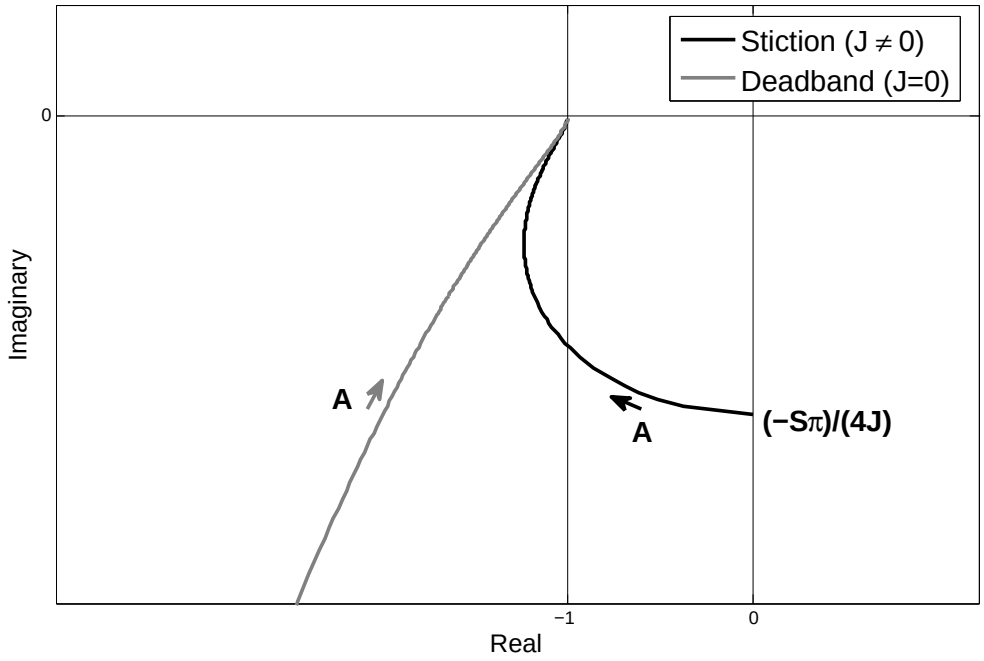

Figure 5.2: Trajectories of $\frac{-1}{N_{(A)}}$ for deadband and stiction.

$$G_{(j\omega)}G_{c(j\omega)} = \frac{-1}{N_{(A)}} \tag{5.11}$$

where $N_{(A)}$ is the stiction describing function (DF), introduced by [7] and discussed in Section 3.2. The fact that the linear and nonlinear parts of the condition are separable, enables us to detect existence of the solution graphically. To do so, the trajectories of both sides of the Equation 5.11 are plotted in a complex plane for different values of frequency (ω) and magnitude (A). Intersection of two curves confirms occurrence of the oscillation.

Table 5.1 shows behavior of the nonlinear part ($\frac{-1}{N_{(A)}}$) for extreme values of the independent variable A. Also, Figure 5.2 shows the related trajectories for stiction ($J \neq 0$) and deadband ($J = 0$).

Table 5.1: Extreme values of $\frac{-1}{N_{(A)}}$.

	Real Part	Imaginary Part
$A \to \frac{S}{2}$	0	$\frac{-\pi S}{4J}$
$A \to \infty$	-1	0

The behavior of the linear side of Equation 5.11 will be studied separately in next sections, based on types of the process and the controller.

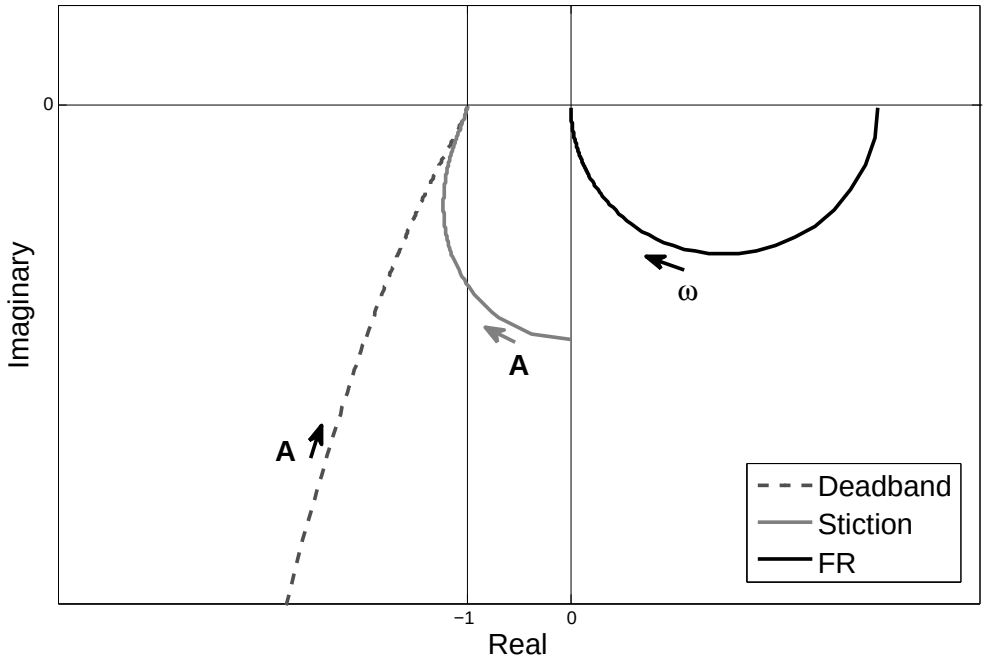

Figure 5.3: Trajectories of $\frac{-1}{N_{(A)}}$ for deadband and stiction and FR for fast self-regulating process controlled by P-only controller.

P-only or PI Controller

The left side of the Equation 5.11 is nothing but the frequency response (FR) of the open-loop system. It can be derived for a pair of process and controller, of which dynamics are known, by substituting $j\omega$ in place of s in their transfer functions. For this case, Equation 5.12 describes the frequency response.

$$G_{(j\omega)}G_{c(j\omega)} = \frac{KK_c}{1+\tau^2\omega^2} - j\frac{KK_c\tau\omega}{1+\tau^2\omega^2} \tag{5.12}$$

Extreme values of the FR are reported in Table 5.2. As it is obvious in Equation 5.12, neither of real and imaginary parts of the FR cannot be zero, i.e., the trajectory of the linear part does not cross any of the axes.

Table 5.2: Extreme values of $G_{(j\omega)}G_{c(j\omega)}$ for fast self-regulating process, controlled by P-only controller.

	Real Part	Imaginary Part
$\omega \to 0$	KK_c	0
$\omega \to \infty$	0	0

Figure 5.3 shows that for such a system, oscillation will not occur because of stiction or deadband, since there is no intersection for two curves.

If P-only controller is replaced with PI, the same results will be implied, since

the only difference between these two cases is the value of FR for small values of ω as illustrated in the following equations:

$$G_{(j\omega)}G_{c(j\omega)} = \frac{KK_c}{1+\tau^2\omega^2}(1-\frac{\tau}{\tau_I}) - j\frac{KK_c}{1+\tau^2\omega^2}(\tau\omega - \frac{1}{\tau_I\omega}) \tag{5.13}$$

$$\lim_{\omega\to 0} G_{(j\omega)}G_{c(j\omega)} = KK_c(1-\frac{\tau}{\tau_I}) \tag{5.14}$$

This slight difference does not affect the overall trajectory of the FR. Therefore, in a system with self-regulating process, controlled by P-only or PI controller, oscillation will not occur due to existence of stiction or deadband in the control valve.

5.3.2 Process with Time Delay ($\theta \neq 0$)

This class of processes are also known as First Order Plus Dead Time (FOPDT), and have the general form shown in Equation 5.9. Frequency response of such processes are different from that of processes without delay, since the exponent can be re-written as summation of sinusoidal terms. This fact causes infinite number of intersection for the trajectory of FR and two axes.

P-only Controller

When an FOPDT process is controlled by a P-only controller, the expression of the open-loop FR can be described as Equation 5.15 shows.

$$\begin{aligned} G_{(j\omega)}G_{c(j\omega)} =& \frac{KK_c}{1+\tau^2\omega^2}[\cos(\theta\omega) - \tau\omega\sin(\theta\omega)] \\ & - j\frac{KK_c\tau\omega}{1+\tau^2\omega^2}[\sin(\theta\omega) + \tau\omega\cos(\theta\omega)] \end{aligned} \tag{5.15}$$

Table 5.3 shows response of the system to extreme values of frequency. At two extreme values, the behavior is identical to that of the process without delay.

Table 5.3: Extreme values of $G_{(j\omega)}G_{c(j\omega)}$ for self-regulating process with delay, controlled by P-only controller.

	Real Part	Imaginary Part
$\omega \to 0$	KK_c	0
$\omega \to \infty$	0	0

As mentioned before, trajectory of FR crosses real and imaginary axes in multiple points. For this analysis, only two points where the curve crosses each axis for the first time are important. Figure 5.4 illustrates these two points for the studied

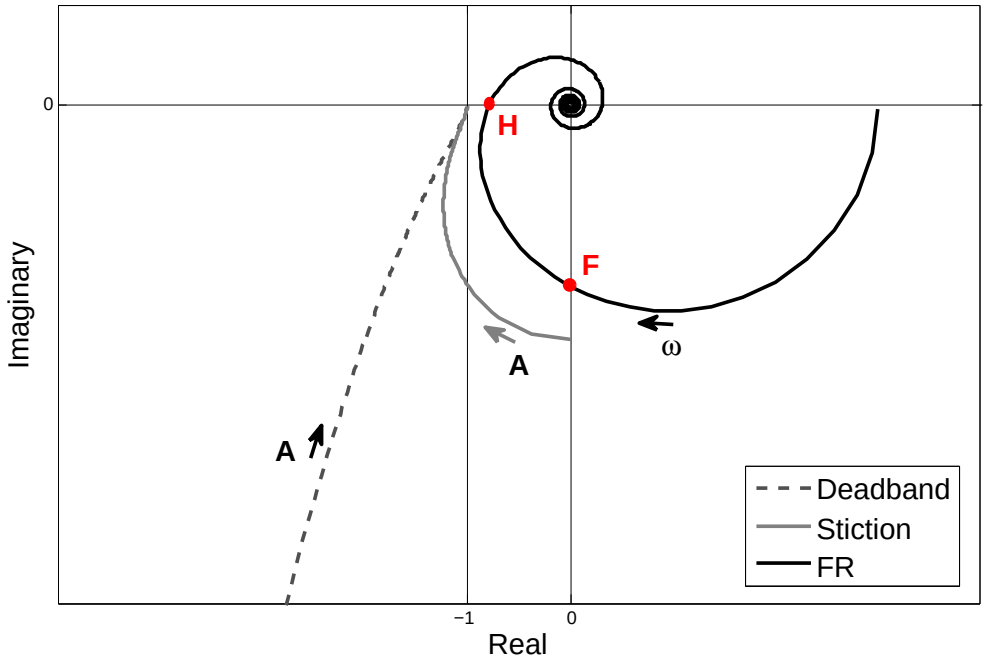

Figure 5.4: Trajectories of $\frac{-1}{N_{(A)}}$ for deadband and stiction and FR for FOPDT process controlled by P-only controller.

case. The projections of these points on the lying axis, and also the corresponding frequencies can be calculated using Equations 5.16 to 5.19.

$$F_{imag} = \frac{-KK_c}{1+\tau^2\omega^{*2}}[\sin(\theta\omega^*) + \tau\omega^*\cos(\theta\omega^*)] \tag{5.16}$$

$$H_{real} = \frac{KK_c}{1+\tau^2\omega^{**2}}[\cos(\theta\omega^{**}) - \tau\omega^{**}\sin(\theta\omega^{**})] \tag{5.17}$$

$$\omega^* = \frac{1}{\theta}\tan^{-1}(\frac{1}{\tau\omega^*}) \tag{5.18}$$

$$\omega^{**} = \frac{1}{\theta}\tan^{-1}(-\tau\omega^{**}) \tag{5.19}$$

where ω^* and ω^{**} are frequencies, at which the trajectory locates at points F and H respectively (see Figure 5.4). It is clear that the values of these critical frequencies are independent of the controller gain. But, the distances of the point F and H can be manipulated by changing K_c.

According to what was mentioned in Section 5.2, the linearized system is stable when the trajectory of open-loop FR (X_4) does not encircle the point $-1 + j0$. Another remarkable point about the stability is that the value H_{real} for the linear system should always have a value greater than -1. This guarantees suitable tuning of the controller in absence of stiction. Also, based on the behavior of the stiction DF, explained in Section 5.3.1, the system will not oscillate due to existence of stiction or deadband, if $F_{imag} > \frac{-\pi S}{4J}$. In contrast, satisfaction of the condition

$F_{imag} \leq \frac{-\pi S}{4J}$ causes the system to oscillate in presence of stiction, but still not for deadband.

To summarize, an FOPDT process, stabilized by a P-only controller, will not oscillate because of deadband. It oscillates because of stiction, for values of K_c satisfying the inequality (5.20).

$$F_{imag} \leq \frac{-\pi S}{4J} \tag{5.20}$$

where F_{imag} is previously described in Equation 5.16.

PI Controller

For this case, the open-loop FR can be expressed using Equations 5.22 and 5.23. It is obvious that its trajectory will have multiple crossings with the axes.

$$G_{(j\omega)} = \frac{K}{1+\tau^2\omega^2}\Big[\cos(\theta\omega) - \tau\omega\sin(\theta\omega)\Big] \tag{5.21}$$

$$- j\frac{K\tau\omega}{1+\tau^2\omega^2}\Big[\sin(\theta\omega) + \tau\omega\cos(\theta\omega)\Big] \tag{5.22}$$

$$G_{c(j\omega)} = K_c - j\frac{K_c}{\tau_I\omega} \tag{5.23}$$

Similarly, extreme values of open-loop FR is reported in Table 5.4. There is a major difference between this system and previously studied ones. For very small values of frequency, the response has infinite imaginary part and finite real part.

Table 5.4: Extreme values of $G_{(j\omega)}G_{c(j\omega)}$ for self-regulating process with delay, controlled by PI controller.

	Real Part	Imaginary Part
$\omega \to 0$	$KK_c(1 - \frac{\theta+\tau}{\tau_I})$	$-\infty$
$\omega \to \infty$	0	0

The real part of the open-loop FR in small frequencies can be positive, negative or zero, depending on parameters of the system and tuning of the controller. If the controller is tuned such that $\theta + \tau = \tau_I$, this real part will be zero, and the FR trajectory will be similar to that of integrating process, which will be discussed in Section 5.4.2. Otherwise, FR has trajectory similar to either of Figures 5.5 or 5.6.

The parameter d, shown in Figures 5.5 or 5.6, can be expressed as follows.

$$d = |KK_c(1 - \frac{\theta+\tau}{\tau_I})| \tag{5.24}$$

Also, the points F and H with the definitions stated before, along with corresponding frequencies (ω^* and ω^{**}), can be calculated using Equations 5.25 to 5.30.

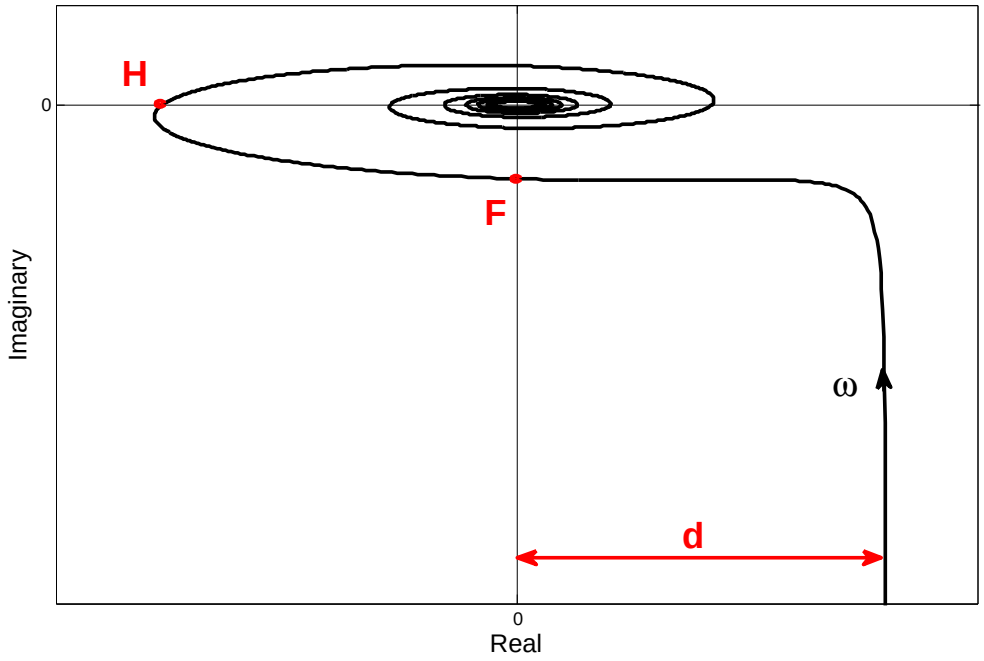

Figure 5.5: Trajectory of open-loop FR for FOPDT process, controlled by PI controller, when $\theta + \tau < \tau_I$.

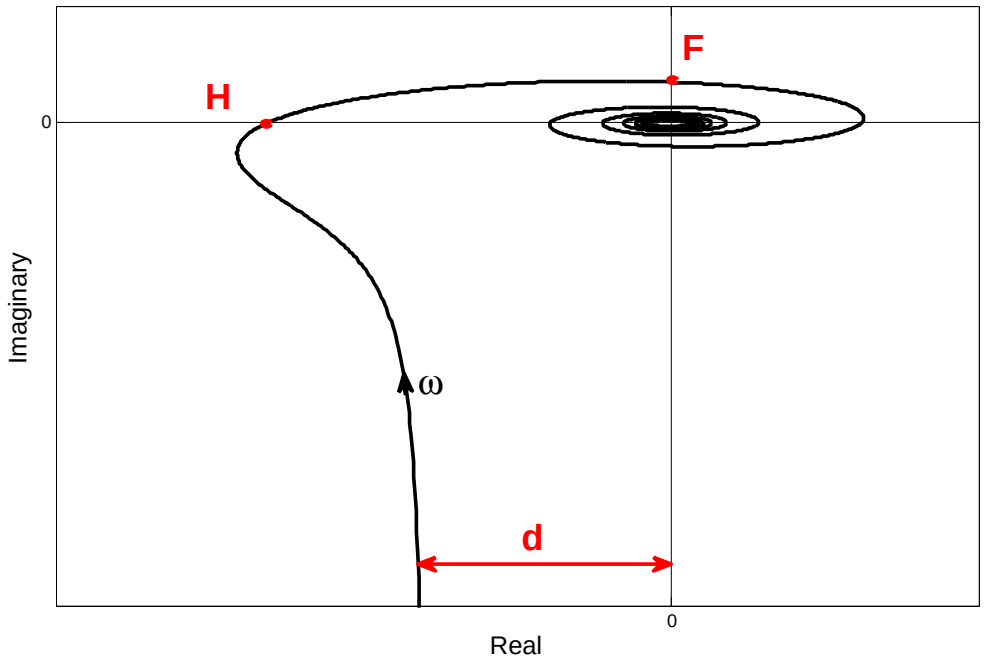

Figure 5.6: Trajectory of open-loop FR for FOPDT process, controlled by PI controller, when $\theta + \tau > \tau_I$.

$$F_{imag} = \frac{-KK_c}{(1+\tau^2\omega^{*2})\tau_I\omega^*}\Big[\cos(\theta\omega^*)[1+\tau\tau_I\omega^{*2}] + \sin(\theta\omega^*)[\tau_I\omega^* - \tau\omega^*]\Big] \tag{5.25}$$

$$H_{real} = \frac{KK_c}{(1+\tau^2\omega^{**2})\tau_I\omega^{**}}\Big[\cos(\theta\omega^{**})[\tau_I\omega^{**} - \tau\omega^{**}] - \sin(\theta\omega^{**})[1+\tau\tau_I\omega^{**2}]\Big] \tag{5.26}$$

$$\omega^* = \frac{\alpha_{(\omega^*)} - \beta_{(\omega^*)}}{\theta} \tag{5.27}$$

$$\omega^{**} = \frac{\beta_{(\omega^{**})} - \alpha_{(\omega^{**})}}{\theta} \tag{5.28}$$

$$\alpha_{(\omega)} = \tan^{-1}(\tau_I\omega) \tag{5.29}$$

$$\beta_{(\omega)} = \tan^{-1}(\tau\omega) \tag{5.30}$$

Any change in controller tuning, affects the values of F_{imag}, H_{real}, d, ω^* and ω^{**}. Again, two conditions for stability of the process in absence and presence of the nonlinearity should hold. If $F_{imag} > 0$ holds (see Figure 5.6), oscillation occurs for stiction regardless of the controller tuning. In the case of $F_{imag} < 0$, situation will be similar to the previous case, when the stiction-induced oscillation can be removed if $F_{imag} > \frac{-\pi S}{4J}$. Otherwise, the system will oscillate due to stiction in the valve. It is noteworthy that, deadband nonlinearity never causes the system to oscillate.

Therefore, for a system with FOPDT process and PI controller, which is oscillating due to stiction, some suggestions can be made in order to eliminate or reduce the oscillations. If $F_{imag} < 0$, it is sufficient to increase value of F_{imag}, while $H_{real} > -1$. In this case, the oscillation will be permanently removed. If $F_{imag} > 0$, the first trial to remove the oscillation should be to tune the controller such that $\theta + \tau < \tau_I$, if possible. Otherwise, one can only decrease the frequency and magnitude of the oscillations by reducing the parameter d. A decrease in d causes the intersection between FR and DF curves to occur in points with smaller values of magnitude (A) and frequency (ω).

5.4 First Order Integrating Process

Equation 5.31 shows the general format of a first order integrating process. Similar to previously discussed ones, this class of processes can also be controlled by P-only or PI controllers.

$$G_{(s)} = \frac{K}{s}e^{-\theta s} \tag{5.31}$$

In this section, the behavior of integrating processes will be studied in presence of stiction.

5.4.1 Process Without Time Delay ($\theta = 0$)

P-only Controller

When an integrating process is controlled by a P-only controller, the open-loop FR can be expressed as follows.

$$G_{(j\omega)}G_{c(j\omega)} = \frac{-KK_c}{\omega}j \tag{5.32}$$

Equation 5.32 confirms that the trajectory of FR for this case is always located on the imaginary axis. Also, Table 5.5 includes the extreme values of this trajectory.

Table 5.5: Extreme values of $G_{(j\omega)}G_{c(j\omega)}$ for fast integrating process, controlled by P-only controller.

	Real Part	Imaginary Part
$\omega \to 0$	0	$-\infty$
$\omega \to \infty$	0	0

It can be observed in Figure 5.7 that the trajectory does not cross real axis and the curve of deadband nonlinearity. In contrast, there are always intersections between two trajectories in presence of stiction. The intersection always occurs at a point on the imaginary axis, where the stiction curve is at minimum value of A. The value of this point is shown in Table 5.1 as $0 + j\frac{-\pi S}{4J}$. Then, the frequency at which the FR locates at the crossing point can be easily found, using Equation 5.32.

$$\omega = \frac{4KK_cJ}{\pi S} \tag{5.33}$$

It is obvious that to decrease the frequency of stiction-induced oscillations, the only solution is to decrease K_c. It is noteworthy that in this case, the oscillations cannot be permanently removed by changing controller tunings only.

PI Controller

For this case, real part of the FR will not be zero for all frequencies. Equation 5.34 and Table 5.6 confirm that the FR curve does not cross any of the axis except in the origin. On the other hand, there are always solutions to the Equation 5.11.

$$G_{(j\omega)}G_{c(j\omega)} = \frac{-KK_c}{\tau_I\omega^2} - j\frac{KK_c}{\omega} \tag{5.34}$$

As observable in Figure 5.8, there are always crossings between FR trajectory and the curves related to nonlinearities for such a system. Similar to the previous case, the oscillations cannot be removed, but can be decreased in terms of frequency and magnitude. An effective way can be achieved by decreasing integral action of

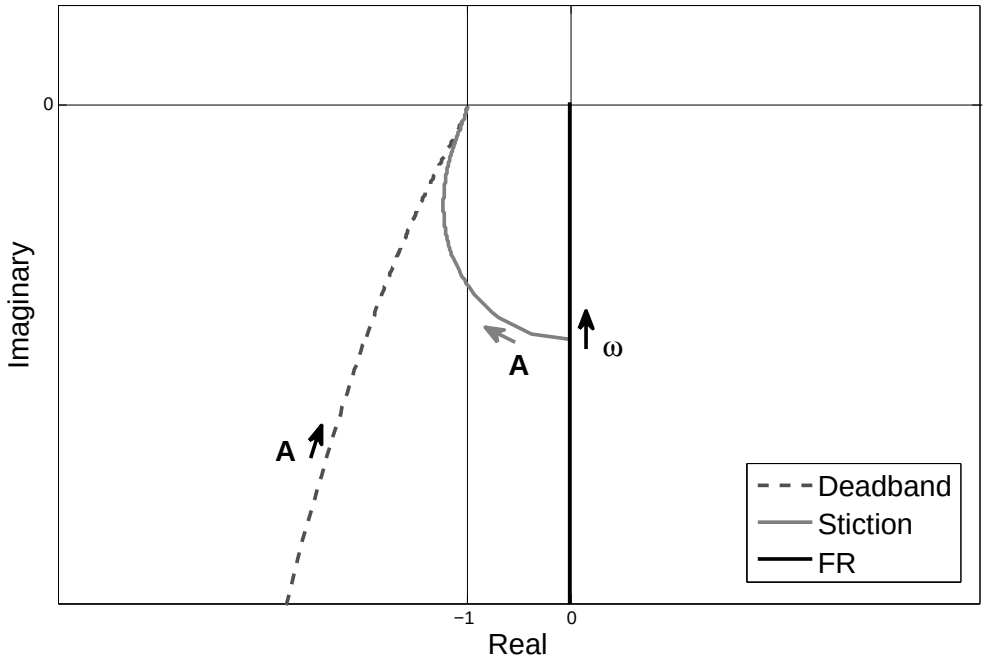

Figure 5.7: Trajectories of $\frac{-1}{N_{(A)}}$ for deadband and stiction and FR for fast integrating process, controlled by P-only controller.

Table 5.6: Extreme values of $G_{(j\omega)}G_{c(j\omega)}$ for fast integrating process, controlled by PI controller.

	Real Part	Imaginary Part
$\omega \to 0$	$-\infty$	$-\infty$
$\omega \to \infty$	0	0

the controller, or even switch to P-only controller, if possible. As a result, oscillations because of deadband will be removed and stiction-induced oscillations will be reduced.

5.4.2 Process with Time Delay ($\theta \neq 0$)

P-only Controller

The open-loop FR for the delayed first order integrating process, which is controlled by P-only controller, can be expressed as Equation 5.35.

$$G_{(j\omega)}G_{c(j\omega)} = \frac{-KK_c \sin(\omega\theta)}{\omega} - j\frac{KK_c \cos(\omega\theta)}{\omega} \tag{5.35}$$

Table 5.7 shows that for small values of frequency, FR has finite value in the real part.

Also, because of the exponential term in process transfer function, there are multiple crossings with the axes. But, the corresponding frequencies (ω^* and ω^{**})

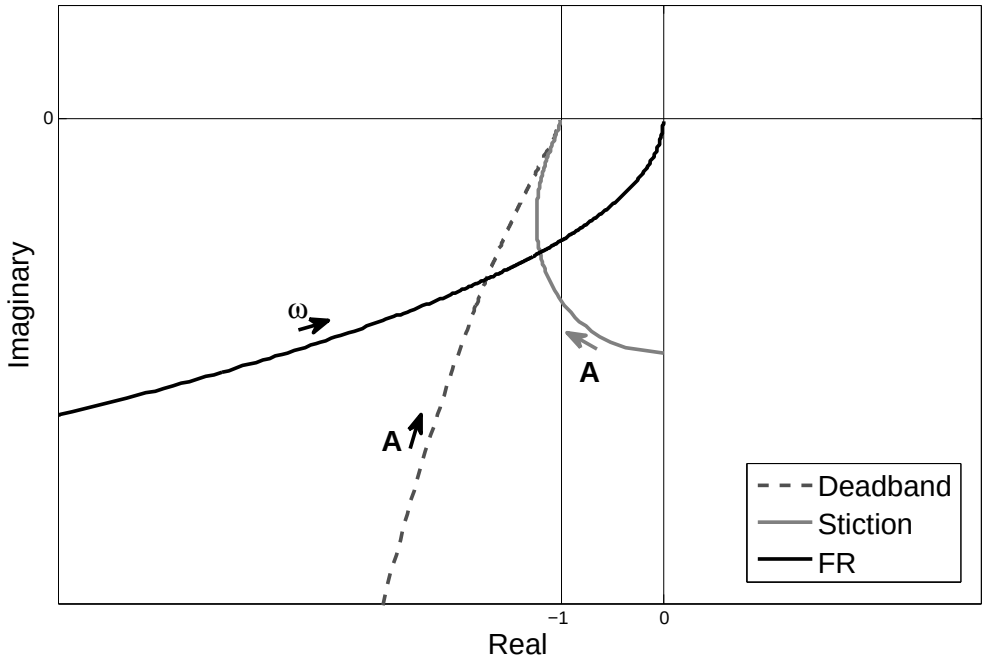

Figure 5.8: Trajectories of $\frac{-1}{N_{(A)}}$ for deadband and stiction and FR for fast integrating process, controlled by PI controller.

Table 5.7: Extreme values of $G_{(j\omega)}G_{c(j\omega)}$ for delayed integrating process, controlled by P-only controller.

	Real Part	Imaginary Part
$\omega \to 0$	$-KK_c\theta$	$-\infty$
$\omega \to \infty$	0	0

for two first crossings (points F and H in Figure 5.9) are independent of controller gain K_c.

If the linear process is stabilized by the controller ($H > -1$), there will be no oscillation in presence of deadband in the control valve. But for stiction, oscillation always occurs. The only solution to decrease the magnitude of the oscillations is to decrease the parameter d (see Figure 5.9). According to Table 5.7, decreasing K_c can be a solution to decrease $d = |KK_c\theta|$.

PI Controller

Equation 5.36 represents the response of the system to frequency changes.

$$G_{(j\omega)}G_{c(j\omega)} = \Big[\frac{-KK_c\sin(\omega\theta)}{\omega} - \frac{KK_c\cos(\omega\theta)}{\tau_I\omega^2}\Big] + j\Big[\frac{KK_c\sin(\omega\theta)}{\tau_I\omega^2} - \frac{KK_c\cos(\omega\theta)}{\omega}\Big] \tag{5.36}$$

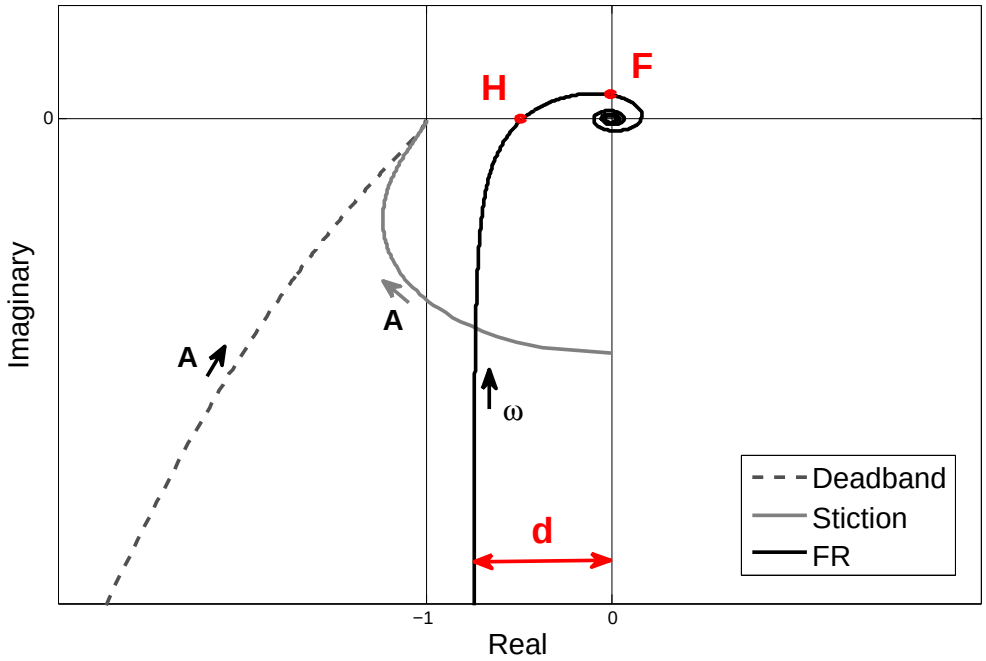

Figure 5.9: Trajectories of $\frac{-1}{N_{(A)}}$ for deadband and stiction and FR for delayed integrating process, controlled by P-only controller.

Table 5.8 shows extreme values of the FR, concluded from Equation 5.36. It can be seen that the imaginary part of the FR can be negative or positive infinite for small values of the frequency.

Table 5.8: Extreme values of $G_{(j\omega)}G_{c(j\omega)}$ for delayed integrating process, controlled by PI controller.

	Real Part	Imaginary Part
$\omega \to 0$	$-\infty$	$KK_c\frac{\theta-\tau_I}{\tau_I\omega}$
$\omega \to \infty$	0	0

Also, there are infinite number of crossings between the FR trajectory and two axes. The positions of the points H and F (see Figures 5.10 and 5.11) and their corresponding frequencies (ω^* and ω^{**}) can be calculated using Equations 5.37 to 5.40.

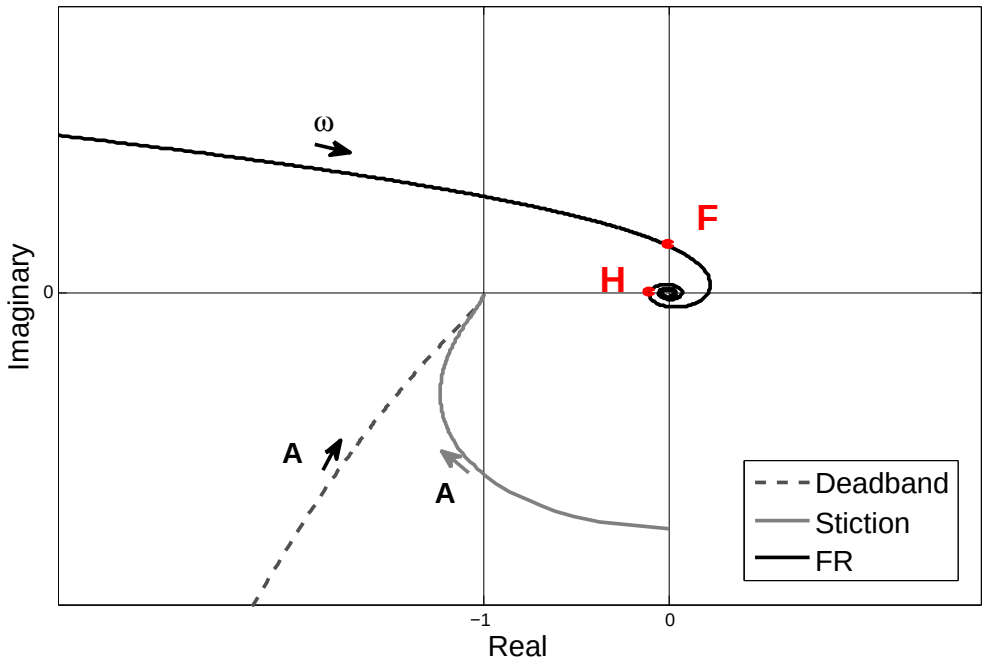

Figure 5.10: Trajectories of $\frac{-1}{N_{(A)}}$ for deadband and stiction and FR for delayed integrating process, controlled by PI controller, when $\tau_I < \theta$.

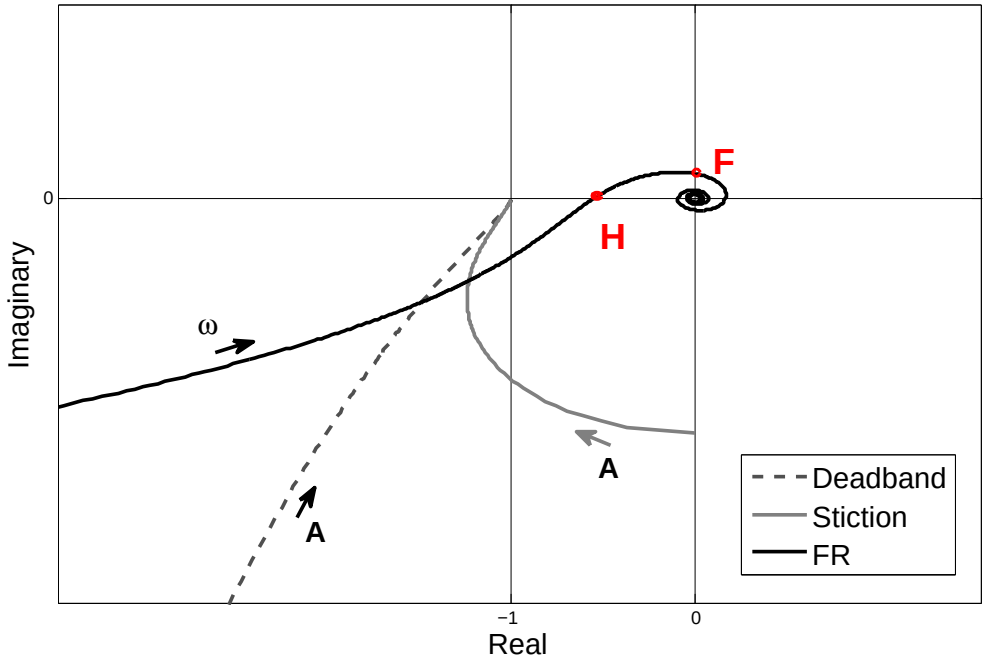

Figure 5.11: Trajectories of $\frac{-1}{N_{(A)}}$ for deadband and stiction and FR for delayed integrating process, controlled by PI controller, when $\tau_I > \theta$.

$$F_{imag} = \frac{KK_c}{1+\tau_I^2\omega^{*2}}\Big[\sin(\theta\omega^*) - \tau_I\omega^*\cos(\theta\omega^*)\Big] \tag{5.37}$$

$$H_{real} = \frac{-KK_c}{1+\tau_I^2\omega^{**2}}\Big[\tau_I\omega^{**}\sin(\theta\omega^{**}) - \cos(\theta\omega^{**})\Big] \tag{5.38}$$

$$\omega^* = \frac{-1}{\theta}\tan^{-1}(\frac{1}{\tau_I\omega^*}) \tag{5.39}$$

$$\omega^{**} = \frac{1}{\theta}\tan^{-1}(\tau_I\omega^{**}) \tag{5.40}$$

Under certain circumstances, elimination of the oscillations induced by deadband and stiction is possible. For systems with relative large time delay, tuning the controller integral time such that $\tau_I < \theta$ will be useful. For systems with small time delays, when $\tau_I < \theta$ is not possible, two options are available: (1) decreasing the integral time (τ_I), which causes the curves intersect in points with higher magnitudes (A), but decreases the frequency of oscillations (see Equations 5.39 and 5.40), or (2) increasing the integral time, which makes the system similar to the last case (P-only controller) and has reverse effects on A and ω. From practical point of view, the first option has better results, since the magnitude of the oscillations cannot exceed certain values in practice.

5.5 Experimental Investigation of the Analysis for Single-loop Systems

In order to evaluate practical efficiency of this compensation method, two different experiments were designed and conducted. The first system includes a coil-heated tank, of which temperature is controlled by a PI controller, by manipulating flowrate of the steam. The valve on the steam pipeline has stiction in some locations. Figure 5.12 illustrates the schematic of this process. For the other experiment, a level control system was considered, which is completely different from the first setup in dynamics. The valve on the input stream to the tank is sticky. The overview of the level control system can be seen in Figure 5.13. The following sections will elaborate the design, experiment runs and results of these experiments. Also, the methodology was validated on a real industrial plant, of which results will be presented.

5.5.1 Pilot-scaled Temperature Control in Coil-heated Tank System

This experiment is designed to investigate effectiveness of the proposed stiction compensation scheme on a temperature control system. The setup includes a cylindrical tank, with constant height of water inside. The level is controlled by input stream

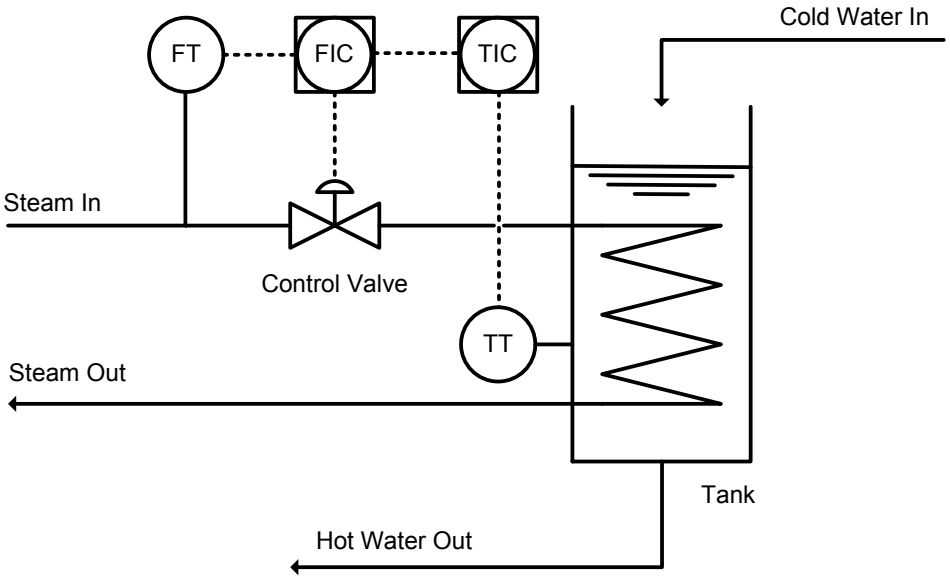

Figure 5.12: Schematic of the temperature control system with sticky control valve.

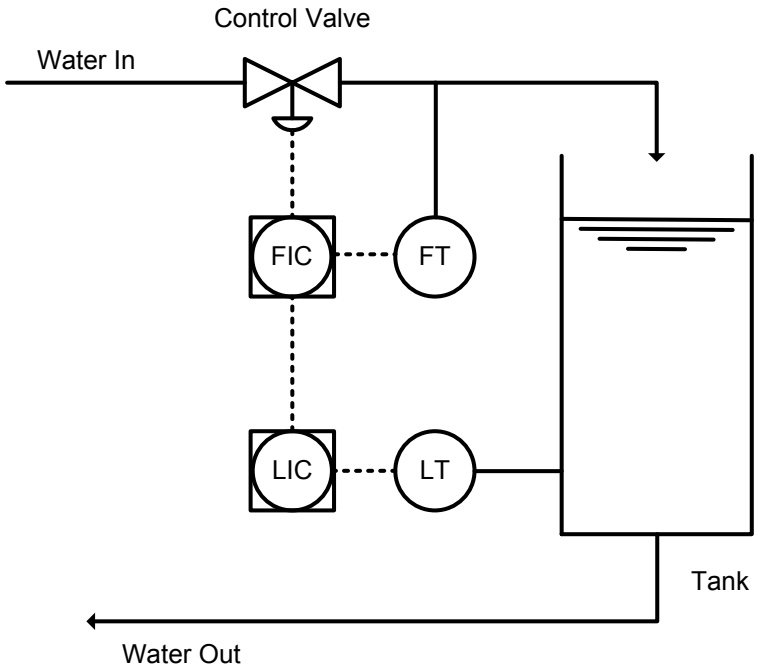

Figure 5.13: Schematic of the level control system with sticky control valve.

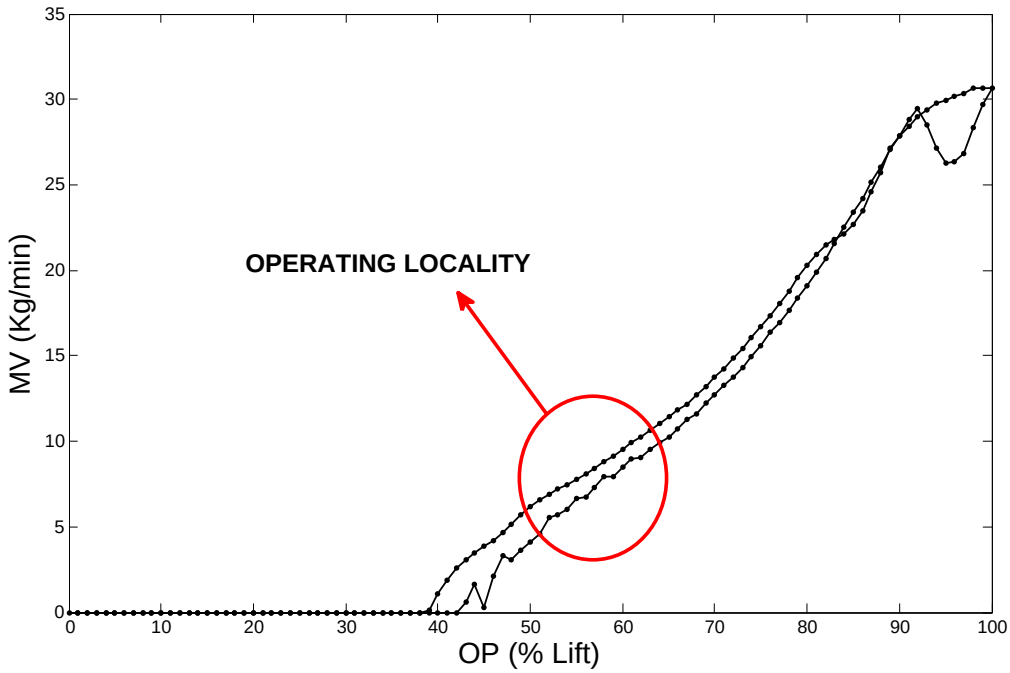

Figure 5.14: Results of the valve characterization for the temperature control valve; actual (MV) vs. expected (OP) valve position.

to the tank. In this experiment, the manipulated variable is flowrate of steam (f_s), which heats the fluid in the tank by passing through a coil. Several thermocouple sets measure the temperature ($^\circ C$) at the outlet of the tank. Based on the nature of the process, it is expected to observe a delay in response of the system.

Valve Characterization

A valve characterization procedure, similar to what was introduced in Section 3.4.2, was carried out for the steam valve. The setpoint is fixed at $25.5^\circ C$ in order to keep the position of the valve between 50 and 60 percent open. According to Figure 5.14, in this region, the valve stem shows static friction in upward direction of movement and the related parameters are estimated as shown in Equation 5.41.

$$S = 4, \quad J = 2 \tag{5.41}$$

Process Model

The FOPDT model was derived for the process, based on first-principle approach. Also, several step tests were carried out to determine the process delay. The identified transfer function for this process is reported by Equation 5.42.

$$\frac{T[^\circ C]}{F_s[\frac{Kg}{min}]} = \frac{0.4346}{27.58s + 1} e^{-6s} \tag{5.42}$$

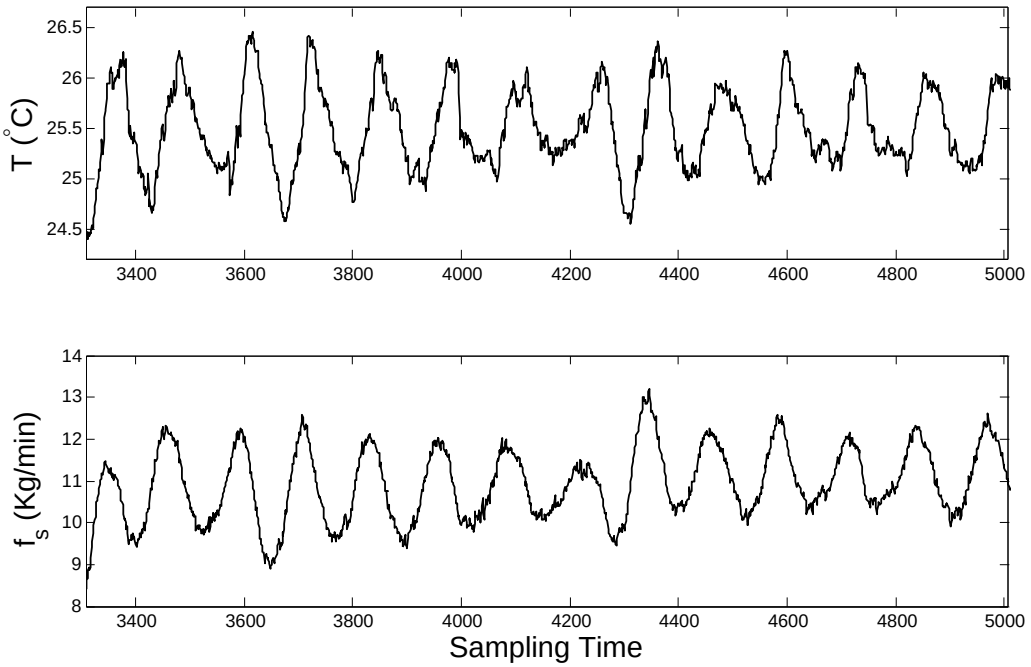

Figure 5.15: Oscillation in the temperature control system, when $K_c = 10\ \frac{Kg}{min°C}$ and $\tau_I = 10\ s$.

where the unit for time delay and time constant of the process is second. The controller used to stabilize this process is PI, tuned as shown in Equation 5.43.

$$G_{c(s)} = 10(1 + \frac{1}{10s}) \tag{5.43}$$

As result of such tuning, considerable oscillation is observed in the control loop. Figure 5.15 illustrates this oscillation in steam flowrate (MV) and outlet temperature of the tank (PV).

Results and Discussion

Figure 5.16 shows the trajectory of frequency response of the system, considering initial tuning ($K_c = 10\ \frac{Kg}{min°C}$ and $\tau_I = 10\ s$). It also illustrates the curve of $\frac{-1}{N_{(A)}}$ for estimated stiction parameters. As expected there is intersection between two trajectories, confirming that oscillation occurs due to stiction.

According to the analysis presented in Section 5.3.2, the controller tuning needs to be changed such that the following conditions hold.

$$\tau_I > \theta + \tau = 33.58\ s \tag{5.44}$$

$$F_{imag} > \frac{-\pi S}{4J} = -1.57 \tag{5.45}$$

Figure 5.17 shows two sub-plots, studying stability of the linear process with and without presence of the stiction. Overlap of two safe areas, where no oscillation is

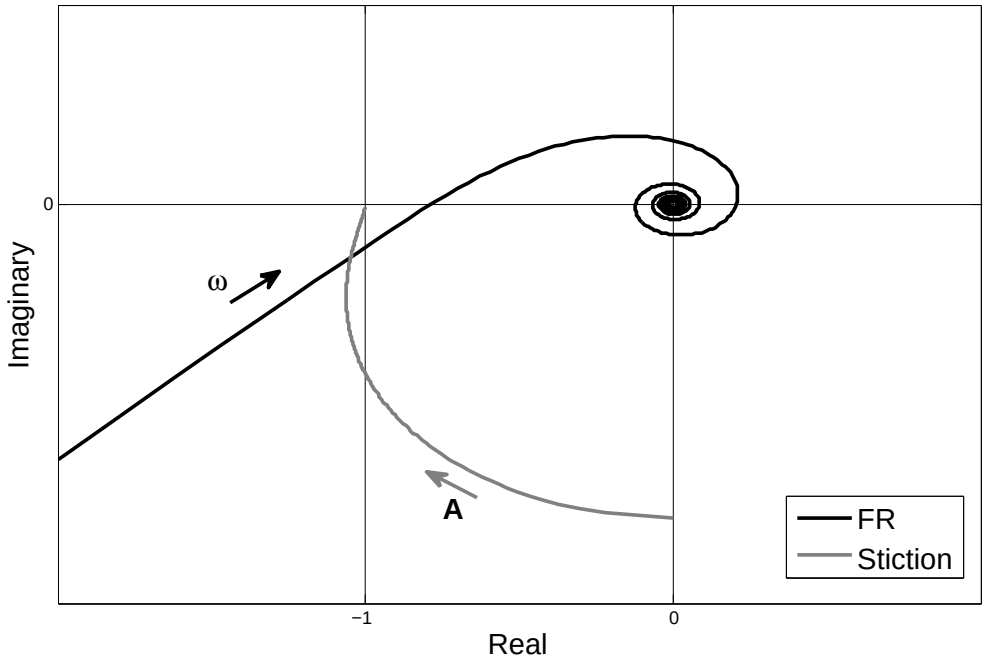

Figure 5.16: Trajectories of $\frac{-1}{N_{(A)}}$ for estimated stiction parameters and FR for temperature control system, when $K_c = 10\ \frac{Kg}{min°C}$ and $\tau_I = 10\ s$.

predicted, will form a new space for tuning parameters. Tunings inside this area will likely lead to a stable process output, i.e., removes the stiction-induced oscillation from the system.

Therefore, elimination of oscillation for this system is feasible. In order to do so, the controller tuning was changed to values shown in Equation 5.46.

$$\begin{aligned} K_c &= 2\ \frac{Kg}{min°C} \\ \tau_I &= 100\ s \end{aligned} \tag{5.46}$$

According to Figure 5.18, which shows the trajectories of the FR and $\frac{-1}{N_{(A)}}$ for the second tuning, oscillation is expected to be removed from the system.

As result of this change, the oscillation was completely removed from the system. Figure 5.19 shows the changes in output of the process, where the dotted line represents the time of the change in controller tuning.

It is obvious that the correct tuning, which is able to remove the stiction-induced oscillation, is not unique. The exact tuning can be found by considering operating conditions, safety issues of the process and flexibility of the control system.

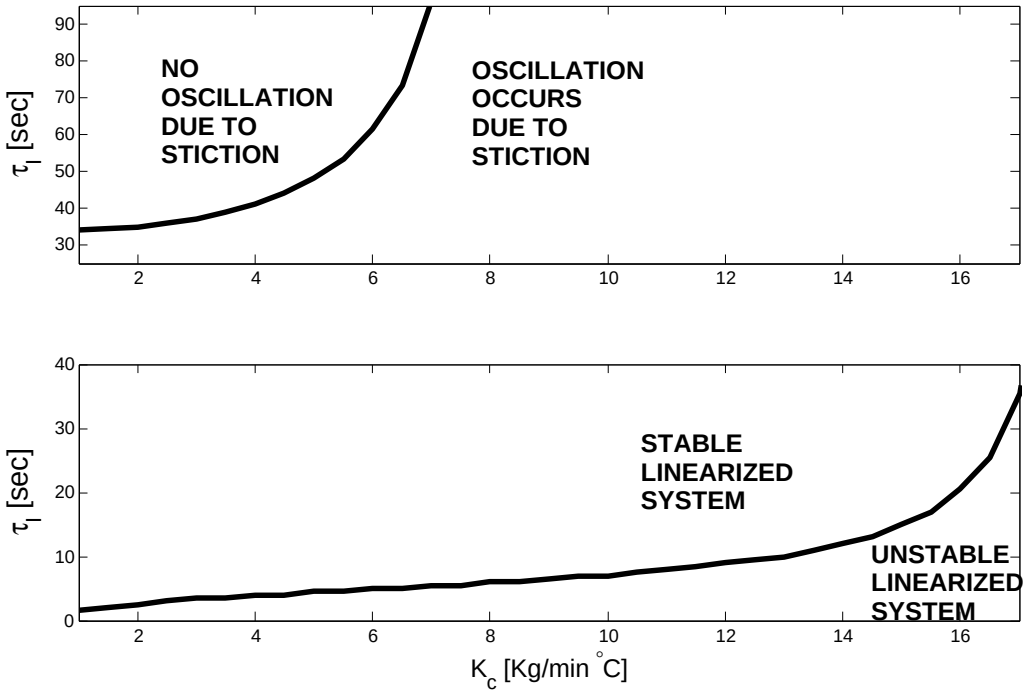

Figure 5.17: Safe and unsafe areas for tuning the controller; stiction included (top) linearized system only (bottom).

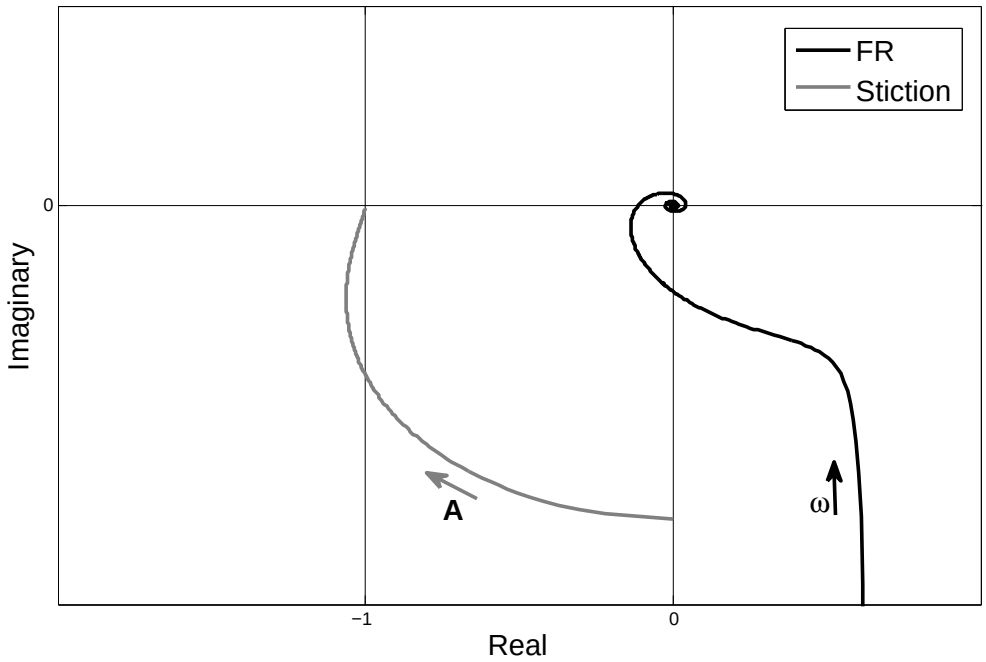

Figure 5.18: Trajectories of $\frac{-1}{N_{(A)}}$ for estimated stiction parameters and FR for temperature control system, when $K_c = 2\ \frac{Kg}{min°C}$ and $\tau_I = 100\ s$.

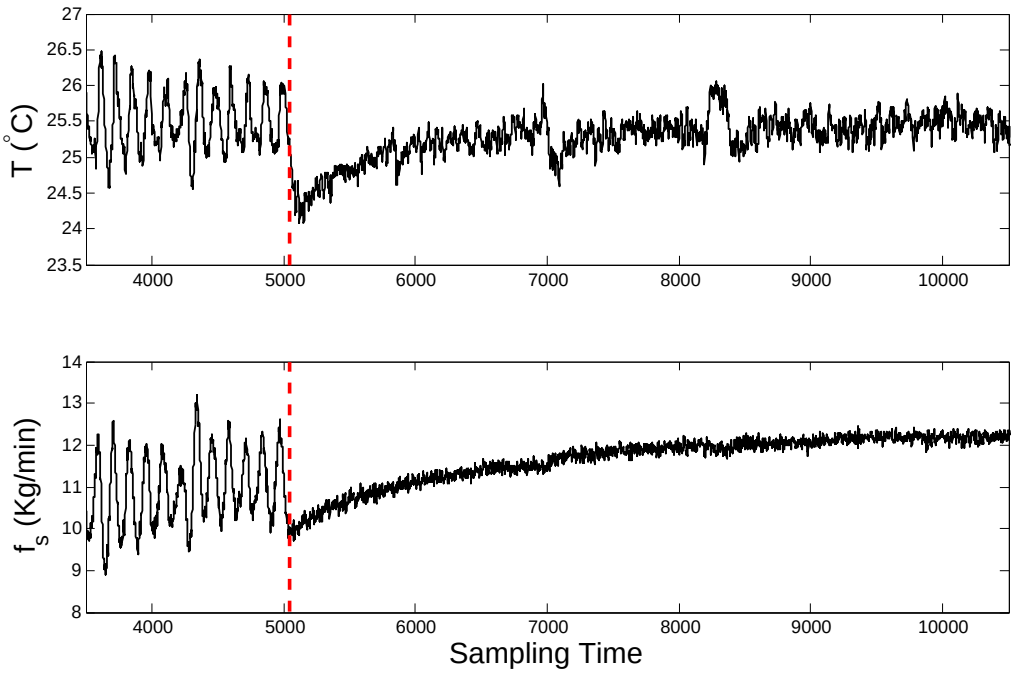

Figure 5.19: Oscillation removal for the temperature control loop using controller tuning only.

5.5.2 Pilot-scaled Level Control in Single-Tank System

The second experiment involves a first order system, with large time constant and no time delay. The experiment setup consists of a cylindrical tank with one input stream and one output. The level of the liquid in the tank (H) is controlled by the input stream (f_{in}). The schematic of the process is shown in Figure 5.13. The control valve on the inlet pipeline has stiction problem. As expected, no significant time delay was observed in this level control system.

Valve Characterization

The inlet water control valve was characterized with gradual changes in the valve position with size of 1% and maximum lift of 50%. As it can be seen in Figure 5.20, the valve has severe stiction problem, especially in positions close to fully closed.

The setpoint is fixed at $0.2m$ and the valve position varies from 3% to 6%. Estimation of the two stiction parameters for this control valve is reported in Equation 5.47.

$$S = 5, \quad J = 1.4 \tag{5.47}$$

According to Figure 5.20, in the operation locality the valve stem shows severe stiction, where the value of stickband (S) is more than slip-jump (J). In such a situation, the valve shows more resistance to changing the direction of its movement.

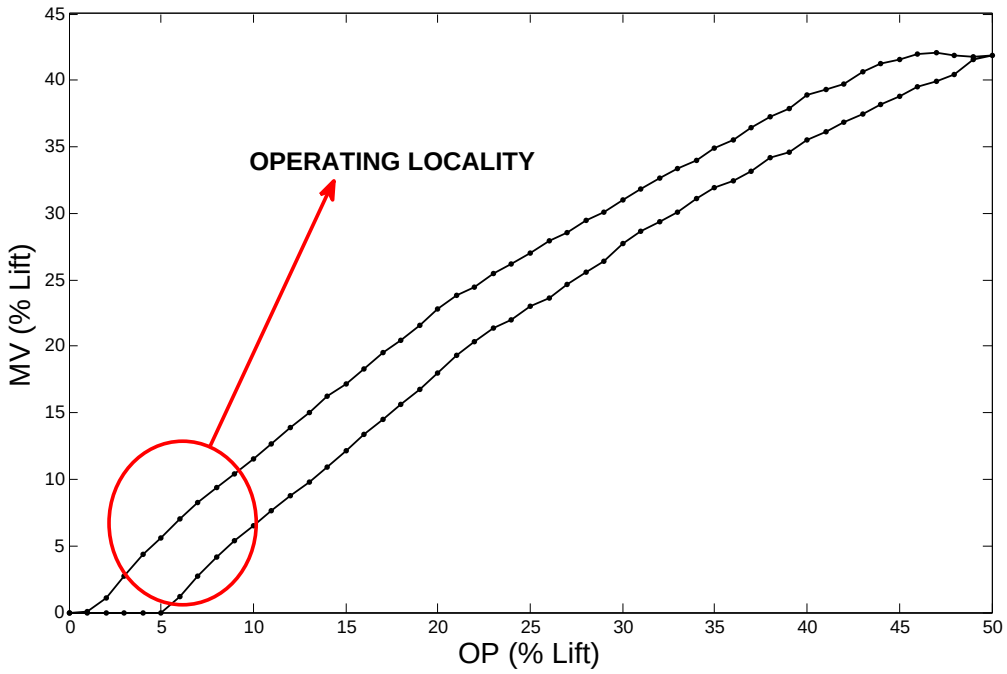

Figure 5.20: Results of the valve characterization for the level control valve; actual (MV) vs. expected (OP) valve position.

During the moving phase there will be no significant jump.

Process Model

Based on first-principle approach, transfer function shown in Equation 5.48 is derived as representative of the dynamics of the process. Similar to the previous experiment, a PI controller is used to control the level of the tank.

$$\frac{H[m]}{F_{in}[\frac{Kg}{min}]} = \frac{0.5717}{544.5s + 1} \tag{5.48}$$

Since the time constant for this process is large ($\tau = 544.5\ s$), the process is expected to show a behavior similar to an integrating process. These systems have been elaborately studied in Section 5.4.1. The PI controller initially has the following dynamics.

$$G_{c(s)} = 2(1 + \frac{1}{10s}) \tag{5.49}$$

This tuning makes the system oscillate because of the stiction. Figure 5.21 illustrates the changes in level of the tank and flowrate of the inlet water.

Results and Discussion

The frequency response of the system with initial values of the controller parameters ($K_c = 2\ \frac{Kg}{min\ m}$ and $\tau_I = 10\ s$) is shown in Figure 5.22. Intersection between two

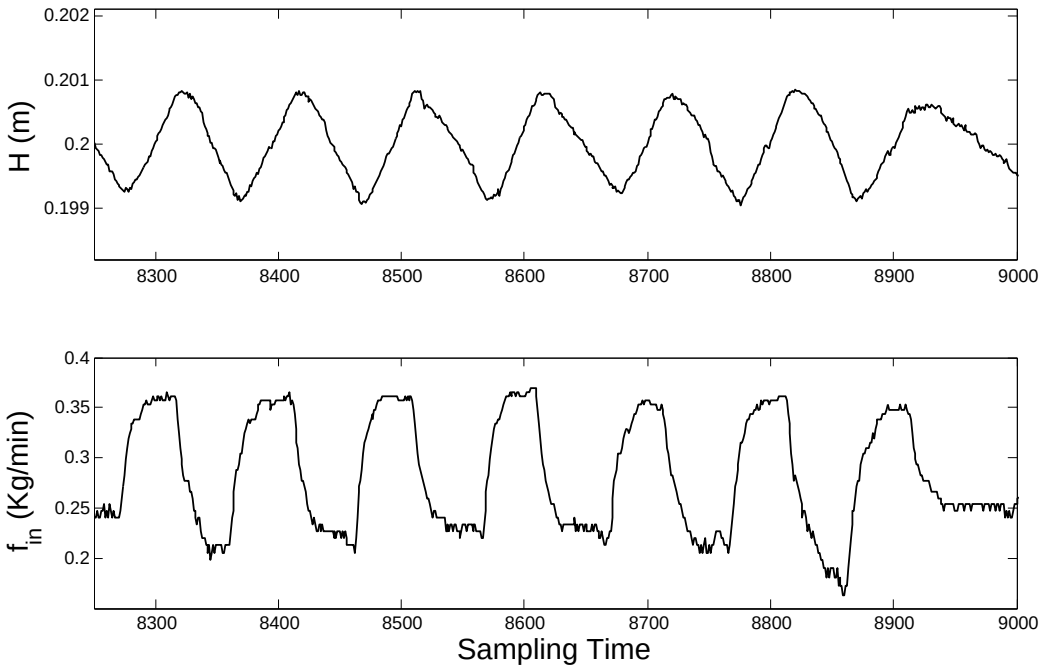

Figure 5.21: Oscillation in the level control system, when $K_c = 2\ \frac{Kg}{min\ m}$ and $\tau_I = 10\ s$.

curves confirms occurrence of the oscillation in the system. As discussed in Section 5.4.1, the stiction-induced oscillations cannot be removed from this system, but its frequency and magnitude may be reduced.

In order to reduce the oscillation in the system, integral action of the controller needs to be reduced. Then, the integral time (τ_I) was increased in several steps. Table 5.9 shows different values of the controller parameters for each step. Also, Figure 5.23 illustrates the frequency responses of these control systems, along with the curve of $\frac{-1}{N_{(A)}}$ for the identified stiction parameters. As the integral time increases, i.e., the integral action of the controller decreases, and the crossing point moves towards the points with less frequencies and magnitudes.

Table 5.9: Different controller tunings for the level control system.

Tuning	$K_c\ [\frac{Kg}{min\ m}]$	$\tau_I\ [sec]$
1	2	10
2	2	20
3	2	100
4	2	500

Results of these changes in controller tuning are illustrated in Figure 5.24, where the oscillations are successfully reduced in terms of frequency and magnitude.

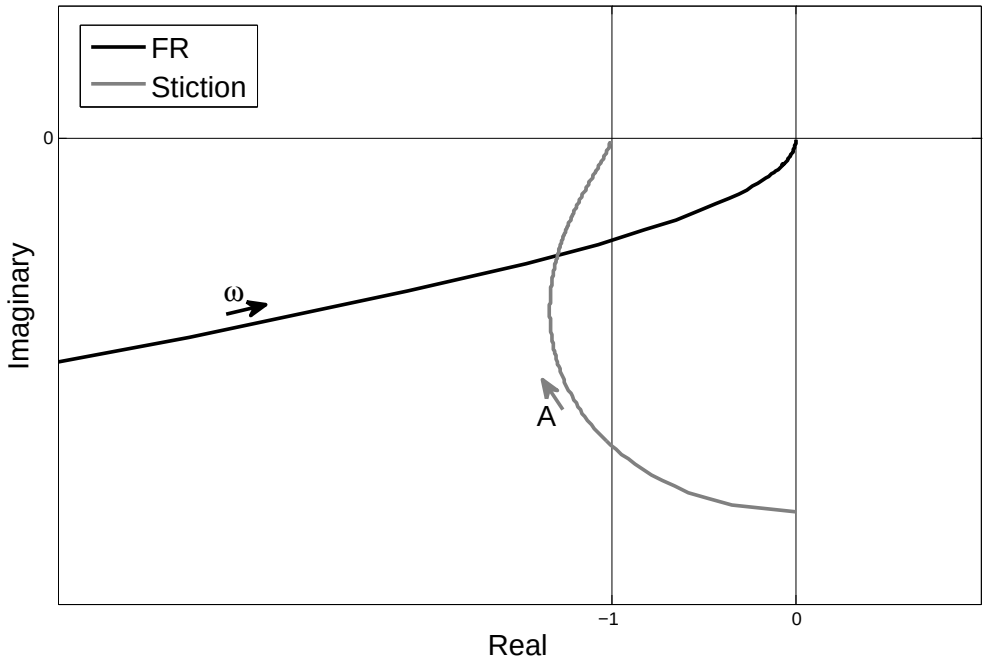

Figure 5.22: Trajectories of $\frac{-1}{N_{(A)}}$ for estimated stiction parameters and FR for the level control system, when $K_c = 2\ \frac{Kg}{min\ m}$ and $\tau_I = 10\ s$.

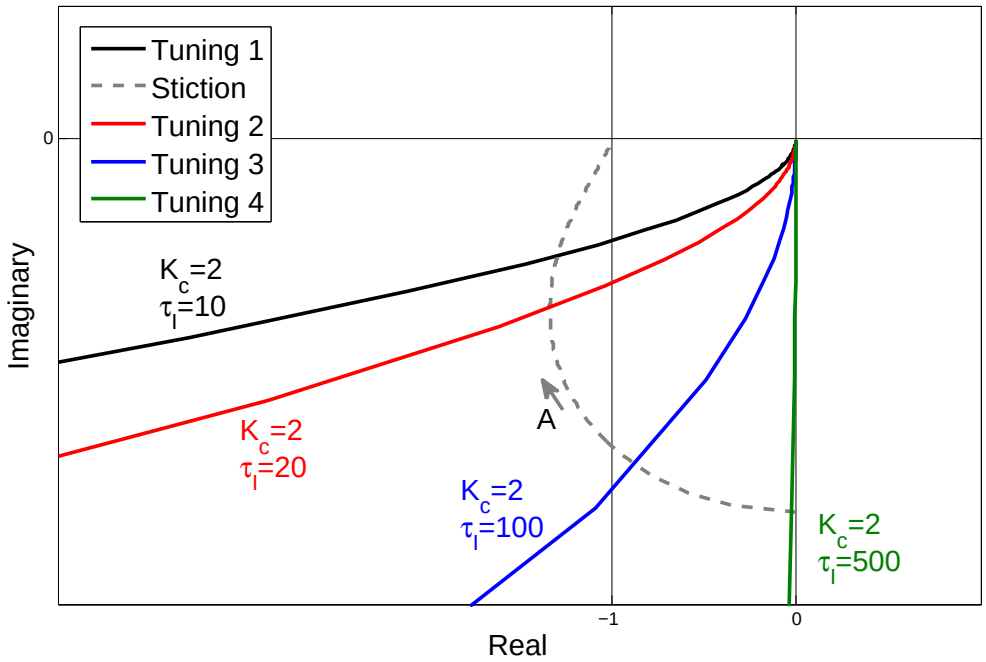

Figure 5.23: Trajectories of $\frac{-1}{N_{(A)}}$ for estimated stiction parameters and FR for the level control system, when $K_c = 2\ \frac{Kg}{min\ m}$ and τ_I is varying.

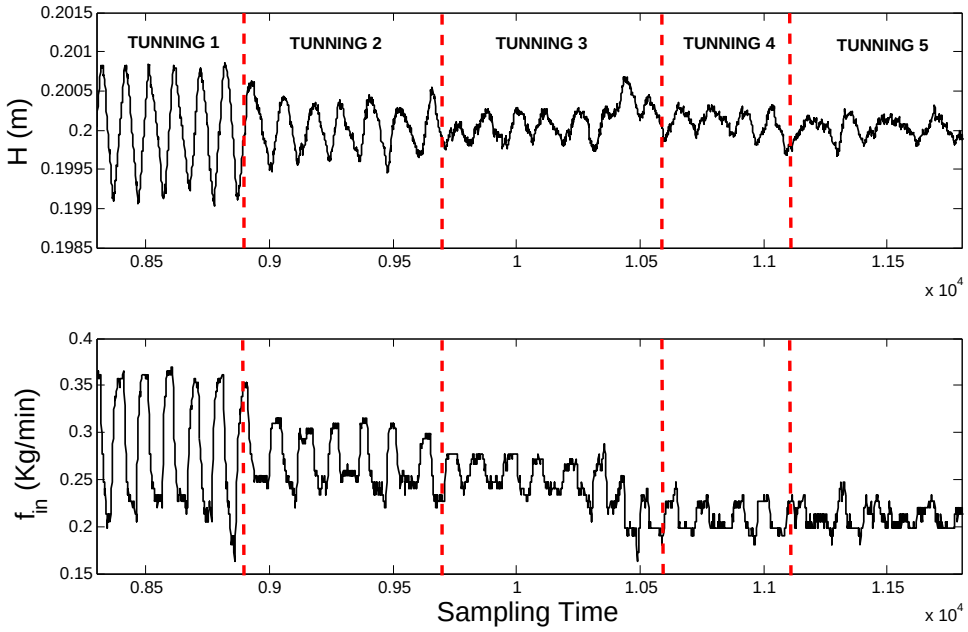

Figure 5.24: Oscillation reduction for the level control loop using controller tuning only.

5.5.3 Industrial Case Study; Level Control System

The problem is concerned with a storage tank in an ammonia plant, of which level fluctuates. The process has been examined for possible root causes of observed oscillations, and stiction in control valve has been identified. The observed oscillation in the process output is shown by Figure 5.25 for a limited time interval. Disappearance of oscillation by changing the setpoint shows that the valve is sticky only in a region around 25% to 26% of the stem travel length.

Process Modeling

All mechanical features of the setup and physical properties of the material are given. In order to execute compensation algorithms on the process, first-principle model is derived for this storage tank system. Results of the modeling is presented in Equation 5.50.

$$\frac{H}{\Delta F} = \frac{0.0092}{s}\, e^{-.08s} \tag{5.50}$$

where $\Delta F = F_{in} - F_{out}$, and units for H, ΔF and time delay are respectively ft, $\frac{USG}{min}$ and min. It is also known that the process is controlled by a PI controller, with the following expression.

$$OP = K_c[(1 + \frac{1}{\tau_I s})PV - \frac{1}{\tau_I s}SP] \tag{5.51}$$

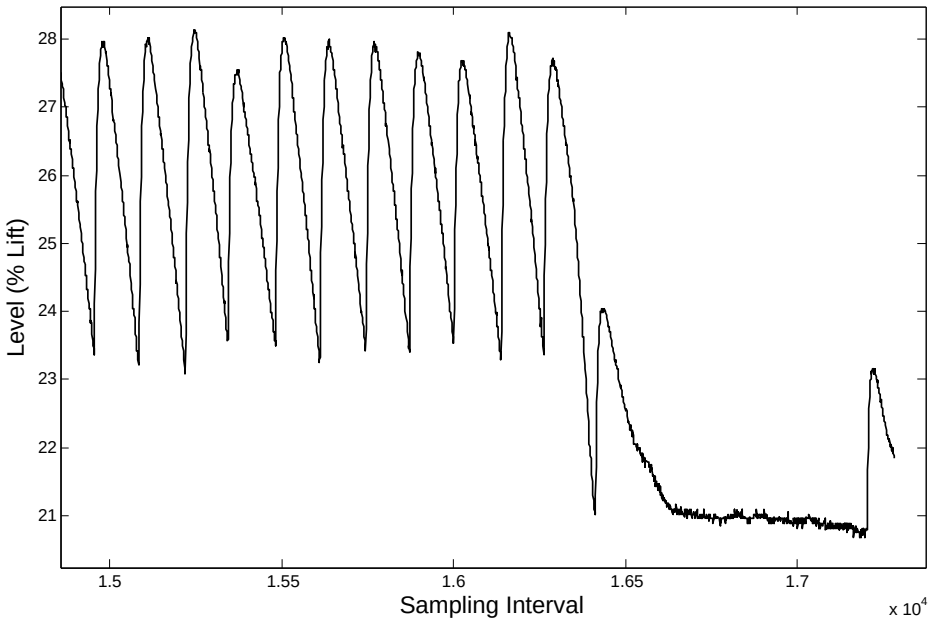

Figure 5.25: Fluctuations of the process output because of stiction in control valve.

Valve Characterization

Severity of the valve problem was determined using the "Stiction Detection and Quantification Package" of "Performance Assessment Technologies and Solutions (PATS)" software. This software is designed and developed in Computer Process Control group in University of Alberta (`http://www.ece.ualberta.ca/~yshardt/index.html`). Description of the designed GUI and the algorithm used in this software can be found in Appendix A.

The estimated values of the stiction parameters f_s and f_d are reported in Equation 5.52.

$$f_s = 3.2, \quad f_d = 0.3 \tag{5.52}$$

The stiction model used for this purpose is a two-parameter model and has been introduced by [17]. The same model will be used in future simulations.

Compensation By Tuning the Controller

When the setpoint to the control system is constant, the dynamics of the process and controller will have the following form:

$$G_{(s)} = \frac{K}{s}\, e^{-\theta s} \tag{5.53}$$

$$G_{c(s)} = K_c(1 + \frac{1}{\tau_I s}) \tag{5.54}$$

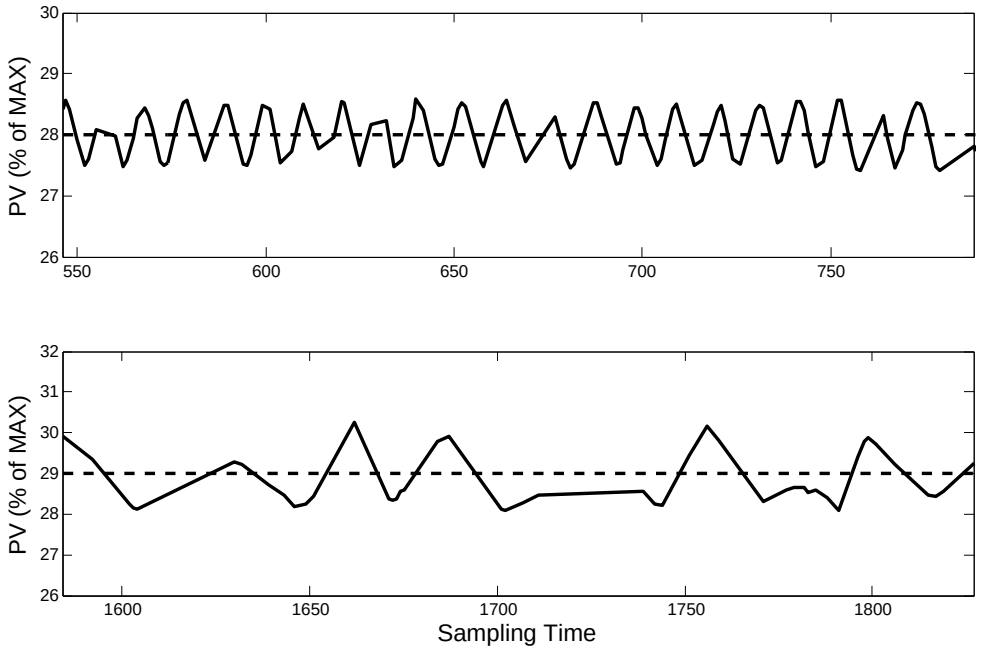

Figure 5.26: Oscillations in the industrial level control system, before the change in controller tuning (top) and after (bottom).

This type of systems have been studied in Section 5.4.2 in detail. In the related discussions, two approaches to cure the oscillations were stated: (1) tune the controller as $\tau_I < \theta$ and (2) decrease the integral time as much as possible. In this particular case, because of the small time delay in response of the system, the first solution is not feasible. Therefore, the suggestion was made to "increase the integral time (τ_I) and/or decrease controller gain (K_c)". This tuning will not permanently remove the oscillations from the system, but is expected to reduce irs frequency and magnitude.

Results and Discussion

To observe the results, the tuning of the controller was changed. The gain reduced from 1.0 to 0.6 and the integral time increased from 1.5 minutes to 15 minutes. The results were satisfactory, as observable in Figure 5.26. The frequency of oscillation is significantly reduced after the change with some increase of the magnitude. According to the engineer, the main interest is to reduce oscillation frequency and this solution has been considered a success.

5.6 Multi-loop Process With Multiple Controllers

It was discussed in Chapter 3 that for a general $n \times n$ system controlled by n controllers, satisfaction of Equation 3.14 confirms occurrence of oscillation in the system because of stiction. It is to say that if interactions between different loops

are ignored, the matrix $\mathcal{H}$ will be of the diagonal form. In other words, each diagonal entry of this matrix represents oscillation condition for one loop of the system and is valid only when there is no interaction. Therefore, for a multi-loop system oscillating due to stiction, tuning the controllers using previously mentioned guidelines, and considering each loop isolated from the others, will not be the definite solution to oscillation problem. Such tuning policy only sets diagonal elements of $\mathcal{H}$ nonzero, while the determinant of this matrix still can have zero value, i.e., oscillation may be observed in the whole system. This fact implies that oscillating multi-loop systems are relatively more difficult to handle.

Based on the mentioned fact, giving a guideline to cure multi-loop systems is not feasible, as the action is case dependant. Process dynamics, interactions of the loops and severity of stiction should be known in order to find the best compensation policy. A two-step compensation algorithm is used here to illustrate the best tuning for all controllers, in order to remove or reduce stiction-induced oscillations.

Given a complete process dynamics and stiction parameters for faulty valves, following these two steps will help finding the best controller tuning for the multi-loop system:

1. Find safe intervals for controller parameters in each loop, considering it isolated from the other loops. The term "safe interval" means the values of tuning parameters which stabilizes the closed-loop process, i.e., the controller is not tuned too aggressively. Obviously, oscillations may not be completely removed from some loops, but the values of controller parameters which reduce oscillations can be found, based on the suggestions previously made for single-loop cases.

2. Find the combination of parameters for all n controllers, for which solving Equation 3.14 for ω gives the least value of frequency.

5.6.1 Experimental Example for Multi-loop System

Experimental System Setup

To investigate the effect of stiction on a system in presence of interaction between loops, a two-input-two-output process was considered. Figure 5.27 shows the schematic of this process.

This setup includes a tank, where level (l) and temperature (T) of the its liquid content are being controlled by two PI controllers. Input to the tank is hot water with flowrate f_h. Saturated steam with flowrate f_s travels through a heating coil inside the tank. Each output is paired with one of the inputs, i.e., flowrates of hot

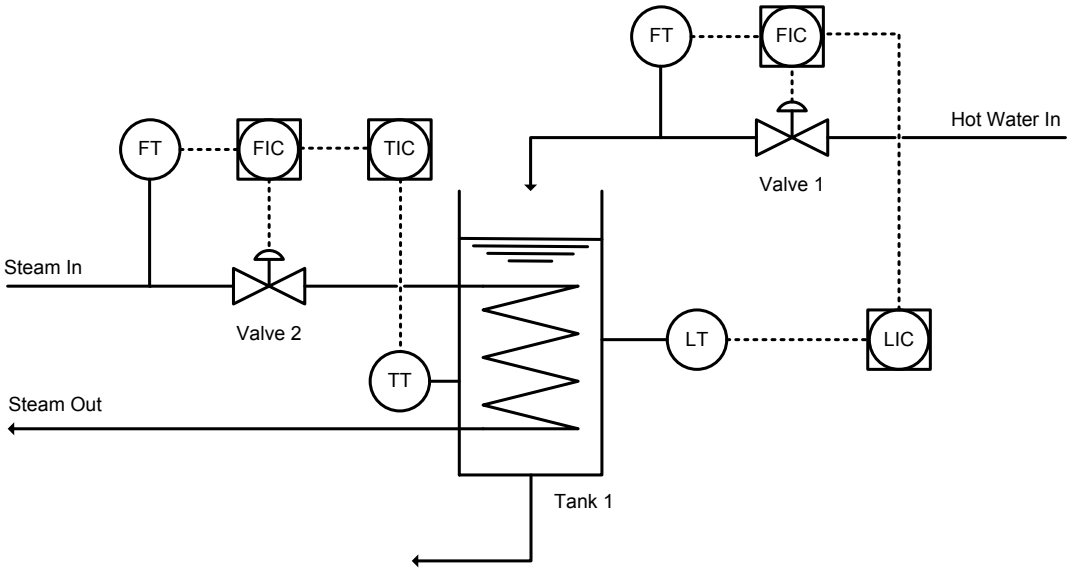

Figure 5.27: Schematic of the studied 2×2 process used for the experiment.

water and steam are manipulated variables to control the level and the temperature, respectively. Also, there are a cascade loops for all flowrate measurement.

Therefore, the dynamics of this process has the form shown in Equation 5.55:

$$\begin{bmatrix} L_{(s)} \\ T_{(s)} \end{bmatrix} = G_{(s)} \begin{bmatrix} F_{h(s)} \\ F_{s(s)} \end{bmatrix} \tag{5.55}$$

where $G_{(s)}$ is a 2×2 matrix, showing the dynamics from the inputs to the outputs of the process.

Valve Characterization

The control valves used in this experiments are same as the ones used in Section 3.4.2. The valve which controls the flowrate of the steam through the coil performs fairly normal, as obvious in Figure 3.5. But, the other valve is sticky with the following estimated parameters:

$$\begin{aligned} S &= 5 \\ J &= 1.4 \end{aligned} \tag{5.56}$$

where both parameters are based on percent of valve travel length.

Process Model

One mass balance equation (for level of the tank) and one energy balance equation (for temperature) were used to model this multivariate process. All the physical properties of the apparatus are stated in Table 5.10.

Table 5.10: Parameters and variable used in modeling of the 2×2 process.

Parameter/Variable	Symbol	Unit	Value (Steady State)
Level of tank 1	l	m	0.2
Temperature	T	$^{\circ}C$	50
Hot water flowrate	f_h	Kg/min	4.3
Steam water flowrate	f_s	Kg/hr	5
Cross section area of the tank	A	m^2	0.016
Resistance of outlet from the tank	R	$m.s/Kg$	3.2488
Heat transfer fraction from coil	k	N/A	0.97
Temperature of inlet to the tank	T_{in}	$^{\circ}C$	38
Reference temperature	T_{ref}	$^{\circ}C$	0
Specific enthalpy of steam[§]	$\Delta\hat{H}$	J/Kg	1994737

[§] *Calculated for saturated steam (*150 *psig) fully condensed, and subject to* T_{ref}.

Differential equations of this dynamic system are given in Equations 5.57 and 5.58.

$$\frac{dl}{dt} = \frac{f_h}{\rho_{(T)}A} - \frac{l}{R\rho_{(T)}A} \tag{5.57}$$

$$\frac{dT}{dt} = \frac{f_h C_{p(T_{in})} T_{in}}{(f_h - \frac{l}{R})C_{p(T)}} - \frac{lT}{R(f_h - \frac{l}{R})} + \frac{k\Delta\hat{H}f_s}{(f_h - \frac{l}{R})C_{p(T)}} \tag{5.58}$$

Liniarization was done for derivatives of l and T, in local neighborhood of the steady state ($\bar{f}_h$,$\bar{f}_s$,$\bar{l}$ and $\bar{T}$). Density and specific heat of the water in the tank were approximated using Equations 3.39 and 3.40 which are valid for temperature interval $40^{\circ}C \leq T \leq 60^{\circ}C$.

$$\begin{aligned}\frac{dl}{dt} &\simeq 6.3909 \times 10^{-4} + 0.0632(f_h - \frac{4.3}{60}) \\ &\quad - 0.0195(l - 0.2) + 2.7192 \times 10^{-7}(T - 50)\end{aligned} \tag{5.59}$$

$$\begin{aligned}\frac{dT}{dt} &\simeq 28.3232 - 955.0638(f_h - \frac{4.3}{60}) \\ &\quad - 6.1009(T - 50) - 660.2484(l - 0.2) + 12.7212(f_s - \frac{5}{3600})\end{aligned} \tag{5.60}$$

Equations 5.59 and 5.60 are transformed to the Laplace domain, rearranged as shown below:

$$L_{(s)} = \alpha F_{h(s)} + \beta F_{s(s)} \tag{5.61}$$

$$T_{(s)} = \gamma F_{h(s)} + \lambda F_{s(s)} \tag{5.62}$$

where

$$A = \frac{0.0632}{s + 0.0195} \tag{5.63}$$

$$B = \frac{2.7192 \times 10^{-4}}{s + 0.0195} \tag{5.64}$$

$$C = \frac{955.0638}{s + 6.1009} \tag{5.65}$$

$$D = \frac{-660.2484}{s + 6.1009} \tag{5.66}$$

$$E = \frac{12.7212}{s + 6.1009} \tag{5.67}$$

$$\alpha = \frac{A + BD}{1 - BD} \tag{5.68}$$

$$\beta = \frac{BE}{1 - BD} \tag{5.69}$$

$$\gamma = E + D\beta \tag{5.70}$$

$$\lambda = C + D\alpha \tag{5.71}$$

$$\tag{5.72}$$

There are time delays only in responses of T to changes in $F_{h(s)}$ and $F_{s(s)}$. Hence, the actual transfer functions can be rewritten as:

$$\frac{T_{(s)}}{F_{c(s)}} = \gamma e^{-20s} \tag{5.73}$$

$$\frac{T_{(s)}}{F_{s(s)}} = \lambda e^{-10s} \tag{5.74}$$

Theoretical Study of the System

The matrix $\mathcal{H}$ for this system is shown in the following equation:

$$\mathcal{H} = \begin{bmatrix} 1 + g_{11(j\omega)} g_{c1(j\omega)} N_{1(A_1)} & g_{12(j\omega)} g_{c2(j\omega)} \\ g_{21(j\omega)} g_{c1(j\omega)} N_{1(A_1)} & 1 + g_{22(j\omega)} g_{c2(j\omega)} \end{bmatrix} \tag{5.75}$$

Because there is no stiction in the valve 2 (steam control valve), the second diagonal entry of the matrix $(1 + g_{22(j\omega)} g_{c2(j\omega)})$ is always nonzero. On the other hand, the process in loop 1, level of the liquid, is considered as first-order integrating process without time delay.

To follow the guidelines suggested in Section 5.6 in order to reduce the oscillations in multi-loop processes, each loop will be considered isolated first. Based on discussions in Section 5.4.1 for single-loop systems, stiction-induced oscillations cannot be permanently removed from the level-control system (loop 1). Oscillation

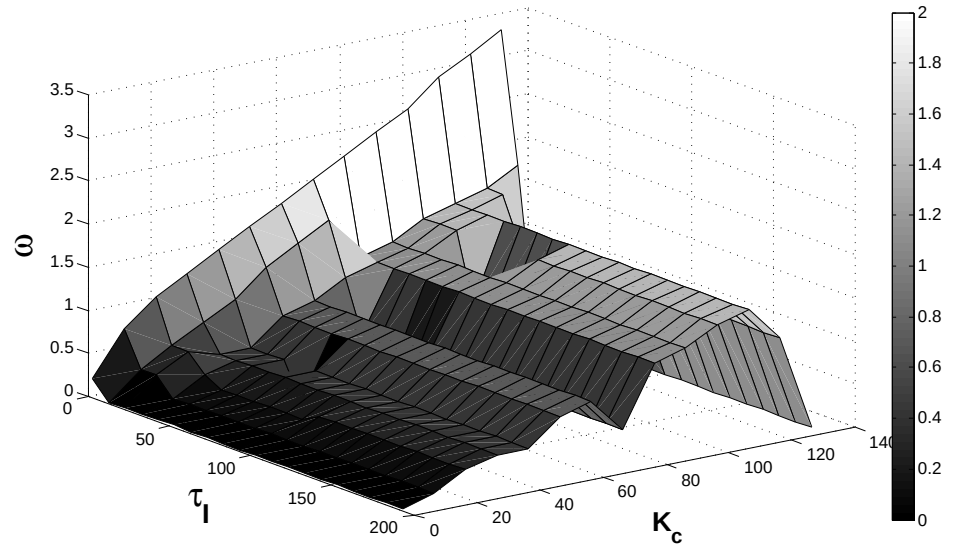

Figure 5.28: Predicted values of frequency for different pairs of K_c and τ_I.

of loop 1 can be reduced by suitable tuning of the controller, i.e., increasing τ_I. The other loop has no stiction and as long as the controller is not tuned aggressively, no oscillation is expected to be observed in this loop. Therefore, tuning parameters of the controller in loop 2 (K_{c2} and tau_{I2}) was fixed at the values shown in Equation 5.76 (the gain of the controller is reported without dimension). This action simplifies solving oscillation occurrence condition.

$$\begin{aligned} K_{c2} &= 4.2 \\ \tau_{I2} &= 40\ sec \end{aligned} \tag{5.76}$$

For the second step, oscillation condition is required to be solved for each pair of parameters of controller 1 (K_{c1} and τ_{I1}). Figure 5.28 illustrates the results of solving the oscillation condition, introduced in Equation 3.14, for the matrix $\mathcal{H}$ in Equation 5.75. This figure implies that increasing integral time, and if possible decreasing controller gain, is expected to decrease the frequency of the oscillations.

Results of the Experiment

According to theoretical analysis of the system, the integral time of the controller 1 was changed from 20 to 50 seconds and the controller gain from 1 to 0.2 (dimensionless). As result, an improvement was observed in the oscillations. Figure 5.29 elaborates the difference between two situations; before and after the change in tuning at $t = 2150\ sec$.

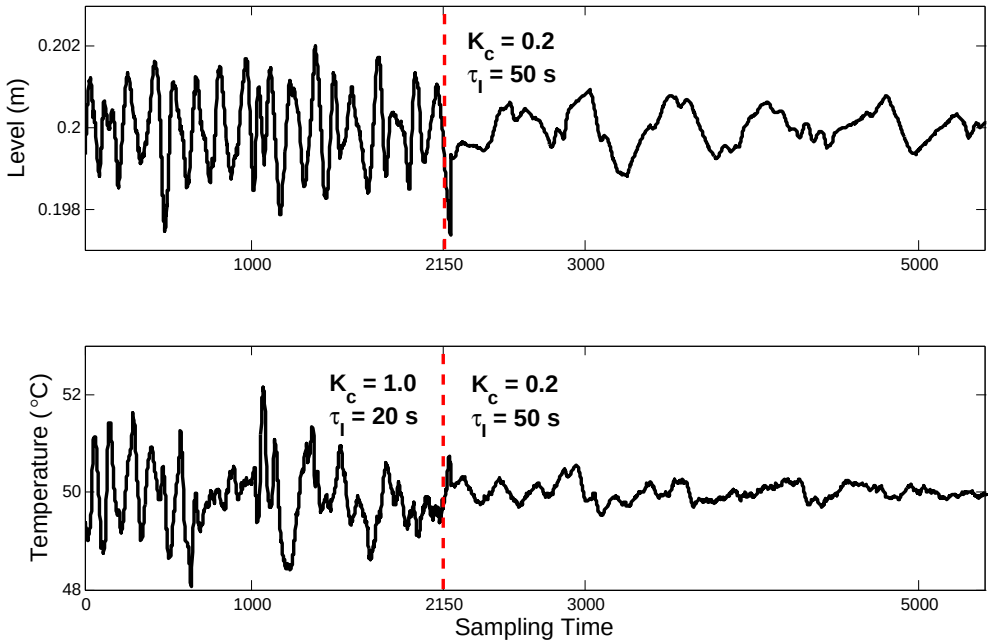

Figure 5.29: Change observed in oscillation of the 2×2 system after change in tuning of the controller 1.

5.7 Conclusion

In this chapter, an approach to compensate for static friction in control valves was presented. The objective of this method is to remove or reduce stiction-induced oscillations by changing controller tuning only. Several combinations of different processes and controllers were analyzed, and qualitative actions to be taken towards the objective were discussed. Also, the theoretical results were validated by two experiments and one industrial level control system. The experiments consist of single control loops for temperature and level, with sticky control valve. Valve characterization procedure, process modeling, and comparison of the theoretical and experimental results are presented for each experiment. Summary of all the compensating actions on controller tunings has been reported in Table 5.11. It is noteworthy that for all systems, the process should be stabilized by controller in absence of stiction nonlinearity and also the guidelines mentioned in Section 5.2 are required to be satisfied.

Table 5.11: Summary of the recommended stiction compensation actions for single-loop control systems with different processes and controllers[§].

Dynamics	Time Delay	Deadband Oscillation	Stiction Oscillation	Action	New Oscillation
SR & P	NO	NO	NO	N/A	N/A
SR & PI	NO	NO	Maybe if $\tau_I > \tau$	$\tau_I \uparrow$	NO
SR & P	YES	NO	Maybe if $F_{imag} < \frac{-\pi S}{4J}$	$K_c \downarrow$	NO
SR & PI	YES	NO	YES if $\theta + \tau > \tau_I$	(1) $\tau_I \uparrow$ (2) $K_c \downarrow$	(1) NO (2) Reduced
Int. & P	NO	NO	YES	$K_c \downarrow$	Reduced
Int. & PI	NO	YES	YES	$\tau_I \uparrow$	Reduced
Int. & P	YES	NO	YES	$K_c \downarrow$	Reduced
Int. & PI	YES	YES if $\tau_I > \theta$	YES if $\tau_I > \theta$	(1) $\tau_I < \theta$ (2) $\tau_I \uparrow$	(1) NO (2) Reduced

§ *P: Proportional Controller; PI: Proportional-integral Controller; SR: Self-regulating Process; Int.: Integrating Process.*

Chapter 6

Summary and Future Challenges

The body of this thesis, consisting of 4 chapters, focused on diagnosis and compensation of destructive effects of static friction on performance of the control system. In the second chapter of the thesis, a new qualitative method for stiction detection in multi-loop control systems was proposed and validated by simulation and industrial data set. The mentioned chapter can be considered as the first step towards solving stiction-induced problem. In fact, after implementing the proposed detection algorithm, potential root causes of the oscillations, i.e, sticky valves in the system, will be known. In the next chapter, the mathematical condition for the occurrence of oscillations induced by nonlinearities in a multi-loop control system was derived. This analysis was performed on a pilot-scaled multi-loop control system and results were successful. The proposed analysis was used to introduce a compensation scheme in Chapter 5. In the proposed methodology, only controller tuning variation was used to control stiction, which is the easiest and cheapest tool. In Chapter 4, a model-based compensation method was introduced. This method can be applied on the systems where the previously proposed method cannot remove the oscillations permanently.

6.1 Contributions of This Thesis

The contributions of this work can be summarized as follows:

- Comparison of existing data-driven stiction models using data set from a pilot-scale plant. Some of the most commonly used one and two-parameter data-driven models were studied and the accuracy of their predictions were discussed.

- A qualitative method for stiction detection in multi-loop control systems was proposed. This new method is able to detect multiple sticky valves in a system, as confirmed by its application on simulation and industrial data.

- General condition for occurrence of nonlinearity-induced oscillations in multi-loop systems was derived mathematically and validated through experimental study. This analysis enables the prediction of variations in frequencies and magnitudes of oscillations due to changes in the system dynamics.
- A methodology to compensate stiction in single- and multi-loop control systems was discussed, which is based on changing the controller tunings. The proposed method uses the previously proposed condition for oscillations, and gives qualitative suggestions to remove or reduce stiction-induced oscillations in the system.
- A new model-based compensation methodology was proposed to remove oscillations induced by stiction from systems from which the effects of friction in valve cannot be eliminated by only changing the controller tuning.

6.2 Future Challenges and Open Discussions

Diagnosis and control of static friction in control systems will stay a major area of research in performance assessment field, as mechanical equipment, more specifically control valves, are still the vital part of the control loops. Further research will uncover more hidden corners of this problem and face future researchers with new questions. Some of these open discussions can be listed as:

- Beside qualitative methods of stiction detection, there always will be a need for methods to quantify stiction parameters. Taking the interactions between different control loops into account makes this procedure computationally expensive. Using nonlinear system identification as the main approach to do this task is a trade-off between high amount of the elapsed time for computations (multi-variate identification) and accuracy of the estimates (considering isolated single-loop processes). More comprehensive study of stiction phenomenon is required to improve the process of quantification. An effective example of this simplifying assumptions is considering the boundaries of search space introduced by [28].
- To improve the compensation proposed in Chapter 5, wider ranges of process and controller types can be included in the method. Prosperity of study of only first-order processes paired with P or PI controllers can be a motivation to expand this analysis to other commonly used types of processes and controllers in industry.
- The proposed model-based method has been validated for FOPDT system controlled by PI controller thorough simulation. It can be predicted that

there will be more challenges in implementation of this method on industrial DCS, or even applying the algorithm on integrating processes.

- In the analysis which was elaborated in Chapter 3 and used as a compensation scheme in Chapter 5, DF of stiction nonlinearity has a remarkable role. The function used in this work is proposed by [7] and is derived based on output of the model developed by the same authors. The comparison of predictions of existing models, which illustrated their differences, can be a motivation for further study of the effects of other stiction models and DFs on the analysis.

Bibliography

[1] B. Armstrong-Hélouvry, P. Dupont, and C. Canudas de Wit. A survey of models, analysis tools and compensation methods for the control of machines with friction. *Automatica*, 30(7):1083–1138, 1994.

[2] W.L. Bialkowski. Dreams versus reality: a view from both sides of the gap. *Pulp and Paper Canada*, 94:19–27, 1993.

[3] S.B. Chitralekha, S.L. Shah, and J. Prakash. Detection and quantification of valve stiction by the method of unknown input estimation. *Journal of Process Control*, 20:206–2016, 2010.

[4] M.A.A.S. Choudhury. *Detection and Diagnosis of Control Loop Nonlinearites, Valve Stiction and Data Compression*. PhD thesis, University of Alberta, Edmonton, Canada, Spring 2000.

[5] M.A.A.S. Choudhury, M. Jian, and S.L. Shah. Stiction - definition, modelling, detection and quantification. *Journal of Process Control*, 18:232–243, 2008.

[6] M.A.A.S. Choudhury, S.L. Shah, and N.F Thornhill. *Diagnosis of Process Nonlinearities and Valve Stiction Data Driven Approaches*. Springer, Berlin, 2008.

[7] M.A.A.S. Choudhury, N.F. Thornhill, and S.L. Shah. Modeling valve stiction. *Control Engineering Practice*, 13:641–658, 2005.

[8] C. Canudas de Wit, H. Olsson, K.J. Åström, and P. Lischinsky. A new model for control of systems with friction. *IEEE Transactions on Automatic Control*, 40(3):419–425, 1995.

[9] L. Desborough, P. Nordh, and R. Miller. Control system reliability: Process out of control. *Industrial Computing*, 8:52–55, 2001.

[10] C.A. Desoer and E.S. Kuh. *Basic Circuit Theory*. McGraw-Hill Book Company, USA, 1969.

[11] D.B. Ender. Process control performance: Not as good as you think. *Control Engineering*, 9:180–190, 1993.

[12] EndTech. Entech control valve dynamic specification. Version 3.0, 1998.

[13] C. Garcia. Comparison of friction models applied to a control valve. *Control Engineering Practice*, 16:1231–1243, 2008.

[14] A. Gelb and W.E. Vander Velde. *Multiple-Input Describing Functions and Nonlinear System Design*. McGraw-Hill Book Company, New York, 1968.

[15] T. Hägglund. A friction compensator for pneumatic control valves. *Journal of Process Control*, 12:897–904, 2002.

[16] B. Halimi and Y. Suh Kune. Analysis of nonlinearities compensation for control valves. In *Proceedings of International Congress on Advances in Nuclear Power Plants (ICAPP 2010)*, San Diego, California, USA, June 13-17 2010.

[17] Q.P. He, J. Wang, M. Pottmann, and S.J. Qin. A curve fitting method for detecting valve stiction in oscillating control loops. *Industrial and Engineering Chemistry Research*, 46:4549–4560, 2007.

[18] A. Horch. A simple method for the detection of stiction in control valves. *Control Eng. Practice*, 7:1221–1231, 1999.

[19] A. Horch. *Condition Monitoring of Control Loops*. PhD thesis, Royal Institute of Technology, Stockholm, Sweden, 2000.

[20] A. Horch. Oscillation diagnosis in control loops- stiction and other causes. In *Proceedings of the 2006 American Control Conference Minneapolis*, Minnesota, USA, June 14-16 2006.

[21] A. Horch and T.I. Isaksson. Detection of stiction in integrating processes. In *In European Control Conference*, Porto, Portugal, 2001.

[22] Z.X. Ivan and S. Lakshminarayanan. A new unified approach to valve stiction quantification and compensation. *Industrial and Engineering chemistry research*, 48:3474–3483, 2009.

[23] M. Jelali and B. Huang. *Detection and Diagnosis of Stiction in Control Loops - State of the Art and Advanced Methods*. Springer, 2009.

[24] M. Kano, H. Maruta, H. Kugemoto, and K. Shimizu. Practical model and detection algorithm for valve stiction. In *In IFAC Symp. on Dyn. And Control of Proc. Syst. (DYCOPS)*, Cambridge, USA, 2004.

[25] D. Karnopp. Computer simulation of stick-slip friction in mechanical dynamic systems. *Transactions of the ASMEJournal of Dynamic Systems, Measurement and Control*, 107(1):100–103, 1985.

[26] S. Karra and M. Nazmul Karim. Comprehensive methodology for detection and diagnosis of oscillatory control loops. *Control Engineering Practice*, 17:939–956, 2009.

[27] K.H. Lee, B. Huang, and E.C. Tamayo. Sensitivity analysis for selective constraint and variability tuning in performance assessment of industrial mpc. *Control Engineering Practice*, 16:1195–1215, 2008.

[28] K.H. Lee, Z. Ren, and B. Huang. Novel closed-loop stiction detection and quantification method via system identification. In *Proceedings of Advanced Control of Industrial Processes (ADCONIP)*, Jasper, Canada, 2008.

[29] K.H. Lee, E.C. Tamayo, and B. Huang. Industrial implementation of controller performance analysis technology. *Control Engineering Practice*, 18:147–158, 2010.

[30] T. Miao and D.E. Seborg. Automatic detection of excessively oscillatory control loops. In *Proceedings of the 1999 IEEE international conference on control applications*, Hawaii, USA, 1999.

[31] B.A. Ogunnaike and W.H. Ray. *Process Dynamics, Modeling, and Control*. Oxford University Press Inc., New York, 1994.

[32] H. Olsson. *Control systems with friction*. PhD thesis, Lund Institute of Technology, Sweden, 1996.

[33] H. Olsson, K.J. Åström, C. Canudas de Wit, M. Gäfvert, and P. Lischinsky. Friction models and friction compensation. *European Journal of Control*, 4:176–195, 1998.

[34] M.A Paulonis and J.W. Cox. A practical approach for large-scale controller performance assessment, diagnosis, and improvement. *Journal of Process Control*, 13:155–168, 2003.

[35] A.R. Romano and C. Garcia. Valve friction quantification and nonlinear process model identification. In *Proceedings of* 9^{th} *International Symposium on Dynamics and Control of Process Systems (DYCOPS)*, Leuven, Belgium, July 5-7 2010.

[36] M. Ruel. Stiction: the hidden menace. *Control Magazine*, 13:69–75, 2000.

[37] ANSI/ISA S51.1-1979. *Process Instrumentation Terminology*. Instrument Society of America, USA, 1979.

[38] C. Scali and F. Ulivari. A comparison of techniques for automatic detection of stiction: Simulation and application to industrial data. *Journal of Process Control*, 15:505–5014, 2005.

[39] D.E. Seborg and T.E. Edgar. *Process Dynamics and Control*. John Wiley & Sons, Inc., 2004.

[40] A. Singhal and T.I. Salsbury. A simple method for detecting valve stiction in oscillating control loops. *Journal of Process Control*, 15:371–382, 2005.

[41] J.J.E. Slotine. *Applied Nonlinear Control*. Ptentice-Hall Inc., Englewood Cliffs, NJ, 1991.

[42] R. Srinivasan and R. Rangaswamy. Stiction compensation in process control loops: a framework for integrating stiction measure and compensation. *Industrial and Engineering chemistry research*, 44:9164–9174, 2005.

[43] R. Srinivasan and R. Rangaswamy. Approaches for efficient stiction compensation in process control valves. *Computer and Chemical Engineering*, 32:218–229, 2008.

[44] R. Srinivasan, R. Rengaswamy, and R. Miller. Control performance assessment 1: Qualitative approach for stiction diagnosis. *Industrial and Engineering Chemistry Research*, 44:6708–6718, 2005.

[45] R. Srinivasan, R. Rengaswamy, S. Narasimhan, and R. Miller. Control performance assessment 2: Hammerstein model approach for stiction diagnosis. *Industrial and Engineering Chemistry Research*, 44:6719–6728, 2005.

[46] A. Stenman, F. Gustaffson, and K. Forsman. A segmentation-based approach for detection of stiction in control valves. *International Journal of Adaptive Control and Signal Processing*, 17:625–634, 2003.

[47] J. Theiler, S. Eubank, A. Longtin, B. Galdrikian, B. Farmer, and J.D. Farmer. Testing for nonlinearity in time-seriesthe method of surrogate data. *Physica D*, 58:77–94, 1992.

[48] N. Thornhill. Finding the source of nonlinearity in a process with plant-wide oscillations. *IEEE Transactions on Control Systems Technology*, 13:No. 3, 2005.

[49] N. Thornhill and A. Horch. Advances and new directions in plant-wide disturbance detection and diagnosis. *Control Engineering Practice*, 15:1196–1206, 2007.

[50] N. Ulaganathan and R. Rengaswamy. Blind identification of stiction in non-linear process control loops. In *Proceedings of American Control Conference*, Seattle, Washington, USA, June 11-13 2008.

[51] J. Wang and W. Wang. Quantification of valve stiction for control loop performance assessment. In *Proceedings of 16th International Conference on Industrial Engineering and Engineering Management (IE&EM)*, Beijing, China, October 21-23 2009.

[52] C. Xia and J. Howell. Loop status monitoring and fault localization. *Journal of Process Control*, 13:679–691, 2003.

[53] Y. Yamashita. Qualitative analysis for detection of stiction in control valves. Technical Report 3214, Part II, pp. 391-397, Lecture Notes in Computer Science, 2004.

[54] H. Zabiri, A. Maulud, and N. Omar. Nn-based algorithm for control valve stiction quantification. *WSEAS Transaction on Systems and Control*, 4, 2009.

[55] X. Zang and J. Howell. Discrimination between bad turning and non-linearity induced oscillations through bispectral analysis. In *Proceedings of the SICE annual conference*, Fukui, Japan, August 4-6 2003.

Appendix A

Performance Assessment Technologies and Solutions (PATS) Software

The Performance Assessment Technologies and Solutions is a collaborative research initiative between the University of Alberta, Syncrude Canada, and the National Science and Engineering Research Council (NSERC) of Canada. The aim of this work is to develop softwares that allows the assessment of controller performance both from practical and economic aspects. The software has been developed primarily in MATLAB®. Trial versions of the software are available in the Download section of `http://www.ece.ualberta.ca/~yshardt/index.html`. This software has been used industrially.

The Stiction Detection and Quantification package of PATS has been developed in order to detect stiction in control valves, and quantify the parameters used in data-driven stiction models, i.e., estimation of numerical values for stiction parameters. Data-driven models try to describe behavior of a faulty control valve, which directly affects performance of the control system, using the least possible number of parameters. This package enables both detection and quantification at the same time.

The developed programme is working based on nonlinear system identification, considering Hammerstein model for the nonlinear system. The stiction model used in this programme, introduced by [17], captures dynamics of a faulty valve accurately using two parameters only. Inputs to the programme are routine process data; the process output (PV) and control signal (OP), and outputs are estimates for stiction parameters. The programme has ability of being fed by multiple data series, downsampling the data series, choosing different time intervals, adjusting linear model structures and the accuracy of estimation. Mentioned features provide a user-friendly environment for this programme. Results of the estimation procedure will be shown visually and numerically.

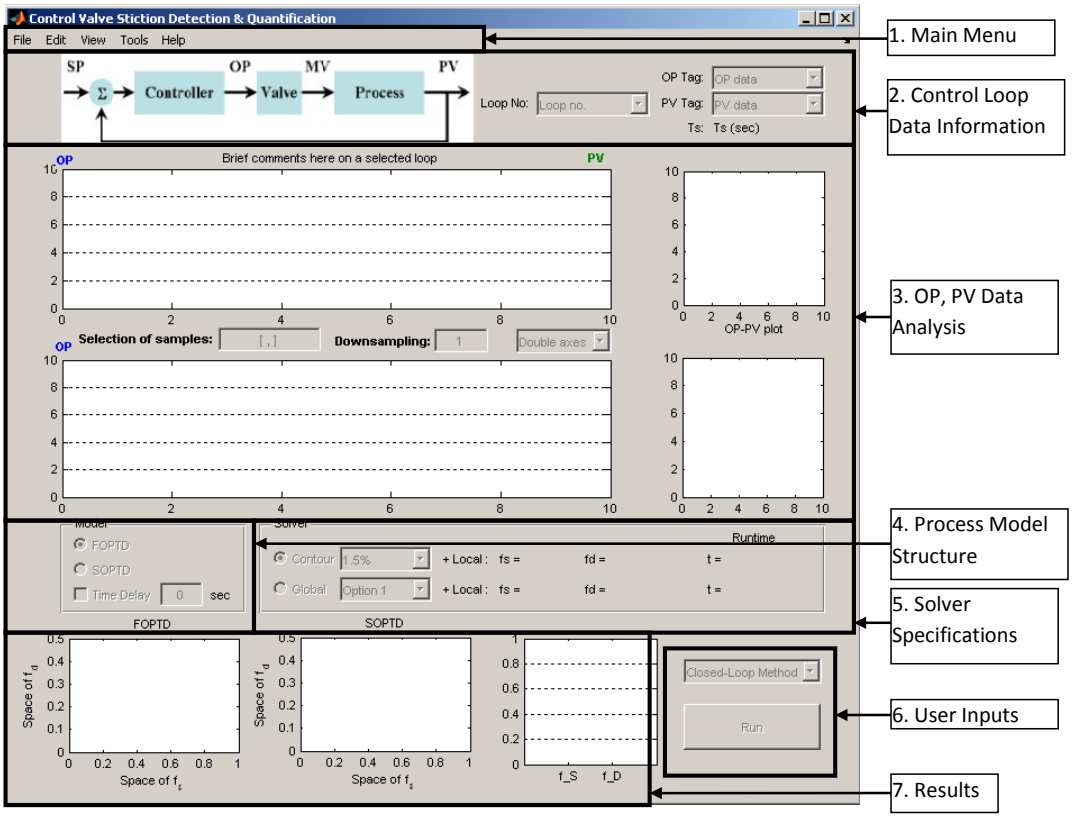

Figure A.1: Different sections of the Stiction Detection and Quantification GUI included in PATS software.

The algorithm used by the programme includes following steps:

1. Generating standard format of the process data.
2. Estimating boundaries of the search space for stiction parameters.
3. Identifying Hammerstein models for values of stiction parameters locating within the search space, and using process data as input-output series.
4. Report the most accurate estimate for parameters based on Mean Square Error (MSE) of the generated output.

Figures A.1 and A.2 show snapshots of the GUI, describing different tasks and methods of reporting the answer after running each run.

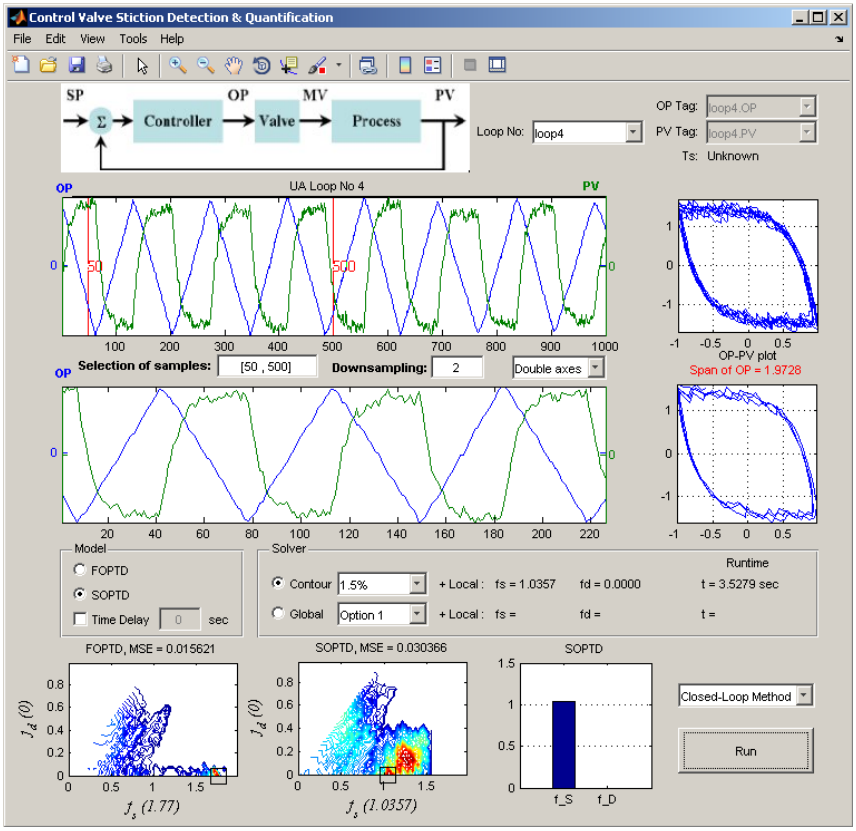

Figure A.2: Results of the estimation procedure shown on Stiction Detection and Quantification GUI.